FACULTY OF MATHEMATICS, PHYSICS AND INFORMATICS
COMENIUS UNIVERSITY
BRATISLAVA

Department of Nuclear Physics

Synthesis and spectroscopic properties of transfermium isotopes with Z = 105, 106 and 107

Accademic Dissertation
for the Degree of
Doctor of Philosophy

by

Branislav Štreicher

Supervisors:
Prof. RNDr. Štefan Šáro, DrSc.
Dr. F.P. Heßberger

Bratislava 2006

Abstract

The quest for production of new elements has been on for several decades. On the way up the ladder of nuclear chart the systematic research of nuclear properties of elements in transfermium region has been severely overlooked. This drawback is being rectified in past few years by systematic synthesis of especially even-even and odd-A isotopes of these elements.

This work proceeds forward also with major contribution of velocity filter SHIP, placed at GSI, Darmstadt. This experimental device represents a unique possibility due to high (up to 1pμA) beam currents provided by UNILAC accelerator and advancing detection systems to study by means of decay α-γ spectroscopy the nuclear structure of isotopes for the elements, possibly up to proton number Z = 110.

As the low lying single-particle levels are especially determined by the unpaired nucleon, the odd mass nuclei provide a valuable source of information about the nuclear structure. Such results can be directly compared with the predictions of the calculations based on macroscopic-microscopic model of nuclear matter, thus proving an unambiguous test of the correctness of present models and their power to predict nuclear properties towards yet unknown regions.

This work concentrates on the spectroscopic analysis of few of such nuclei. Namely it deals with isotopes ^{261}Sg and ^{257}Rf with one unpaired neutron, as well as isotopes ^{257}Db and ^{253}Lr with one unpaired proton configuration. Moreover, the analysis of odd-odd nuclei of the the decay sequence ^{262}Bg$\rightarrow$^{258}Db$\rightarrow$^{254}Lr$\rightarrow$ produced in various experiments at SHIP is discussed in detail.

Exhaustive spectroscopic analysis of these data is provided, revealing new information on α, γ, EC and SF decay modes of these very heavy isotopes, and deepening the knowledge of the low lying single-particle level structure.

Outcomes resulting from the comparison with the systematics of experimentally derived nuclear properties as well as with the predictions of the theoretical models is given. Some aspects and proposals for the further investigation in this region of nuclei are also discussed.

Acknowledgement

I express my gratitude to my supervisor, Prof. Štefan Šáro, for giving me the opportunity to work on this project and for introducing me to the world of physics.

My special appreciation goes to Dr. Fritz Peter Heßberger for all his valuable advices, suggestions and patient guidance during last few years.

I am deeply indebted to Prof. Sigurd Hofmann for his help, and for giving me the chance to periodically visit Darmstadt and to work at GSI over the past few years.

I am very grateful to Dr. Andrei N. Andreyev for many fruitful discussions and enlightenment of physical issues.

Many thanks go to my colleagues at the department especially to Dr. Stanislav Antalic and Martin Venhart for many enthusiastic discussions and for helping me to solve everyday problems and Ivan Brida for thoughtful remarks and corrections.

I would like to thanks also to Barbara Sulignano and Dr. Pasi Kuusiniemi for many cheerful moments and helpful discussions during my stays at SHIP.

Finally, I want to thank my parents for their continuous help, my girlfriend Mirka for her love and understanding and Frank Zappa and Virgil Donati for their endless inspiration.

Contents

Chapter 1

Introduction and Motivation

The quest to find the limits of stability for nuclei has been one of the major driving forces in nuclear physics for about forty years now. In the region of heaviest elements where the liquid drop model fission barriers tend to decrease to zero, nuclear shell structure is of special importance for the stability of nuclei. Special emphasis was put on the doubly magic nuclei which possess two special features, namely that the nuclear binding energies as deduced from the nuclear masses are exceptionally high and that the nuclei are spherical and stiff against deformation. Based on these features, various theoretical models [1] were proposed that predicted the next double closure shell beyond ^{208}Pb at proton numbers Z=114 or 126, and at neutron number N=184. Recent models based on the Nilsson-Strutinsky approach predicted strong shell correction energies and spherical shapes for nuclei with Z=114 [2], whereas Hartree-Fock calculations predict highest stability at proton number Z=126 [3].

Shortly after these assumptions were made a hypothesis of the existence of the "island of stability" located around this closed shell has appeared. The nuclei in this region were assumed to have the spontaneous fission half-lives exceeding the age of universe [4] and such an indication was also true for the other modes of radioactive decay such as α and electron capture (EC) decays. Therefore the physicists put an enormous effort to find these elements in nature but their endeavor was not successful. To find out the truth about the "island of stability" the consecutive synthesis of heavy elements was started in laboratories on which more information can be found in chapter 3.

In reality, given experimental conditions allow to reach with high certainty only into the region around Z $\sim$ 100 and N $\sim$ 152, which on the opposite consists of neutron deficient nuclei that are still quite far from supposed next double shell closure.

Presently this region of very neutron deficient nuclei far above uranium can be accessed essentially by means of complete[1] fusion reactions. One of the most important characteristics of such a production is that it leaves the compound nucleus (CN) with excitation energy in the region of $10-50$ MeV, which results in

[1] Also the incomplete fusion can be of special interest.

prevailing tendency of prompt fission. From the experimental point of view another mode is interesting, when in the first stages the CN cools by emission of a few (usually 1-5) neutrons and at excitation energies below the neutron binding energy by emission of γ-rays and conversion electrons and finally reaches the ground-state. The residual nucleus, having an atomic mass number smaller than that of the CN by the number of emitted neutrons is usually called evaporation residue (ER). After additional separation from the scattered beam and unwanted transfer products this residue can be detected and identified by means of its decay properties. Rapidly decreasing production cross sections down to the pbarn region as well as short half lives introduce serious problem for their successful production and identification.

It seems that in order to unfold the myth about the superheavy elements two conditions have to be fulfilled at first. Most of all there is a need for new experimental devices in principle which will be needed in order to reach directly such defined island of superheavies. This is given by the impossibility of today's experimental set-ups to deliver extra ten to twenty neutrons to the compound nucleus. Such a task can nowadays be achieved only by utilizing the radioactive beams, that already start to be used in nuclear physics experiments. However, for successful engagement into heavy element research their intensity needs to be increased by few orders of magnitude. Another task that lies in front of the heavy element research is to look more closely at the spectroscopic properties of already known transfermium elements. This information is vital in further exploration of the superheavies from two aspects: the first one is to gain more precise spectroscopic data from the region of isotopes in which we expect the future elements' decay chains to occur. The second one is even more difficult and focuses on the 'fine-tuning' of the existing and possible development of new theoretical models describing the basic nuclear properties measured in the experiments such as partial half-lives, decay energies and the nature and ordering of the corresponding nuclear levels. This information in conjunction with the experimental findings is crucial in understanding the physics of nuclear matter at the borders of stability and will be beneficial in planning the future experiments.

1.1 Project of PhD. Thesis

Presented work is closely connected with the investigation of spectroscopic properties in the transfermium region of nuclei. More specifically it deals with the analysis of several experimental runs performed at the velocity filter SHIP in GSI (Gesellschaft für Schwerionenforschung) Darmstadt utilizing the reactions ^{208}Pb(^{54}Cr,1n-2n)^{260,261}Sg, ^{209}Bi(^{54}Cr,1n)^{262}Bh and ^{209}Bi(^{50}Ti,1n-2n)^{257,258}Db. Although the isotopes of the interest here do not lie in the region of possible decay chains from the doubly magic nuclei near e.g. Z=114, 126 and N=184 which would represent one possible combination with predicted enhanced shell effects, the improvement of their spectroscopic properties will be beneficial as underlined before. In general the objectives of the presented PhD. project can be summarized in following

points:

- This PhD. thesis attempts to give the complete spectroscopic analysis of the aforementioned experiments with respect to produced isotopes. The methods of particle decay spectroscopy are used to identify individual isotopes down to the limit of a few, possibly even one nucleus, and extract all possible physical quantities, discussed in more detail in chapter 2. Possible modes of decay that can be measured at SHIP directly are α-decay, γ-decay, spontaneous fission and recently even electron signals from internal conversion. Indirectly, through just mentioned modes also electron capture and/or β^+-decay can be identified.

- It needs to be mentioned that all analyzed isotopes have been identified previously, however due to already mentioned difficulties with their production many of them with only poor statistics that did not allow for precise measurement of the physical quantities and left many questions opened. Therefore new set of experiments to refine those measurements were performed at SHIP having specific tasks related to each isotope discussed in this work. These tasks had physical as well as technical nature and are addressed in detail in separate sections of chapter 4.

- Furthermore, to demonstrate the evolution of the nuclear properties in respect to the isotopes discussed here, the derived physical quantities are examined and compared over extended sequences of nuclei - that is, a nuclear *systematics*, while at the same time contributing and expanding them. Interpretation of these comparisons is put into a general picture of the systematics of the nuclear properties in transfermium region.

- The most direct data on the single-particle energies and J^π values come from the odd-A nuclei, providing the motivation to investigate isotopes ^{261}Sg, ^{257}Rf, ^{257}Db and ^{253}Lr among the others discussed in this work. These data provide the most direct link between the experimental findings and theoretical models. In this work both, single-neutron and single-proton levels are deduced to possible extent in the mentioned isotopes. These are compared against a few theoretical calculations available based on a macroscopic-microscopic approach. Again possible interpretations and conclusions about the predicting power and usability of these models are given.

- Derived spectroscopic information and the conclusions stemming from physical interpretation attempt to contribute to the knowledge of nuclear properties of transfermium isotopes and will be beneficial in planing of the future experiments aimed at the production of either these isotopes or the ones generically connected. Opened questions arising from the current analysis and underlined in each section should serve as a motivation for further measurements.

Chapter 2

Background on Physical Properties

Following sections are dedicated to explain in brief the basic physical phenomena connected with the production, decay and identification of nuclei in transfermium region. It should merely serve as the apparatus to better understand the problematics of the later chapters where the analysis of the experiments is described and the interpretation of these data is put into perspective using the physical terms and ideas described here.

2.1 Process of Element Synthesis

Production of new elements and their isotopes through the process of neutron capture in high-yield reactors and their successive β^- decay ended at the element ^{258}Fm due to its short half-life of 0.38 ms. Two other methods can be used as possible alternatives for further production of heavy elements.

One of them is based on the process of transferring the desired number of nucleons from one nucleus to the other, hence forming the final product. In such a process many different isotopes will be produced beside the wanted ones. This feature along with the facts that the excitation energy of the final product increases with increasing number of nucleons transferred and cross sections drop steeply when going away from the target nucleus makes this method less usable in heavy element production. However, in later chapters of this work, such products will be used for detector calibration purposes.

Another approach is the complete amalgamation of two nuclei in a fusion process. Compound system formed in this manner carries an excitation energy expresses as:

$$E^* = Q + \frac{M}{M+m} E_p, \tag{2.1}$$

where $Q = (M + m - M_{CN})c^2$ is the reaction Q-value, E_p is the projectile's energy in the laboratory frame and M, m and M_{CN} are masses of target nucleus,

projectile and compound nucleus, respectively. This excitation energy is taken away by emission of particles[1], predominantly neutrons, and γ-rays, thus forming an evaporation residue. In principle two different approaches can be taken to produce superheavy nuclei by means of complete fusion reaction:

- Cold Fusion utilizes ^{206,207,208}Pb and ^{209}Bi targets in combination with the projectile of appropriate mass. Resulting compound nucleus has an excitation energy approximately 10 - 20 MeV and cools down desirably by emission of 1 - 2 neutrons.
- Hot Fusion on the other hand uses very heavy targets like ^{238}U bombarded with projectiles from the region ^{12}C - ^{48}Ca. Following the reaction kinematics, the final product is left with substantially larger excitation energy of about 40 to 60 MeV.

2.2 Production Cross Sections

The cross section for synthesis of SHEs is very small and decreases rapidly with increasing atomic number down to the value of 13 ± 5 pb for element ^{271}110 and $2.9^{+1.9}_{-1.3}$ pb and $0.5^{+1.1}_{-0.4}$ pb [6] for elements ^{273}111 and ^{277}112, respectively. The experimental investigation of excitation functions for the SHE production becomes increasingly difficult due to the very small cross sections and narrow width of the excitation function of about 4 MeV FWHM [24].

Theoretical evaluation of the SHE formation, schematically also shown in Fig. 2.1 can be treated in three stages:

- The amalgamation of two nuclei and the formation of a common shape of the two touching nuclei. Low energy surface vibrations and a transfer of few nucleons are taken into account at the first step of a reaction
- The formation of a spherical or nearly spherical compound nucleus.
- The survival of excited compound nucleus during evaporation of neutrons and γ-ray emission which compete with fission - formation of evaporation residue.

In general, the evaporation residue cross-section of dinuclear system can be evaluated [7] as follows:

$$\sigma_{er}(E) = \sum_{l=0}^{\infty} (2l+1)\sigma_l^{fus}(E,l)W_{sur}(E,l), \tag{2.2}$$

[1]The fission of the excited compound nucleus is usually prevailing in competition with particle emission.

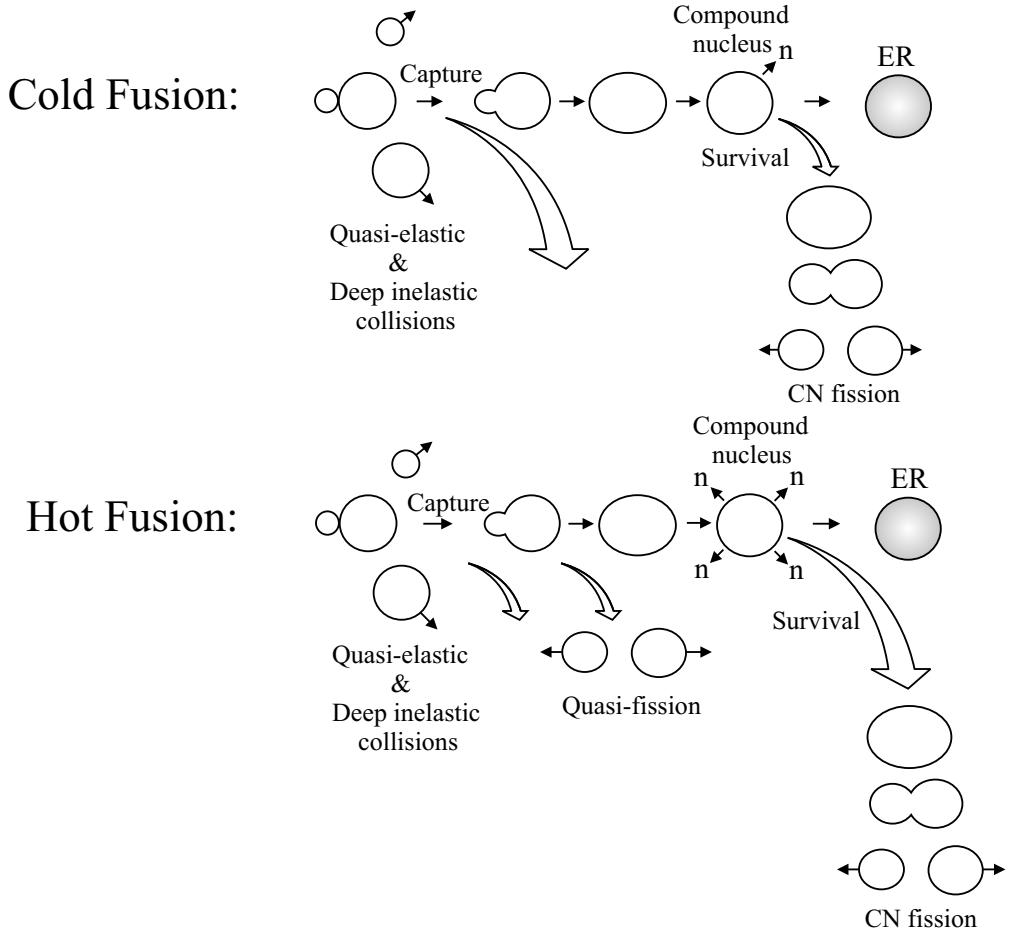

Figure 2.1: Simple scheme showing principal differences between cold and hot fusion reaction mechanism [5].

where the entrance channel effects are included in the partial fusion cross-section $\sigma_l^{fus}(E)$ defined by the expressions:

$$\sigma_l^{fus}(E) = \sigma_l^{capture}(E) P_{CN}(E, l), \tag{2.3}$$

$$\sigma_l^{capture}(E) = \frac{\lambda^2}{4\pi} P_l^{capture}(E). \tag{2.4}$$

Here λ is the de Broglie wavelength of the entrance channel, $P_{CN}(E, l)$ is a factor taking into account the decrease of the fusion probability due to brake-up of the dinuclear system before fusion, $P_l^{capture}(E)$ is the capture probability which depends on the collision dynamics and determines the amount of partial waves leading to capture and $W_{sur}(E, l)$ is survival probability of the compound nucleus for a given angular momentum l.

2.3 Properties of α-Decay

A nucleus in an energetically unstable state can decay sequentially by means of particle or γ-ray emission until the final nucleus in a stable ground-state is reached. The type of emission depends on the energetics of the possible process and on the structure of the initial and final states. When particle emission is energetically possible it is usually preferred followed by γ-ray emission. When ground-state of the nucleus is reached, further γ-ray emission is impossible but if the nucleus is still unstable it can either decay by β-emission to Z $\pm$ 1 isobar or by α-emission to the nucleus with Z-2 and A-4, respectively. Moreover both of these decays can populate the ground-state in the daughter nucleus as well as an excited state whose energy can be again carried away by γ-ray emission and so on. In many cases all of these decay modes are in competition.

Alpha radioactivity has been known in heavy nuclei for a long time. It might be thought remarkable that α-decay happens at all, but it can be explained by high binding energy of the α-particle ($B_\alpha = 28.3$ MeV). Total energy release in α-decay Q_α can be expressed in two different ways, either through masses of mother and daughter nuclei and α-particle:

$$Q_\alpha = (m(Z, A) - m(Z-2, A-4) - m_\alpha)c^2, \tag{2.5}$$

or binding energies of the objects involved:

$$Q_\alpha = B(Z-2, A-4) - B_\alpha - B(Z, A). \tag{2.6}$$

When quantity Q_α becomes positive, the α-particle will no longer be a trapped particle inside the nucleus and will be emitted after tunnelling through the Coulomb barrier from the mother nucleus ${}^{A}_{Z}\mathrm{X}_{N}$. Looking at the periodic chart of isotopes one can see that this starts to occur[2] at A $\approx$ 150.

From the experimental point of view the quantity Q_α is distributed between the excitation energy of the daughter nucleus E_d^*, if this is not left in the ground-state ($E_d^* = 0$), kinetic energy of α-particle E_α and recoil daughter nucleus E_R:

$$Q_\alpha = E_d^* + E_\alpha + E_R. \tag{2.7}$$

Following the conservation of momentum in α-decay to the ground-state, the energy is shared between the α-particle and daughter nucleus as the ratio of their masses:

$$E_R = \frac{m_\alpha}{m(Z-2, A-4)} E_\alpha. \tag{2.8}$$

The sum of elektronic signals measured in the experiment gives the Q_α, which can be then easily calculated from the measured α-energy E_α. In case of decay to the ground-state one gets:

[2]There is also a small island of α-emitters just above tin around A $\approx$ 110.

$$Q_{\alpha a} = E_\alpha + E_R = \frac{m(Z,A)}{m(Z-2,A-4)} E_\alpha. \tag{2.9}$$

The quantity $Q_{\alpha a}$ represents an atomic Q_α (difference of the atomic masses). For theoretical calculations a nuclear $Q_{\alpha n}$ value, computed from nuclear masses, is more important. This can be evaluated as:

$$Q_{\alpha n} = E_\alpha + E_R + \triangle E_\alpha, \tag{2.10}$$

where $\triangle E_\alpha = (65.3Z^{7/5} - 80Z^{2/5})$ eV [8] is a "screening correction", which evaluates the energy loss of α-particle passing the atomic shell.

2.3.1 Relationship Between Q_α and $T^\alpha_{1/2}$

The α-particles from radioactive[3] nuclei have discrete energies appreciably smaller than the Coulomb barrier and well-defined mean ranges $\Re$ in air, which are connected with the α-particle energies by $\Re \approx 0.325 E_\alpha^{3/2}$ (E_α is given in MeV and $\Re$ in cm). Based on these empirical observations and by fitting the experimental data, Geiger and Nuttall [9] came up with the formula connecting the energy of the α-particle with the corresponding decay constant λ for even-even natural emitters:

$$\log \lambda_\alpha = C \log E_\alpha - D, \tag{2.11}$$

where C and D are constants.

For analytical explanation of this feature of α-decay Gamow [10] and Gurney and Cordon [11], independently, developed a quantum theory of α-particle tunnelling through the Coulomb barrier. Since the α-particles have considerably smaller energy than the Coulomb barrier, their wavefunction is exponentially attenuated as they pass through the barrier and the emission probability is therefore very sensitive function of the α-particle energy. This explains the huge range of experimental half-lives.

According to this theory, the α-decay constant λ_α can be expressed as the product of the frequency ω which expresses, in a simple way, the frequency of impacts on the barrier and the probability of transmission through the barrier P:

$$\lambda_\alpha = \omega P. \tag{2.12}$$

The first term can be approximated as a fraction of 'internal' α-particle velocity and the nuclear radius, giving $\omega = v_{in}/R$. The barrier penetration factor P can be in case of one dimensional barrier expressed in WKB (Wentzel-Kramers-Brillouin) approximation:

$$P \approx e^{-G} = \exp\left\{ -2\frac{\sqrt{2m_\alpha}}{\hbar} \int_R^b [V(r) - E_\alpha]^{1/2} dr \right\}, \tag{2.13}$$

[3]This seems to be true for all α-emitters, but was historically realized for α-particles from natural sources.

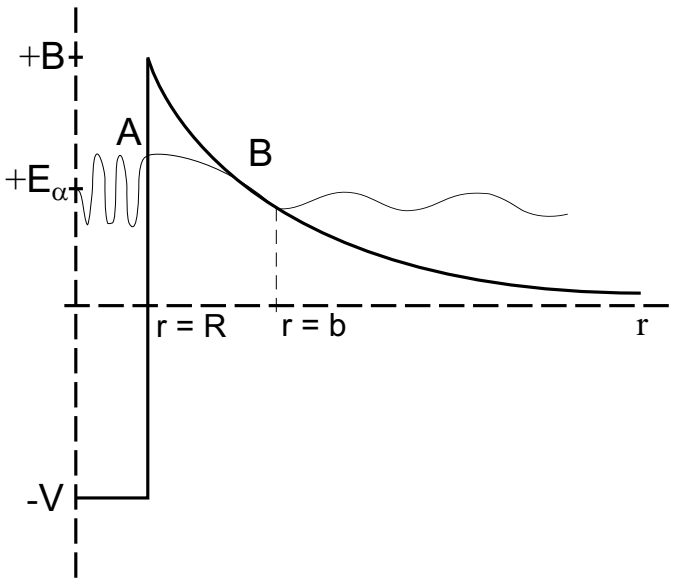

Figure 2.2: Schematic diagram of the nuclear potential V, barrier hight B and the α-wavefunction tunnelling through the Coulomb barrier.

where G is the Gamov factor, R and b are the classical turning points A and B shown in Fig. 2.2 and $V(r)$ is the Coulomb barrier. Omitting the details of the calculations it can be shown from the mentioned assumptions, that the relation between $T^{\alpha}_{1/2}$ and Q_α is:

$$\log T^{\alpha}_{1/2} = A + \frac{B}{\sqrt{Q_\alpha}}, \tag{2.14}$$

where A is a constant and B depends on Z. This is the Geiger-Nuttall law of α-decay, since $\lambda_\alpha = \ln 2/T^{\alpha}_{1/2}$.

2.3.2 Branching Ratios and Partial Half-lives

The α-decay probability λ_α as derived in previous section describes decay carrying away zero-angular momentum and involves decay of a nucleus in its ground-state. Many α-particle emitters, though, show a spectrum of α-groups corresponding to α-transitions to various nuclear excited states in the final nucleus. This is confirmed by the fact that γ-rays have been observed along with the energies corresponding to the energy differences between various α-groups.

As it was mentioned in the beginning of section 2.3, decay schemes can be quite complex, involving various decay modes as can be seen on Fig. 2.3. In such a case the decay constant λ consists of sum of partial decay constants for individual decay modes:

$$\lambda = \sum_i \lambda_i \ , \quad i = \alpha,\ \beta^+, \beta^-, EC,\ SF \ldots . \tag{2.15}$$

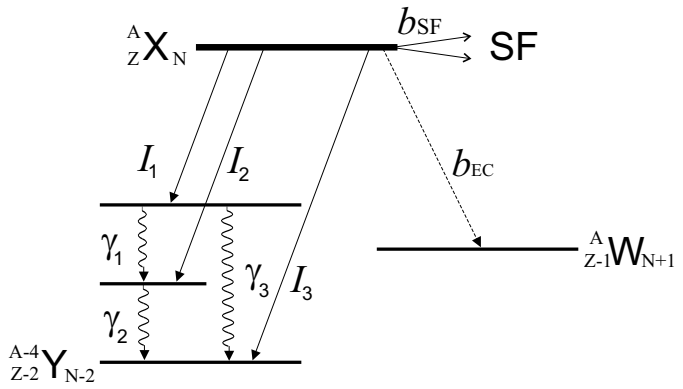

Figure 2.3: Diagram introducing various decay modes.

Following from this, for each corresponding decay mode the branching ratio can be defined:

$$b_i = \frac{\lambda_i}{\lambda}, \tag{2.16}$$

as well as the partial half-life:

$$T_{1/2}^{i} = \frac{\ln 2}{\lambda_i}. \tag{2.17}$$

The partial half-life is another way to represent branching ratios. The activity would be observed to decay only with the total half-life.

Similar situation appears within the α-decay mode itself. Here several α-lines can be observed populating the ground-state and excited states in daughter nuclei as shown on Fig. 2.3. In this situation the α-decay constant λ_α can be expressed as a sum of individual decay constants of all α-lines:

$$\lambda_\alpha = \sum_i \lambda_i, \quad i = 1, 2, 3 \ldots. \tag{2.18}$$

For practical purposes we define relative intensities I_i for individual α-lines as a ratio of number of observed events for each α-line n_i divided by total number of observed α-decays N:

$$I_i = \frac{n_i}{N}, \quad \sum_i I_i = 1, \quad i = 1, 2, 3 \ldots. \tag{2.19}$$

2.3.3 Reduced α-widths δ_α^2

The α-decay provides us with a sensitive probe of configuration and structure in the parent and daughter nuclei. By means of experimental measuring of its half-life, according to [12] a reduced α-width δ_α^2 can be calculated as follows:

$$\delta_\alpha^2 = \lambda h / P, \tag{2.20}$$

where λ_α is a decay constant, h is Planck's constant and P is a probability of the α-particle to penetrate through the barrier, calculated using similar expression as 2.13 except for added centrifugal term taking into account orbital momentum l carried away by α-particle. The potential $V(r)$ was derived from the optical model analysis of the elastic scattering of the α-particles in [13] and has a form of:

$$V(r) = -1100 \exp\left\{ -\left[\frac{r - 1.17A^{1/3}}{0.574}\right]\right\} MeV. \tag{2.21}$$

A reasonable assumption is, that this should represent the potential experienced by α-particle emitted in α-decay. On the contrary to relative intensities I_i, reduced α-width δ_α^2 is stripped off the simple energy dependance and carries basically all nuclear information. In practice we can draw some conclusions about the structural changes in the parent and daughter nuclei in α-decay, if we know that one of it has oblate, prolate or spherical shape. Based on this information one can say something about the overlap of parent-daughter nuclear wavefunctions.

2.3.4 Calculation of α-Decay Half-lives

Semiempirical formula for partial half-life calculation using the measured Q value of α-decay can be derived from the fission theory of α-emission [14]. It is a second order expression of the arguments N and Z with six parameters B_i $(i = 1, 2, \ldots, 6)$ determined from a fit to experimental data. In accordance to [15] it can be finally obtained:

$$T_{1/2}^{\alpha} = 10^{(B_1+B_2y+B_3z+B_4y^2+B_5yz+B_6z^2)K_s/ln10-20.446}, \tag{2.22}$$

where y and z are reduced variables expressing the distance of N and Z for the isotope of interest from the closest magic numbers of neutrons and protons N_i, Z_i relative to the next magic number N_{i+1}, Z_{i+1} for both nucleons as can be seen from expressions in 2.23. The other parameters are as follows:

$$\begin{aligned}
y &= (N - N_i)/(N_{i+1} - N_i); \qquad N_i < N \leq N_{i+1};\\
z &= (Z - Z_i)/(Z_{i+1} - Z_i); \qquad Z_i < Z \leq Z_{i+1};\\
N_i &= 51, 83, 127, 185, \ldots\\
Z_i &= 51, 83, 115, 121, \ldots\\
Q &= E_\alpha A/A_d;\\
K_s &= 2.52956 Z_d (A_d/AQ)^{1/2} [\arccos\sqrt{x} - \sqrt{x(1-x)}];\\
x &= 0.4253Q(1.5874 + A^{1/3})/Z_d;\\
A_d &= A - 4; \qquad Z_d = Z - 2;\\
B_1 &= 0.988662; \qquad B_2 = 0.016314;\\
B_3 &= 0.020433; \qquad B_4 = 0.027896;\\
B_5 &= B_6 = -0.003033,
\end{aligned} \tag{2.23}$$

where A and A_d represent the masses of mother and daughter nuclei, respectively and E_α is the measured α-particle energy in MeV. The original work of Poenaru et al. introduced different parameter $B_6 = -0.16820$, but it was found out [16], that setting parameter B_6 equal to B_5 reproduces much better the experimental results.

The value of $T^\alpha_{1/2}$ from equation 2.22 is obtained in seconds if $Q = E_\alpha A/A_d$ is expressed in MeV.

It should be noted that odd A nuclei have substantially longer half lives that their even-even neighbors do. Consequently the decays of the odd A nuclei are referred to as 'hindered' and the hindrance factor may be defined as the ratio of the measured partial half-life for a given α-transition to the half-life that would be calculated from a simple one-body theory applied to even-even nuclides.

2.4 Internal Conversion

Internal conversion is a competing process to gamma-ray emission and electron-positron pair formation (provided that the excitation energy is above 1.022 MeV). Its importance as a decay mode increases towards the region of heavier nuclei.

The internal conversion coefficient (ICC) is defined as the ratio of the number of electrons N_i ejected from the i-th atomic shell ($i = K, L, M, ...$) to the number of gamma quanta N_γ leaving the nucleus at the same time. By definition,

$$\alpha_i = \frac{N_i}{N_\gamma}. \tag{2.24}$$

The total ICC, α_T, is the sum of partial ICCs for all atomic shells having the binding energy ε_i in which the process is energetically possible ($E_\gamma > \varepsilon_i$). Thus

$$\alpha_T = \sum_i \alpha_i. \tag{2.25}$$

The kinetic energy of a conversion electron e^- is determined by the law of energy conservation,

$$T_{e^-} = E_\gamma - \varepsilon_i, \tag{2.26}$$

where E_γ is the gamma-ray energy[4].

Internal conversion occurs when nucleus transfers its excitation energy through the interaction of its electromagnetic field with the electron. In this precess conversion electron receives angular momentum with magnitude l from the nucleus. The multipolarity type τ of this angular momentum (electric $\tau = E$ or magnetic $\tau = M$) is associated with the parity of the radiation field:

[4]This is equal to transition energy, if nuclear recoil is neglected.

$$\pi_\gamma = (-1)^l \text{ for electric transitions,}$$
$$\pi_\gamma = (-1)^{l+1} \text{ for magnetic transitions} \quad (2.27)$$

The probability P_{IC} for the nucleus to deexcite by internal conversion is in general govern by these rules:

- P_{IC} increases as Z^3, so it plays much important role in heavier nuclei.
- It decreases with the transition energy.
- For high multipole transitions (higher l) it is more probable than gamma emission.
- P_{IC} decreases for higher atomic shells approximately as $1/n^3$.

Based on mentioned conditions one can conclude that IC plays a dominant role for low energy, high multipolarity, K-shell transitions in heavy nuclei. According to well established notation also used here, in later sections discussing the experimental results the multipolarity of the transitions together with the angular momentum will be labelled as E1, M1, etc..

2.5 Nilsson Levels in Heavy Nuclei

All nuclear properties are trying to be explained within the framework of appropriate nuclear model. Important decay quantities of transfermium nuclei e.g. ordering and J^π values of excited levels are well enough understood by the concept of deformed nucleus consisting of independent particles moving in a deformed well. Because of its importance to the later discussions of spectroscopic data and the fact that it is based on the nuclear shell model a brief explanation is presented in the next sections.

2.5.1 Shell Model

Shell model was developed in the late 1940s [17],[18] as a reaction to unsuccessful attempts of previous models to explain a number of nuclear phenomena, most importantly the existence of magic numbers among the others. The idea behind shell model lies in particles moving independently in the central potential. The short range of nuclear force that creates this potential makes it to resemble nuclear density distribution. The way to successful explanation of magic numbers and other features connected to the shell structure of the nucleus leads through finding the best form for this potential. The solution of the Schroedinger's equation:

$$\nabla^2\psi - \frac{2m}{\hbar^2}(E - V)\psi = 0, \quad (2.28)$$

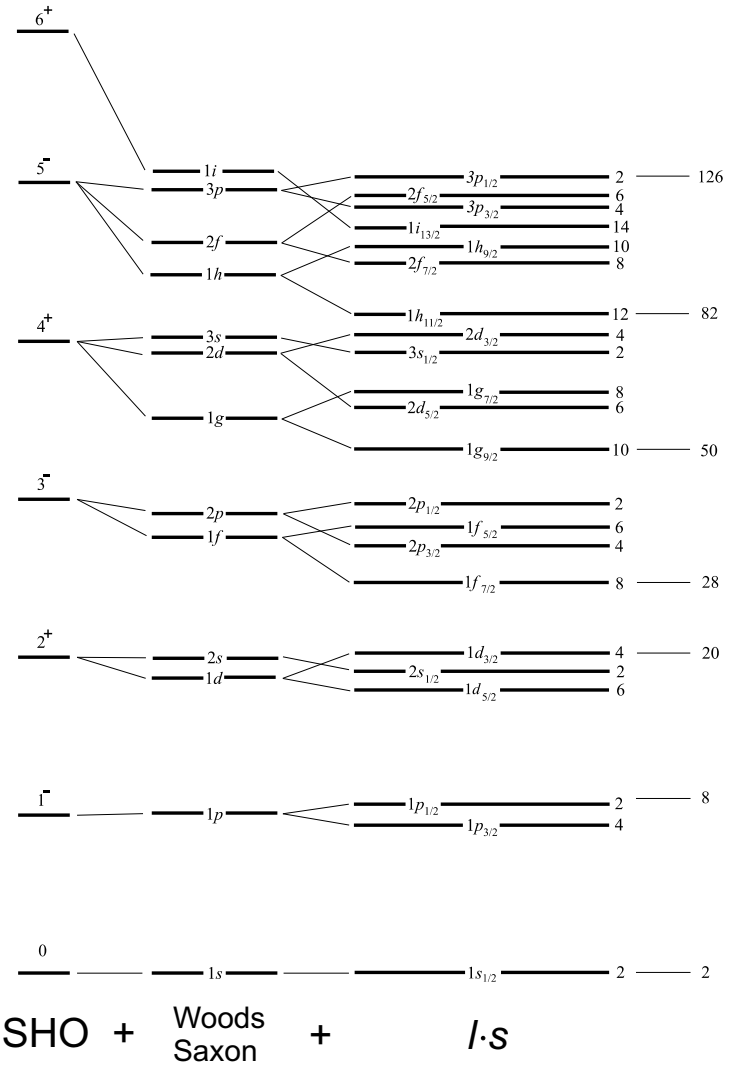

Figure 2.4: Approximate level pattern for nucleons calculated using three potentials. The number of nucleons in each level calculated as $j \times 2$ with $j = l + s$ and the cumulative totals are shown.

with such potential V has to reproduce experimental results and yet to have meaningful physical interpretation for its form. Resulting energy levels are shown in Fig. 2.4 with few most simple potentials:

$$V_1(r) = -V_0 + \frac{1}{2}M\omega^2 r^2, \quad V_2(r) = \frac{-V_0}{1 + exp(\frac{r-R}{a})}, \tag{2.29}$$

where $V_1(r)$ is simple harmonic oscillator potential with M being the nucleon mass, ω is oscillator frequency and $V_2(r)$ is Woods-Saxon potential [19] with R denoting the half-density radius and a the diffuseness parameter. The later potential resembles nuclear density distribution much better and with its use the degeneracy of Simple Harmonic Oscillator (SHO) levels is broken as shown in Fig. 2.4.

In 1949 Mayer and Jensen, following a suggestion of E. Fermi, proposed the additional spin-orbital term $V_{ls} = C_{ls} l \cdot s$ corresponding to the interaction between the nucleon spin s and its orbital angular momentum l. This causes additional splitting of nl levels (middle column in Fig. 2.4) into nlj states, and this happens for each $l \neq 0$. It was not until the introduction of this correction that proper magic numbers *2, 8, 20, 28, 50, 82, 126* were reproduced.

The next meaningful extension of this idea directly applicable to spectroscopic data is a treatment of the single-particle states constructed from the closed shell nucleus plus one valence nucleon. Because closed shell has always total angular momentum J=0 and even parity π, the ground-state J^π value of nucleus with closed shell + one nucleon is carried by this valence nucleon. Such approach can really explain the ground state J^π of nuclei like ^{17}O$(5/2^+)$ or ^{209}Pb$(9/2^+)$. As long as this simplification assumes that only the valence nucleon itself is being excited with the core left undisturbed this model can explain the excitation J^π values up to a few MeV when breaking of the nucleon-nucleon pair in the closed core becomes possible. It is clear that such treatment must result in failure of explaining the nuclear levels of more complex systems. This can be improved by introduction of corrections briefly outlined in the following:

- All particles outside the major closed shell are considered and angular momenta of these particles are combined in various ways to get the resulting angular momentum. Two main schemes represent LS and jj coupling.
- Residual forces between the particles outside the closed shells are introduced. This further influences the form of the potential V causing it to become noncentral which has an effect on additional splitting of otherwise degenerate states created by interaction of nucleons in the level with the same j value.
- It is known that many nuclides are permanently deformed and hence can not be described by a spherical potential. This is especially true for the region of interest of this work around Z $\sim$ 100 and is discussed in the next section.

2.5.2 Deformed Shell Model

Since many nuclei possess large permanent deformations[5] in 1955 S. G. Nillson [20] introduced shell model describing ellipsoidal deformed nuclei. Nucleons in such nucleus do not move in a spherical potential. Nillson used deformed harmonic oscillator potential, which enables much of the calculation to be made analytically:

$$V_{def} = \frac{1}{2} m[\omega_\perp^2 (x_1^2 + x_2^2) + \omega_3^2 x_3^2] + C\langle ls \rangle + Dl^2, \tag{2.30}$$

In eq. 2.30 factor ω is related to the energy of an oscillator level, the second term is the spin-orbital potential and the third one is an empirical addition to maintain

[5] All isotopes treated in this work are well deformed - see discussions in chapter 4.

the observed ordering of the higher states. For a pure quadrupole deformation with the deformation parameter ϵ coefficients $\omega_\perp$ and ω_3 follow:

$$\omega_3 = \omega_0(1 - \frac{2}{3}\epsilon)$$
$$\omega_\perp = \omega_0(1 + \frac{1}{3}\epsilon) \tag{2.31}$$

The parameter ϵ is connected to the geometric deformation parameter δ as $\delta = \epsilon(1 + \frac{1}{2}\epsilon)$ with $\delta = \Delta R/\bar{R}$. This expresses the difference of the average nuclear radius $\bar{R}=\frac{1}{2}(a+b)$ on the difference of two axes a and b of the ellipsoid $\Delta R = a-b$ (see Fig. 2.5a)). As a result, V_{def} is determined by four parameters ω_0, C, D and ϵ, with only ϵ depending strongly on the nuclear shape.

Typical levels in deformed nucleus of small A in dependance of ϵ are shown in Fig. 2.5b). For zero deformation the levels agree with those at right side of Fig. 2.4, while for $\epsilon \neq 0$ deformation breaks the $2j+1$ degeneracy of the spherical shell model. This gives a raise to $\frac{1}{2}(2j+1)$ different energy levels for each spherical state, that further behave according to the magnitude of ϵ as schematically shown in Fig. 2.5b). In Nillson model each orbital is characterized by a set of quantum numbers $\Omega^\pi[\mathrm{Nn}_z\Lambda]$ (used in later sections to label single-particle states) shown in Fig. 2.5 and described as:

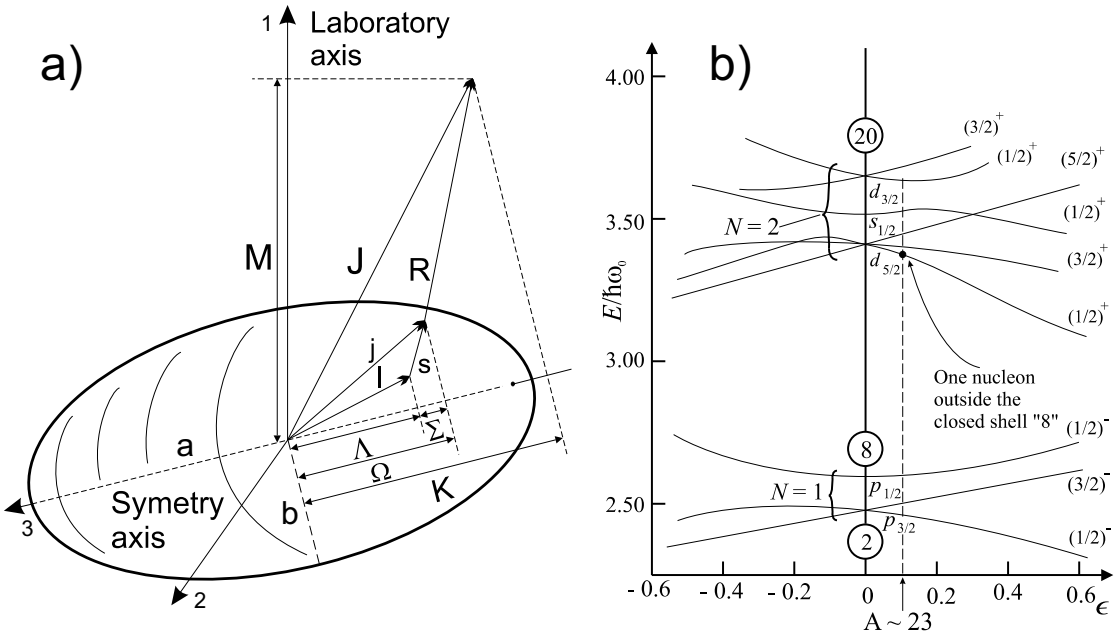

Figure 2.5: **a)** The description of quantum numbers in deformed nucleus. **a)** Schematic representation of the levels in Nilsson model.

- **N** - the total oscillator shell quantum number.

- $\mathbf{n}_z$ - the number of oscillator quanta in the z direction.
- **M** - projection of total angular momentum J of the nucleus on the laboratory axis.
- Ω - the projection of the total angular momentum j (orbital l plus spin s) of the odd nucleon on the symmetry axis.
- **R** - angular momentum from the collective motion of the nucleus.
- Λ - the projection of angular momentum along the symmetry axis, Ω=Λ+Σ, where Σ is the projection of the intrinsic spin along the symmetry axis.
- **K** - projection of total angular momentum J of the nucleus on the symmetry axis[6].

Since the nucleus can rotate in any state of deformation, each intrinsic level (Nilsson level) can form a band-head of the rotational band. Derivations of the described model with more sophisticated potentials are successfully applied in explanation of the levels in the deformed odd mass nuclei and will be used in discussions in later sections.

2.5.3 Interconnection Between Nuclear Spectroscopy and Model

Measurements of the nuclear rotational bands up to spins as high as $> 20\hbar$ by means of in-beam spectroscopy provide crucial information about the spins and parities of the band-heads of these rotational bands in deformed nuclei. These bands in odd-A nuclei de-excite by series of E2 and M1 transitions (see Fig. 2.6) to the band-head that represents the corresponding single-particle level with the same $\Omega^{\pi}[\mathrm{Nn}_z\Lambda]$ in Nilsson model. The strength of E2 and M1 transitions can be expressed by their experimentally measured half-lives $T_{1/2}$ and energies E_γ of the transitions within the band:

$$B(\mathrm{E2}) = \frac{0.0566}{T_{1/2}(\mathrm{E2})E_\gamma^5}(eb)^2$$
$$B(\mathrm{M1}) = \frac{0.0394}{T_{1/2}(\mathrm{M1})E_\gamma^3}\mu_N^2. \qquad (2.32)$$

The quantities B(E2) and B(M1) can be also expressed in terms of intrinsic quadrupole moment Q_0, nuclear g-factors g_K and g_R, and quantum numbers J and K as:

[6]When the spin difference $\lambda = j_i$ - j_f of initial and final states from two different rotational bands having K_1 and K_2 in γ-decay follows $\lambda \not\geq \Delta K$, such a decay is K-hindered. These so called K-isomers are being intensively studied nowadays also at SHIP.

$$B(\mathrm{E2}) = B(J, K \to J-2, K) = \frac{5}{16\pi}^{2} Q_0^2 \big\langle JK20|J-2K\big\rangle^2 (eb)^2$$
$$B(\mathrm{M1}) = B(J, K \to J\pm 1, K) = \frac{3}{4\pi}(g_K - g_R)^2 K^2 \big\langle JK10|J\pm 1K\big\rangle^2 \mu_N^2, \quad (2.33)$$

The rotational g-factor defined as $g_R \approx Z/A$ arises from the collective rotation of the core and the intrinsic g-factor defined as g_K is the result of the motion of valence nucleons.

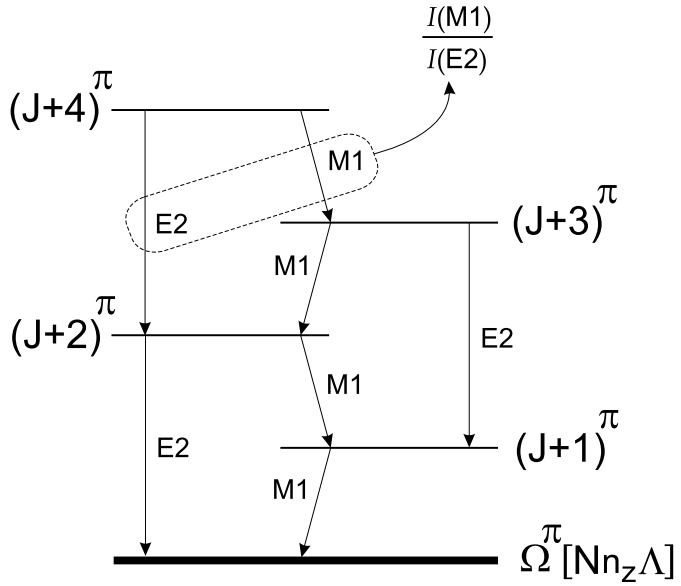

Figure 2.6: Schematic structure of the rotational band. In consistency with the notation in previous section the spin and parity of the band-head is denoted Ω^π and that of higher levels as $(J+x)^\pi$ with $x = 1, 2, 3, \ldots$ and $J = \Omega$.

The possibility to derive aforemention information in in-beam experiments has fundamental connection to spectroscopy experiments in the region of transfermium isotopes. The basic physical idea and experimental procedure is schematically described in the following points:

- ♣ Experimentally measured ratio of M1 and E2 transition intensities for each level is the same throughout the rotational band (see Fig. 2.6). This ratio is proportional to the ratio of calculated transition strengths $B(\mathrm{M1})/B(\mathrm{E2})$ which is further reducible using eq. (2.33) to the form expressed as $C \times (g_K - g_R)/Q_0$, where C is a constant from all other equation members. Providing that we know the value of Q_0 we can estimate the intrinsic g-factor g_K. This quantity depends on Ω^π[N,n$_z$,Λ] of the band-head and therefore is directly connectable to theoretical predictions of J^π[Nn$_z\Lambda$] values of Nilsson levels in various isotopes.

- ♣ Transition strength $B(\mathrm{E2})$ can be obtained in so called 'plunger measurements' enabling to record the transition times within the rotational band down to ps time region. Knowing the value $B(\mathrm{E2})$ and using corresponding expressions from (2.32), (2.33) we can obtain the value for Q_0. By this procedure it is possible to experimentally deduce the intrinsic quadrupole moment Q_0 and providing that $Q_0 = 0$ for spherical nuclei, $Q_0 > 0$ for prolate (rugby-ball shaped) and $Q_0 < 0$ for oblate (disk shaped) make judgements about nuclear shape. Quadrupole moment Q_0 is also related to the quadrupole deformation parameter ε_2. The energy variance of different $J^\pi[\mathrm{Nn}_z\Lambda]$ Nilsson levels is usually dependent on parameter ε_2 and thus providing another connection between experimental results on heavy deformed nuclei and theoretical predictions resulting from the deformed shell model.

It is straightforward to see that in-beam data can have a significant contribution to the spectroscopy experiments in transfermium region. Although there is a lack of available data and so far the heaviest isotope studied in-beam is ^{255}Lr [21], it can be of a benefit to know unambiguously assigned J^π value of a ground-state or at least one of the low-lying Nilsson states of the isotope through which the isotope of our interest decays. This provides the anchor for attributing the J^π values to other levels in the decay scheme arising from the data. Based on the hindrance factors for fine structure α-decays, internal conversion coefficients between nuclear levels and decay half-lives of the transitions the multipolarity of these transitions can be estimated and hence J^π of connected levels can be derived. Providing that the in-beam information about spins and parities of some lighter decay-connected isotopes is known, many spectroscopic experiments can be performed on heavier nuclei, since these can be done with few nb crossections giving about $\sim 10^3 - 10^4$ decays at reasonably long irradiation times. In present state of the research however this information is scarce and the assignment is usually based on the systematics and/or few theoretical calculations whose predicting power is quite limited and most importantly needs to be confronted with the experimental results.

Chapter 3

Experimental Devices and Techniques

At the beginning of the heavy elements research the new isotopes beyond uranium were produced artificially by bombardment of uranium target with either neutrons (Np) or protons (Pu). The element Americium was first identified by breeding it from Pu in a reactor. The beam of He ions was used for synthesis of elements up to Mendelevium, whereas elements of Einsteinium and Fermium were first identified in radioactive debris from thermonuclear explosion.

The new technique of heavy-ion reactions was developed to reach the region of elements beyond Fermium. In this case the complete fusion takes place between heavy-target element together with heavy-ion projectile from the accelerator. There are basically three possible combinations of targets and projectiles possible for complete fusion reactions, each of them having its unique pros and cons: fusion of actinide target elements irradiated with light projectile nuclei from neon up to calcium, targets of lead or bismuth irradiated with heavier projectiles from calcium to krypton, which is the combination used in the production of isotopes analyzed within this work, and finally symmetric reactions of for example two tin nuclei up to samarium plus samarium combination.

3.1 Velocity Filter SHIP

The velocity filter SHIP has been put into operation in 1976 [22] at GSI in Darmstadt, Germany. It had been designed to get a high yield of separated heavy ion induced reaction products especially from fusion reactions. During the first decade of SHIP operation three new elements with a proton numbers Z = 107, 108 and 109 were discovered [23]. Then after the upgrade and detector modernization in 1994 the elements with Z = 110, 111 and finally in 1996 the element with Z = 112 were successfully synthesized [24].

3.1.1 Beam and Target

SHIP is installed on a beam line of UNILAC (Universal Linear Accelerator). UNILAC delivers the beams of heavy ions up to 10^{13}/s particles of C to U at energies up to 20 MeV per nucleon. A new ECR (Electron Cyclotron Resonance) ion source provides a high quality beam at low consumption of material. The beam energy is variable and defined by a set of single resonators. A relative accuracy of the beam energy is ±0.003 MeV/u. The absolute energies are accurate to ±0.01 MeV/u. The beam intensities are rather high, for example, the following values could be obtained at the target: 3.0 pμA for $^{40}Ar^{8+}$, 1.2 pμA for $^{58}Fe^{8+}$ and 0.4 pμA for $^{82}Se^{12+}$ (1 pμA = 6.24 x 10^{12} particles/s) [24].

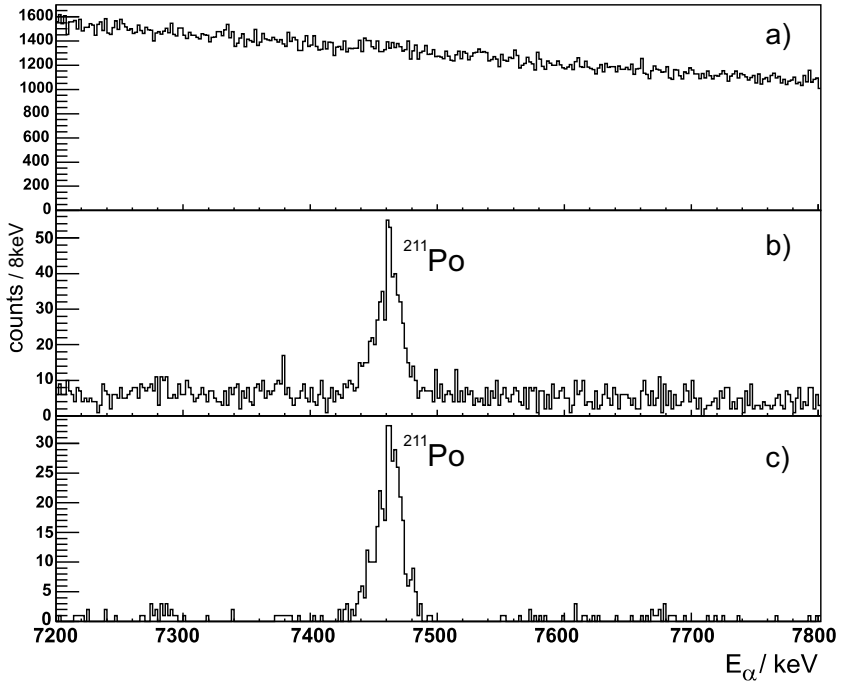

Figure 3.1: Comparison of various low energy spectra from reaction $^{58}Fe+^{208}Pb$ showing the region of transfer product ^{211}Po: **a)** All events from nuclei registered in Si-detector after they exit from SHIP plus their decays. **b)** Events in anticoincidence with TOF system which reduces the background by factor better than 100. **c)** Events that occurred in beam pause, mainly α-decays.

SHIP experiments use a pulsed beam from UNILAC accelerator with frequency of 50 Hz and duty cycle of 27.5% (5.5 ms pulse, 14.5 ms pause). The disadvantage of a pulsed beam is that it poses higher thermal stress on the target than the continuous beam, since higher intensities during the pulse are needed to obtain the same average beam current. This is of a special importance for low melting point materials such as Pb and Bi used widely in cold fusion reactions. Therefore a rotating target wheel was developed which moves eight target segments across the

beam axis synchronously to the accelerator pulsing with a step motor. Each target is irradiated at intervals of 160 ms. On the other hand the pulsed beam creates a possibility to obtain almost clear α-spectra (without the scattered projectile background) when only the signals coincident to beam pause are taken (see Fig. 3.1).

3.1.2 Separator

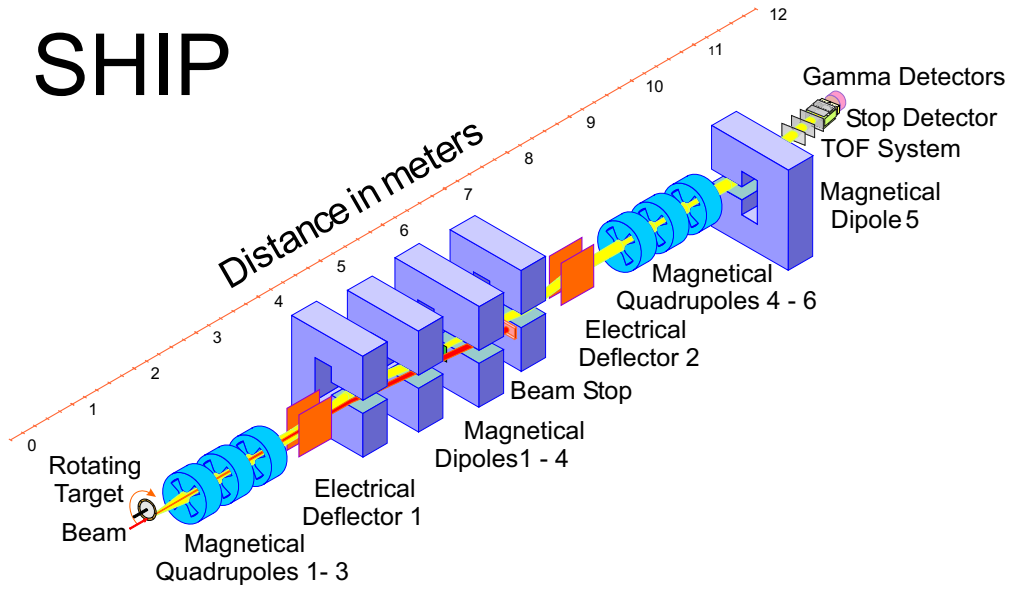

Figure 3.2: Schematic drawing of SHIP together with the detection system at it's end. It is constructed as a two stage velocity filter with spatially separated electric and magnetic fields. At the tail additional 7.5° deflection magnet is placed behind the second quadrupole triplet providing supplementary reduction of high energy background by a factor of 10 - 50.

The velocity filter separates the evaporation residues recoiling from a thin foil target in-flight from the primary beam taking advantage of their kinetic properties. The law of momentum conservation gives us fusion product with the velocity v:

$$v = \frac{v_{\mathrm{p}} A_{\mathrm{p}}}{A_{\mathrm{p}} + A_{\mathrm{t}}}, \tag{3.1}$$

where v_{p} is projectile's velocity and A_{p} and A_{t} are the masses of projectile and target, respectively. The separation time is determined by the flight time through the filter and is of the order of $10^{-6}s$.

The separation properties of SHIP can be most efficiently utilized by reactions of the type:

- Light to medium heavy projectile + Pb or Bi target $\rightarrow$ Compound nucleus

This is given by the angle between the beams of evaporation residues and projectiles following the relation:

$$\frac{v_\mathrm{p} - v}{v} = \frac{A_\mathrm{t}}{A_\mathrm{p}}, \tag{3.2}$$

which means that for light projectiles only evaporation residues pass the filter. For more symmetric reactions where $A_\mathrm{p} \approx A_\mathrm{t}$ greater amount of scattered projectiles can pass the separator and for systems where $A_\mathrm{p} > A_\mathrm{t}$ this angle given by eq. 3.2 is so small that unretarded projectiles may pass all slits [74].

As the evaporation residues recoil in beam direction, the primary accelerator beam has to be suppressed effectively. To achieve this high background suppression SHIP is constructed from two velocity filters with separated fields (see Fig. 3.2).

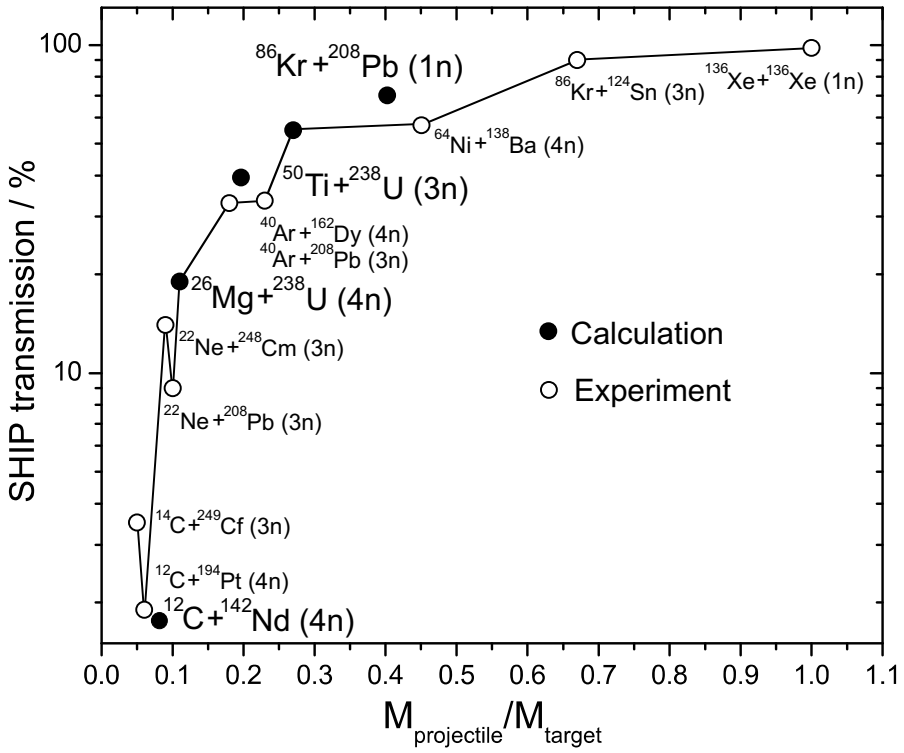

Figure 3.3: Ship transmission $\varepsilon_\mathrm{trans}$ depends heavily on the ratio of the masses of projectile and target nucleus. More symmetric reactions should result in higher $\varepsilon_\mathrm{trans}$.

At each filter consisting of one electrostatic deflector and two magnetic dipoles separation through both electric and magnetic fields happens. The first filter stage begins with quadrupole triplet that collects the recoiling fusion products and focuses them into the velocity slit in the middle of the separator, where the reaction products are separated from the primary beam. Second filter stage is operating in inverse-symmetric mode, i.e. the senses of deflection of all fields are alternating, and ends with the second quadrupole triplet that focuses the separated

recoils on the silicon detector in focal plane of the separator. The electric dipole is required to achieve sufficient resolution and to transport a wide energy over charge (E/q) distribution at the same time. The C-type magnetic dipoles have deflection angles of the same order as the electric field. The separator accepts a relative velocity width of $\pm 5\%$ and a relative charge width of $\pm 10\%$ [22]. The calculated transmission $\varepsilon_{\mathrm{trans}}$ of SHIP is shown in Fig. 3.3 superimposed over experimental points measured for various combinations of projectile - target nucleus.

3.1.3 Detectors

Detector system of SHIP consists of three large area Time-Of-Flight (TOF) detectors, each with two foils, position-sensitive silicon detector (PSSD) divided into 16 strips, backward detector (32 strips), three silicon 'veto' detectors and germanium detector. Schematic block scheme of basic SHIP detectors and the electronics is shown in Fig. 3.4

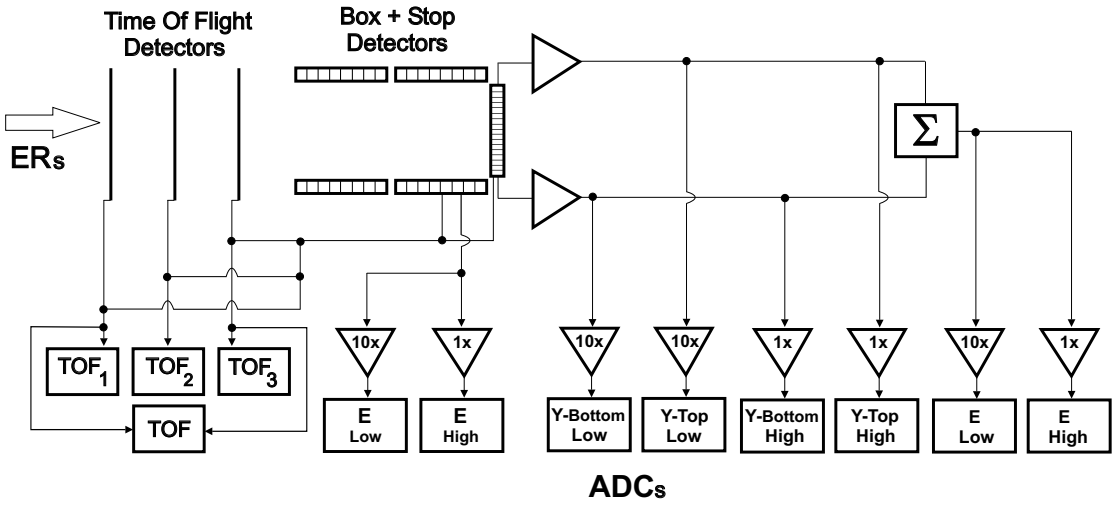

Figure 3.4: Block scheme of SHIP electronics.

Schematic drawing of a single TOF detector is presented on Fig. 3.5. Two foils made of 30 μg/cm^2 thick carbon are needed for each detector. Between the foils an electric potential of 4 kV is applied in order to accelerate electrons emitted from the first foil when a heavy ion passes through. Perpendicularly, a magnetic field is applied in order to bend the electrons onto a microchannel plate for further amplification. The foils are selfsupporting and their transmission is 100 %. Such TOF system can be used in anticoincidence with the Si-detector to distinguish between the real decays in the Si-detector (such signals would lack the coincidence signal from the TOF system) and the fake ones. For this purpose it is needed to determine the TOF detector efficiency $\varepsilon_{\mathrm{TOF}}$:

$$\varepsilon_{\mathrm{TOF}} = \frac{N_{\mathrm{E_{keV}}} - N_{\mathrm{EA_{keV}}}}{N_{\mathrm{E_{keV}}} - (N_{\mathrm{EP_{keV}}})/\bar{t}}, \quad \bar{t} = (t_{\mathrm{pause}}/t_{\mathrm{macropulse}}), \tag{3.3}$$

where $N_{\mathrm{E_{keV}}}$, $N_{\mathrm{EA_{keV}}}$ and $N_{\mathrm{EP_{keV}}}$ represent the total number of counts in low energy spectra, anticoincidence low energy spectra and pause low energy spectra, respectively and coefficient $\bar{t}$ represents the correction for the number of counts in $N_{\mathrm{EP_{keV}}}$. It can be also used to roughly estimate the mass of ion passing through the foils and being stopped in the Si-detector placed at distance l downstream the last TOF detector. From the measured time of flight t and the energy E, we can calculate the mass m, following the classical formula $E = \frac{1}{2}m(l/t)^2$. Three TOF detectors in a row are used to increase detection efficiency very close to 100 % [26].

Because of the high efficiency of each of these detectors, the background due to projectiles in the decay spectra is suppressed by a factor of a hundred to thousand as seen from Fig. 3.1b), and the time window for measuring generic parent-daughter decays is significantly prolonged. The time resolution of the foil detectors is about 700 ps.

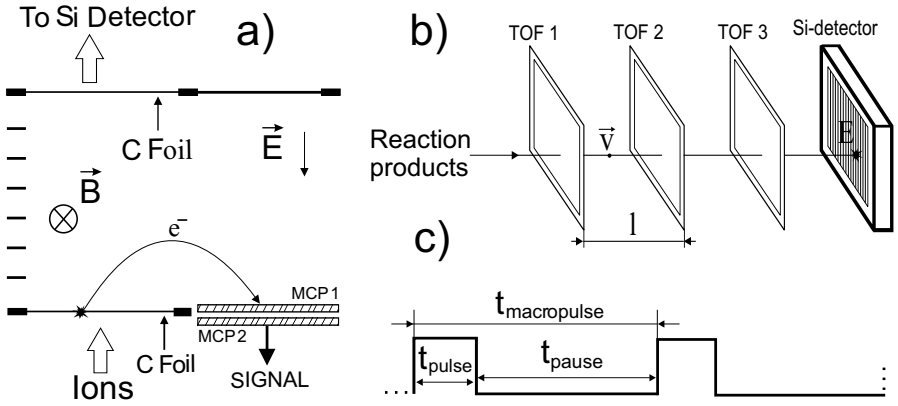

Figure 3.5: **a)** Schematic drawing of Time-Of-Flight detector working principle taken from [26]. Each detector consists of two electron emitting foils. MCP = Microchannel Plate. **b)** Position of TOF in front of the PSSD. **c)** Beam's macrostructure.

The active area of the PSSD silicon wafer is 80 × 35 mm^2. Each strip on this wafer is 5 mm wide and position sensitive in the vertical direction with a relative resolution of 150 μm (FWHM) for the α-decays. For that reason, the stop detector is equivalent to $\sim$ 3700 single detectors, each with an active area of 5 × 0.15 mm^2. The energy resolution is 14 keV for α-particles from a ^{241}Am source measured in a single strip. The resolution is worse (about 20 keV FWHM) when a summed spectrum from all stripes is generated. Figure 3.6 shows an intensity, position and energy distribution of the α-particles and also particles implanted into the detector (background) across the focal plane. The energy spectrum also contains background from scattered projectiles and β-decay.

Six similar wafers are mounted in the back hemisphere facing the stop detector. This configuration called box detector is designed to measure escaping α-particles or fission fragments with a solid angle of 80 % of 2π. In the case of the back detectors, neighboring strips are connected galvanically, forming 24 energy sensitive segments. The energy resolution obtained by summing the energy-loss signal from the stop detector and the residual energy from the box detector can be about 40 keV for α-particles in best strips. All silicon detectors are cooled to 263 K.

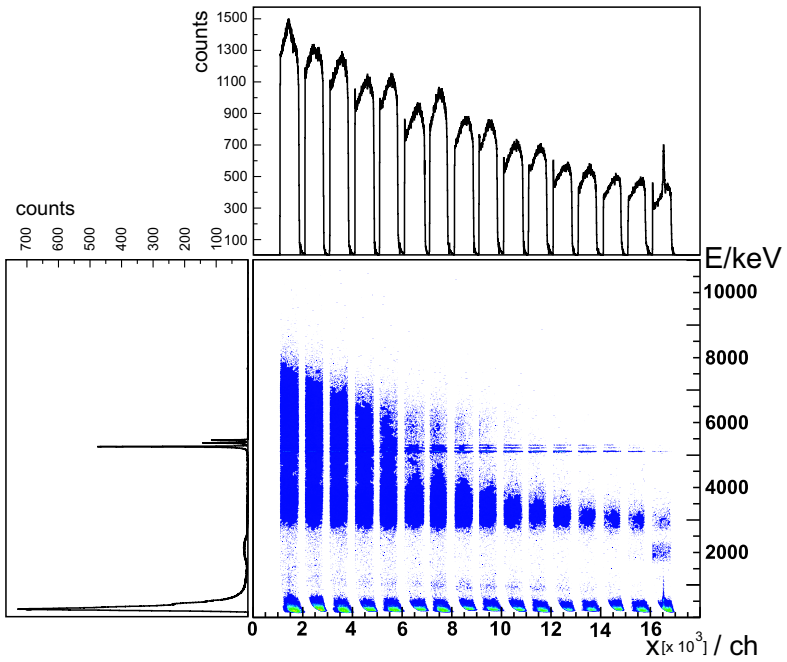

Figure 3.6: Energy over horizontal position spectrum for all 16 strips of silicon detector. Each point within the central plot represents one event. Position is defined as: (strip number $\times$ 1000 + position in the strip) and the energies are in keV. The integral distributions are plotted outside.

The term detector efficiency $\varepsilon_{\mathrm{det}}$ denotes geometrical efficiency of the silicon detector to catch the signal either from α-decay or spontaneous fission (SF). EC-decay branch can not be registered directly and we have to evaluate its contribution some other way, usually by looking for correlations with the EC-decay products. Because spontaneous fission produces two fragments flying in the opposite directions the detector efficiency for SF is very close to 100% and does not depend on the implantation depth of the evaporation residues. Different situation applies for the α-particles as shown on figure 3.7. From the typical ranges of heavy ions ($d_{\mathrm{Re}} \approx 5\mu m$ for ^{238}U) and α-particles ($d_\alpha \approx 50\mu m$ for 8 MeV) in silicon we can evaluate:

$$\frac{d_{\mathrm{Re}}}{d_\alpha} = cos\varphi \Rightarrow \varphi_\alpha = 84.3^\circ, \tag{3.4}$$

from which follows the estimation of detector efficiency for α-particles:

$$1 - \frac{2 \times 84.3^\circ}{360^\circ} = 0.53 \Rightarrow 53\%. \tag{3.5}$$

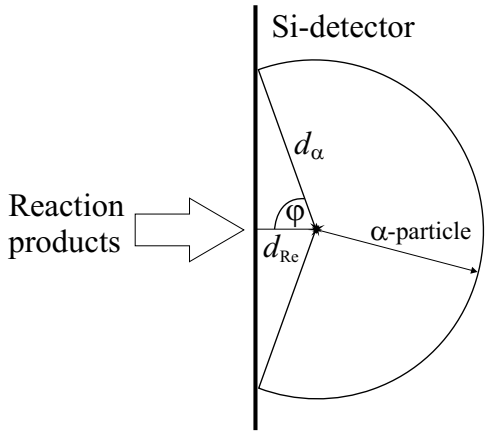

Figure 3.7: Schematic drawing of the range d_{Re} of impinging evaporation residues and d_α of α-particles in Si-detector. Example of realistic calculation of $\varepsilon_{\mathrm{det}}$ for α-decays to be registered in stop detector is shown.

Behind the stop detector another silicon detector (Veto detector) is placed. The signals from this detector are used to eliminate from the analysis the high energy light particles (mainly protons), which are not recognized by the time-of-flight system, and pass through the stop detector.

The germanium CLOVER detector consists of four crystals, measuring the X-rays or γ-rays that are coincident within a time window of 5 μs with signals from the silicon detectors. This allows for the detection of α-transitions to excited levels in the daughter nucleus, which decay by gamma emission. In coincidence with stop detector signal from high energy region, the γ- rays could be used as a confirmation of spontaneous fission signal. The probability for detecting coincident event $\alpha - \gamma$ was estimated to be about $\approx$ 14 % in the energy region of interest (100-300) keV.

3.2 Recoil-Decay Tagging Technique

For the heavier proton rich nuclei exceeding Z=70 and A=150 α-emission is becoming predominant decay mode, hence α-spectroscopy is a useful identification method. This fact combined with possibilities of velocity filter and its detection system gives us a powerful tool for investigating new isotopes and elements.

3.2.1 $\alpha - \alpha$ correlation method

So far the only method that has proved itself usable in search for very neutron deficient isotopes[1] and in investigation of their spectroscopic properties is the one of delayed $\alpha - \alpha$ coincidences. This method is based on analysis of generic decay chain starting with implantation of ER to the silicon multi-strip detector, followed by consequent series of alpha decays according to scheme:

$$\overset{\text{ER}}{\downarrow}\\ \mathsf{mother} \overset{\alpha_1}{\rightsquigarrow} \mathsf{daughter} \overset{\alpha_2}{\rightsquigarrow} \mathsf{granddaughter} \overset{\alpha_3}{\rightsquigarrow} \ldots \tag{3.6}$$

Such a process allows us to search for intrinsic correlations in specified energy and time windows for each of its members, corresponding to their expected α-decay energies and half lives. Inevitable condition for recognition of the correlation chain is the occurrence of all its members at the same position in detector strip within the spatial resolution of the detector which is around ± 0.3 mm. Such a process links the previously identified α-energies and half-lives of daughter and/or granddaughter generations to the corresponding values of unknown mother nuclei.

The method also allows the determination of branching ratios. Introducing the possibility of spontaneous fission or EC-decay of neutron deficient nuclei produces more complicated modes of decay which will be discussed in more detail in chapter 4.

3.2.2 $\alpha - \gamma$ coincidences

Due to low production cross-section information on nuclear structure in transfermium region has been restricted to depend almost entirely on the tools of α-decay measurements. Only the limited information on nuclear structure could be drawn on the basis of Nilsson levels for transfermium isotopes in connection with the hindrance factors of α-decays. Enhanced sensitivity of experimental set-ups makes it now possible to detect γ-rays and conversion electrons in coincidence with α-decay of a given recoil.

These γ-rays are emitted in cascade de-exciting the daughter nucleus to provide us an insight into the structure of the level scheme. Along with γ-rays, X-rays can be observed in coincidence to α-decays, indicating that the levels populated by this α-decay de-excite by internal conversion.

Successful decay studies by the $\alpha - \gamma$ coincidence method were recently performed at SHIP, for example on isotopes ^{253}No [35] and ^{255}No [34]. Positive results gave way to new investigation of neutron deficient isotopes of mendelevium, nobelium and lawrencium. In this work the results from [35] will be compared with $\alpha - \gamma$ coincidence measurements for indirect production of ^{253}No in section 4.1.

[1] The technique of α-α correlation is in general useful for identifying unknown isotopes. For known isotopes it is sometimes useful to distinguish them, if several isotopes have similar decay energies.

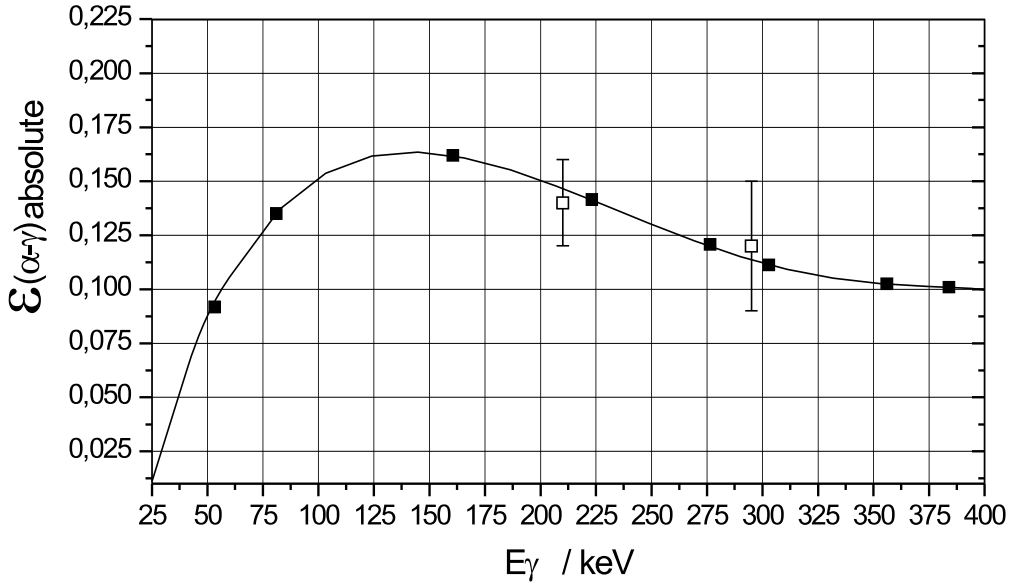

Figure 3.8: The response-function of the Clover detector for α-γ coincidences showing the absolute efficiency $\varepsilon_{\alpha-\gamma}$(geometrical + detection) as a function of the γ-transition energy. Full points represent relative measurement with ^{133}Ba source while opened points denote absolute measurement using γ-lines of ^{247}Md(210 keV) and ^{251}Md(295 keV). Relative points are fitted using the fifth grade polynomial.

3.2.3 Electron tagging technique

Recently, a new tagging method was put in operation in data analysis of experimental runs at SHIP. For the sake of identification of new isomeric states in transfermium isotopes α-γ correlation analysis method was introduced. In contrast to α-γ coincidences this procedure requires a time difference between the α-particle and the γ-quantum larger than 4μs (time defining a single event). In order to do this, γ-acquisition must run in a 'free' mode, meaning that all γ-events are being recorded, not just those accompanying other events within 4μs time window. This of course introduces a large γ-background and in many cases makes it impossible to observe true γ-events coming from the isomeric-state populated either by an preceding α-decay or a recoil implantation. Therefore an advantage was taken from the fact that the de-excitation of such isomeric levels often proceeds through the series of several levels decaying by both internal conversion and γ-decay in one prompt cascade. Internal conversion electrons coming from such a cascade are recorded in low part ($\sim$50-600 keV) of the low energy spectra. An idea came to practice to require the coincidence between these electrons and the γ-events to clear the spectra from unwanted background. Indeed, by such Re$\rightarrow$e$^-$-γ correlation analysis we were able to identify K-isomers in isotopes ^{252,254}No in experiments at SHIP.

3.2.4 Decay chain confidence analysis

It is an essential knowledge that the background suppression could never be 100%. A stochastic fluctuations of background give raise to random correlations, which could be mixed up with the real ones. In this section a mathematical apparatus is given which allows to establish the significance of mother-daughter relationship obtained from delayed coincidence measurement. Here, a method described in [36] is applied.

Suppose a chain composed of K members going in fixed order, first event E_1 followed by a second event E_2 and so on, up to the last event E_K. Each event belongs to the different interval characterized by a minimum and maximum value of energy. The probability density that stochastically an event E_i is followed by an event E_{i+1} after the time period t, is given by the random time interval distribution of events E_{i+1} times the probability of not observing an event of any other group in between:

$$\frac{dp_{i,i+1}}{dt} = \lambda_{i+1} e^{-\lambda_{i+1} t} \prod_{j \neq i+1} e^{-\lambda_j t} = \lambda_{i+1} e^{-\sum_{j=1}^{K} \lambda_j t} \tag{3.7}$$

where λ_i is the mean counting rate of the event group E_i.

The probability to observe the sequence E_i, E_{i+1} within a time interval t_i, t_{i+1} is given by integrating 3.7 from zero to $\Delta t_i, t_{i+1}$. The expected value for the number of stochastically created complete sequences n_b within the time T is given by the product of all the probabilities for the sequences E_i, E_{i+1} (with $i = 1$ to $K-1$) times the number n_1 of events of type 1 ($n_1 = \lambda_1 T$):

$$\begin{aligned} n_b &= n_1 \prod_{i=1}^{K-1} \left\{ \int_0^{\Delta t_{i,i+1}} \frac{dp_{i,i+1}}{dt} dt \right\} = \\ &= \lambda_1 T \prod_{i=1}^{K-1} \left\{ \int_0^{\Delta t_{i,i+1}} \lambda_{i+1} e^{-\sum_{j=1}^{K} \lambda_j t} dt \right\} = \\ &= T \frac{\prod_{i=1}^{K} \lambda_i}{(\sum_{i=1}^{K} \lambda_i)^{K-1}} \prod_{j=1}^{K-1} \left\{ 1 - e^{-\sum_{i=1}^{K} \lambda_i \Delta t_{j,j+1}} \right\} \end{aligned} \tag{3.8}$$

$\Delta t_i, t_{i+1}$ are maximum time limits given for the sequences E_i, E_{i+1}. If the conditions

$$\sum_{i=1}^{K} \lambda_i \Delta t_{j,j+1} \ll 1 \tag{3.9}$$

are fulfilled for all possible j values, n_b can be approximated:

$$n_b \approx T \prod_{i=1}^{K} \lambda_i \prod_{i=1}^{K-1} \Delta t_{i,i+1}. \tag{3.10}$$

Now assume that a number of n_{ex} events mentioned above was observed in the experiment. The probability[2] that a fluctuation of background produces n_{ex} or more events is given by the sum over Poisson's distribution:

$$P_{err} = \sum_{n=n_{ex}}^{\infty} \frac{{n_b}^n}{n!} e^{-n_b}. \tag{3.11}$$

If condition $n_b \ll 1$ is fulfilled, the following approximation can be made:

$$P_{err} \approx \frac{{n_b}^{n_{ex}}}{n_{ex}!}. \tag{3.12}$$

In many cases the order of the events in an event chain is not fixed, typical example of which is when the energy intervals of chain members are overlapping. In the limiting case, it is only known that the sequence starts with the leading event E_1 and all others event intervals (E_2 to E_K) are overlapping, i.e. they may appear in any order. A single condition must be fulfilled, that at least one event E_i must appear within the time limit $\Delta t_{1,t_i}$. In a consideration similar to the above one a following formula is obtained for the value of expected number of complete sequences produced randomly:

$$\begin{aligned} n_b &= \lambda_1 T \prod_{i=1}^{K-1} \left\{ \int_0^{\Delta t_{1,i+1}} \frac{dp_{1,i+1}}{dt} dt \right\} = \\ &= T \frac{\prod_{i=1}^{K} \lambda_i}{(\sum_{j=2}^{K} \lambda_1 + \lambda_j)} \prod_{i=2}^{K} \left\{ 1 - e^{(-\lambda_1 + \lambda_i)\Delta t_{1,i}} \right\} \end{aligned} \tag{3.13}$$

If the conditions $(\lambda_1 + \lambda_i)\Delta t_{1,i} \ll 1$ are fulfilled for all possible j values, the following approximation can be made:

$$n_b \approx T \prod_{i=1}^{K} \lambda_i \prod_{i=2}^{K} \Delta t_{1,i} \tag{3.14}$$

The error probability is calculated following the equations 3.11 and 3.12.

3.3 Data Acquisition

Altogether up to 42 parameters are measured for each event by the electronic system. The data are read from the CAMAC crates using a GSI developed acquisition software called Multi-Branch System (MBS) [39] running on the CAMAC

[2]This probability is equal to the error probability of a different interpretation of these events. In our case it is the origin of the $\alpha - \alpha$ chain in decay of a single mother nuclei what one should understand by different interpretation.

PowerPC processor board (CES RIO2). The data are stored in the list mode on large capacity magnetic tapes and can be simultaneously analyzed on-line. During the experiment, a continuous experiment control and an on-line data analysis are running on the VAX station under VMS operating system. Both, control and analysis, are combined in the analysis program written as a part of GSI on-line off-line analysis system (GOOSY) [40]. Similar program is used in the off-line data processing. The analysis part of the program is modified each time to match the individual settings and small experimental changes in each experimental run. These changes include for example positions of electronic modules in CAMAC crates or setting of the correlation conditions.

The calibrations and calibration reactions as well as results primarily based on the correlation analysis are described in section 4.

3.4 The Go4 analysis framework

Experimental data presented in this work were analyzed using the Go4 [41] (GSI Object Oriented On-line Off-line) Analysis Framework that is based on the ROOT [42] system of CERN. It has been designed as an on-line monitoring and off-line analysis framework with the specific requirements of the low and medium energy nuclear and atomic physics experiments.

The analysis itself can be run in remote GUI (Graphical User Interface) controlled mode or in batch mode from the command line, which is about 30 % faster. The Go4 separates analysis and GUI in two tasks which could run on different nodes within a specific computer cluster and communication is done through threads and sockets. The analysis framework provides the syntax to organize the analysis in steps which can be controlled from the GUI with each step having its own inputs, outputs and processing classes. The Go4 GUI includes a browser and tree viewer which can be used without analysis to process standard ROOT files.

The Go4 has been developed on Linux (Debian, tested on RedHat and Suse). It should be portable to other UNIX platforms supporting ROOT.

Chapter 4

Results

Experiments performed at SHIP separator in GSI Darmstadt obtain for bookkeeping purposes a nicknames in the form "R-xxx", where R stands for Run and xxx denotes the consecutive number of the experiment. Presented PhD. thesis is connected with experimental runs R-205, R-212, R-218 and R-238. Some data such as α-γ coincident matrices are also added for the increasement of the statistics from runs 210 and 226. The bulk of the discussed results deals with spectroscopic analysis of the data collected during runs R-212, R-218 and R-238 and are presented in following sections.

4.1 Isotope ^{261}Sg and its decay products

The isotope ^{261}106 was produced and studied for the first time along with ^{259}106, ^{260}106 by Münzenberg *et al.* [43] at the velocity filter SHIP using the reactions of ^{54}Cr beam on ^{207}Pb and ^{208}Pb targets. The experimental results collected at that time showed the evidence for the island of purely shell stabilized nuclei in the region of deformed transfermium isotopes. Since then four more experimental runs were performed at SHIP in quest to learn more about these isotopes, namely R-212 and R-238 dedicated to ^{261}Sg and R-228 plus R-231 focused on the search for K-isomer in ^{260}Sg [28]. This work concentrates on the analysis of first two of these runs.

4.1.1 Experiments

R-212

Isotope ^{261}Sg was produced in the experimental run 212 performed from 29.5. 2003 until 24.6. 2003 at the velocity filter SHIP at GSI, Darmstadt. The used beam of ^{54}Cr ions had intensity between 800 to 1000 pnA and was focused on ^{208}Pb target. Approximately 3.35×10^{18} projectiles were collected at the target[1]. For each target eight lead foils were mounted on the rotating wheel speed and phase of which was

[1] For more information about targets see also section 4.1.4

synchronized to the pulse's macrostructure[2]. In order to measure the excitation functions for the reactions ^{208}Pb(^{54}Cr,1n-2n)^{260,261}Sg beam energies of 4.696, 4.733, 4.771, 4.809, 4.844, 4.926, 4.997, 5.113 and 5.167 AMeV for the ^{54}Cr beam were chosen. Recoiling nuclei had an average energy of about $\approx$ 50 MeV. Effective in-flight separation of evaporation residues from unwanted transfer products and projectile-like nuclei was reached by passing through the velocity filter SHIP with estimated separation efficiency of 40 % and efficiency of TOF system $\varepsilon_{\mathrm{TOF}} =$ 99.5%. Three peaks from long living activities produced in a preceding experiment and one fast decaying transfer product were used to calibrate the stop detector, namely ^{206,208,210}Po and ^{211}Po (see the table 4.1 for energies). Resulting stop detector resolution[3] was 22.7 keV for ^{211}Po. Back detector calibration was done using the same procedure resulting in resolution of 74 keV for peak of ^{208}Po. Gamma detectors were calibrated using the γ-sources of ^{152}Eu and ^{133}Ba with resolution of FWHM = 2.3 keV for 356.02 keV line of ^{133}Ba. This calibration was periodically checked throughout the experimental run.

Isotope	^{206}Po	^{208}Po	^{210}Po	^{211}Po	^{211}At
E/keV	5223.3	5114.9	5304.4	7450.3	5869.5
$\triangle E$/keV	1.5	1.4	0.1	0.5	2.2

Table 4.1: Energies and their uncertainties for the lines used in calibration of R-212. All values are taken from [70].

R-238

This run took place at SHIP from 5.3 to 15.3. 2006 and its major focus was to investigate ^{257}Rf using indirect production via ^{261}Sg α-decay which was produced using the reaction ^{208}Pb(^{54}Cr,n)^{261}Sg. As a beam ^{54}Cr^{7+} with the energy of E_{beam}=4.77 AMeV was used and run from the ECR source with the average intensity of 650 pnA. The average energy of implanted ERs was deduced from Re-α_1-α_2 correlations to be 27.9± 3.9 MeV which is in agreement with the SRIM [44] calculation of 29.1 MeV for the fusion in the middle of the target, passage through the separator and implantation into the silicon. Two targets of standard SHIP construction were used with the compound ^{208}PbS and average thickness of 492 μg/cm^2 PbS (426 Pb) and 478 μg/cm^2 PbS (414 Pb), respectively. The targets were covered in average with 43 μg/cm^2 (upstream) and 10 μg/cm^2 (downstream) of carbon backing. In total about 2.2×10^{18} projectiles were delivered to the targets The efficiency of TOF detector system was calculated to be 98.9 %. Test reaction of ^{164}Dy(^{54}Cr,4n)^{214}Th was run before the main reaction and used for calibration of the stop and box detectors. Namely the most intensive α-lines of ^{214}Th, ^{210}Ra,

[2] 4 to 6 ms of beam was followed by 16 to 14 ms pause.

[3] All resolutions in this work are taken as FWHM (Full Width at Half Maximum) of particular peak.

^{206}Rn, ^{210}Fr and ^{214}Ac were chosen. The contribution from 5n channel products of ^{213}Th, ^{209}Ra and ^{205}Rn whose α-energies overlap with their aforementioned neighboring isotopes was taken into account by weighted average of the α-energies. The relative production intensities of these neighboring isotopes were taken from the HIVAP [45] calculations. Final resolution for the stop detector was 20 keV FWHM for 6039 keV peak of ^{209}Rn. Although there was a problem with the noise in the box detector resulting in substantial loss of positions for the box detector signals, quite good resolution was achieved with the value of FWHM = 40 keV for the same isotope. It was also possible to do a rough high energy calibration using the same peaks as for the stop detector (low energy) calibrations from the signals that were recorded in the high energy branch of acquisition system. The new four segmented CLOVER detector of smaller volume than the SUPERCLOVER used in R-212 was calibrated using standard ^{152}Eu source. Resolution of 1.3 keV and 1.6 keV was achieved for 121.8 keV and 344.3 keV peaks of ^{152}Eu, respectively. It was found that this detector had in about 10 to 20 % better resolution in 100 to 400 keV region than the old one. The gamma calibration was checked in the middle of the run and also at the end. After the main reaction ^{164}Dy(^{54}Cr,4n)^{214}Th was run again to check the stability of α-calibration. It can be concluded that all calibrations held steady throughout the whole duration of the experiment.

4.1.2 Spectroscopy of ^{261}Sg

Since the primary study of isotopes ^{259,260,261}106 and their decay properties in the early 1980s, there was no careful investigation carried out aimed at exploring the nuclear structure of ^{261}Sg. To compensate for this a little, the experiment R-212 was performed at SHIP dedicated to measurement of the excitation functions for ^{260,261}Sg and testing of compound targets, and together with R-238 enabling to investigate the nuclear structure of ^{261}Sg and its decay products. Analysis and interpretation of acquired data is presented in the following. The Re-α_1 and Re-α_1-α_2 correlations were searched for in pause for R-212 because of rather high background in anticoincidence spectrum and both in pause and pulse for R-238. Because of rather precise and well aligned box detector calibration also events found in the box were added to the analysis. For spectroscopic purposes files produced by both types of targets - metallic and PbS were considered. The correlation search was run with the various position windows to find the best ratio between encountered statistics and the background that can be estimated from the number of found double correlations[4]. Finally, the position windows for the Re-α and α-α was chosen to be 0.8 mm and 0.5 mm for the stop detector and 1.3 mm for the correlation with escaped α-particles recorded in the box. The energy and time windows for first and second generation were as follows:

[4]By double correlation we usually mean two correlation chains of the kind Re-α_1 or Re-α_1-α_2 where α_1-events are the same for both chains with different ER found (because of the countrate being much higher for ER than for αs)

Isotope	E_α / keV	$I/\%$	$T_{1/2}$/s	HF	$b_{EC}/\%$	$b_{SF}/\%$
^{261}Sg	9345	0.8±0.2	$0.21^{+0.09}_{-0.05}$	232	1.3±0.3	0.6±0.2
	9420	13.9±1.1	0.18 ± 0.01	21	-	-
	9470	26.8±1.6	0.17± 0.01	15	-	-
	9550	55.0±2.5	0.16 ± 0.006	11	-	-
	9620	3.6±0.5	$0.19^{+0.03}_{-0.02}$	325	-	-
^{261}Db	8927	∼100	$4.1^{+1.4}_{-0.8}$	5	-	73±29
^{257}Rf	8360	0.9±0.3	$5.8^{+3.1}_{-1.5}$	36	19.4±1.4	1.3±0.3
	8440	6.3±0.9	$5.9^{+0.9}_{-0.7}$	10	-	-
	8510	6.2±0.9	$5.3^{+0.8}_{-0.6}$	15	-	-
	8550^{m}	5.1±0.8	$5.5^{+1.0}_{-0.7}$	26	-	-
	$8660^{m,t}$	3.7±0.7	$5.8^{+1.2}_{-0.9}$	82	-	-
	8686	5.5±0.8	$6.0^{+1.0}_{-0.8}$	73	-	-
	8710^{m}	9.5±1.1	$5.2^{+0.6}_{-0.5}$	44	-	- -
	8755	16.2±1.5	$5.1^{+0.5}_{-0.4}$	35	-	-
	8778^{m}	39.4 ±2.5	5.6± 0.3	19	-	-
	8950	7.0±1.0	$5.2^{+0.8}_{-0.6}$	326	-	-
^{257}Lr	8615^{t}	14.2±2.6	$6.6^{+1.4}_{-1.0}$	34	-	-
	8815^{m}	57.5±6.2	5.8± 0.5	63	-	-
	8870	28.3±4.0	$6.3^{+0.9}_{-0.7}$	50	-	-
^{253}No	7.9-8.1 MeV	-	1.5±0.1 min	-	-	-
^{260}Sg	9675^{t}	8.5±2.1	$2.0^{+2.7}_{-0.7}$ ms	21	-	77 ± 9
	9715	8.6±2.4	$6.7^{+9.1}_{-2.5}$ ms	5	-	-
	9758	82.9±11.5	$3.0^{+0.7}_{-0.5}$ ms	2	-	-
^{256}Rf	8786	∼100	$5.1^{+1.0}_{-0.7}$ ms	0.7	-	97^{+2}_{-6}

Table 4.2: Summarized spectroscopic data derived from reaction ^{54}Cr(^{208}Pb,1-2n)^{260,261}Sg from both R-212 and R-238 except for ^{260}Sg and ^{256}Rf which were analyzed using the data only from R-212. The energies have systematic uncertainties ± 10 keV caused by calibration and ± 27 keV FWHM resulted from the detector resolution. Unless stated otherwise the half-lives are in seconds. Symbol ^{m} denotes the α-lines from the isomeric-state of ^{257}Rf and ^{t} marks the lines whose assignment is only tentative.

E_{α_1}: (9250-9670) keV, ΔT:(0-1400)ms
E_{α_2}: (8200-9100) keV, ΔT:(0-26000)ms

Derived spectroscopic properties of ^{260,261}Sg along with their decay products are summarized in table 4.2. The α-spectrum of ^{261}Sg can be divided into five regions corresponding to fine structure α-decay as can be seen in Fig. 4.1. The statistics from both R-212 and R-238 is taken. Although there is a slight indication for a separate peak at 9520 keV from Re-α_1-α_2 correlation search, at this quality of

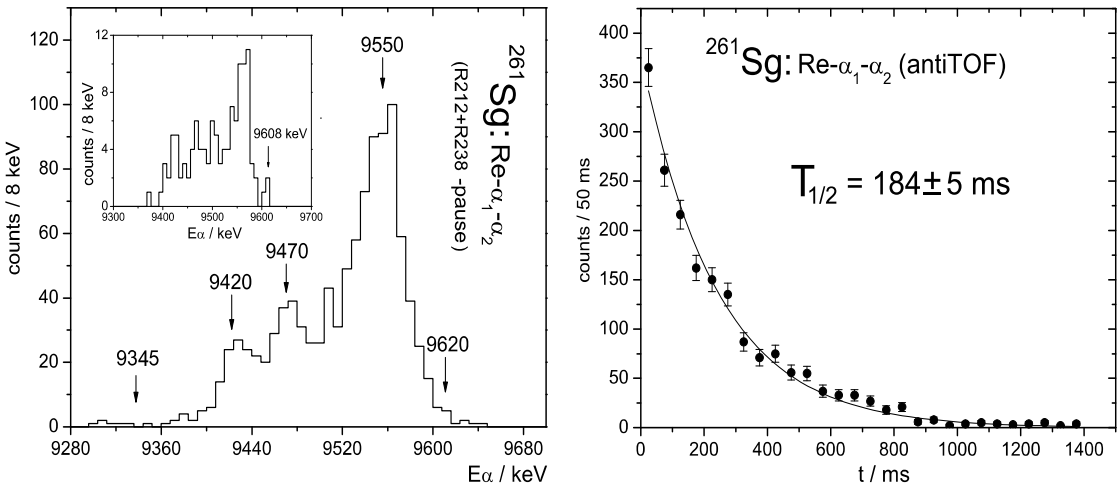

Figure 4.1: The energy region of α-decay of ^{261}Sg taken from Re-α_1-α_2 correlations from both R-212 and R-238. Embedded picture represents ^{261}Sg from Re-α_1-α_2-α_3 correlations with strict conditions (all α-events in pause, both positions [top and bottom] required with $\Delta x = 0.3$ mm) showing the ground state transition. The spectrum at the right shows the decay curve for ^{261}Sg decay times taken from these correlations.

data it does not seem reasonable to assign it to a real α-line. This shoulder on the left side of 9555 keV α-line could be due to summing of broad peak at 9470 keV with the conversion electrons causing it to appear as a hint for peak in Re-α_1-α_2 spectrum. Similar case applies for 9620 keV peak which could represent the g.s. to g.s transition. There is only a small indication for a separate peak visible in the data acquired from Re-α_1-α_2-α_3 correlation search, therefore it is consider only as a tentative α-transition.

Together with this simple assignment based solely on α-structure of the correlation and/or α-spectrum taken between the beam bursts also α-γ two dimensional coincidence matrix is considered providing more in-depth nuclear structure information. From spectra in Fig. 4.2 one clear γ-line at E$_\gamma$=107 keV is visible and two more groups of coincidences located at E $\in$ (125-160) keV and E $\in$ (15-40) keV corresponding to K and L X-rays from the isotope ^{257}Rf, respectively. This is the first reported experimental observation of X-rays from the vacancies in the atomic shell of the element as heavy as Z = 104. Their experimental energies and number of counts found for each energy group are listed in table 4.3 together with theoretically calculated relative intensities taken from [70]. It can be concluded that the K X-ray energies reported for this element agree with the measured ones within $\pm$ 0.4 keV. Considering the acquired statistics also the number of counts for these energies are in agreement with the calculated relative intensities. As the ratio $I_{K_{\alpha_1}}/I_{K_{\alpha_2}}$ = const. for given Z, the experimentally observed value of 2.2 $\pm$ 1.2 can be compared against theoretical intensity ratio of 1.5 taken from [70]. De-

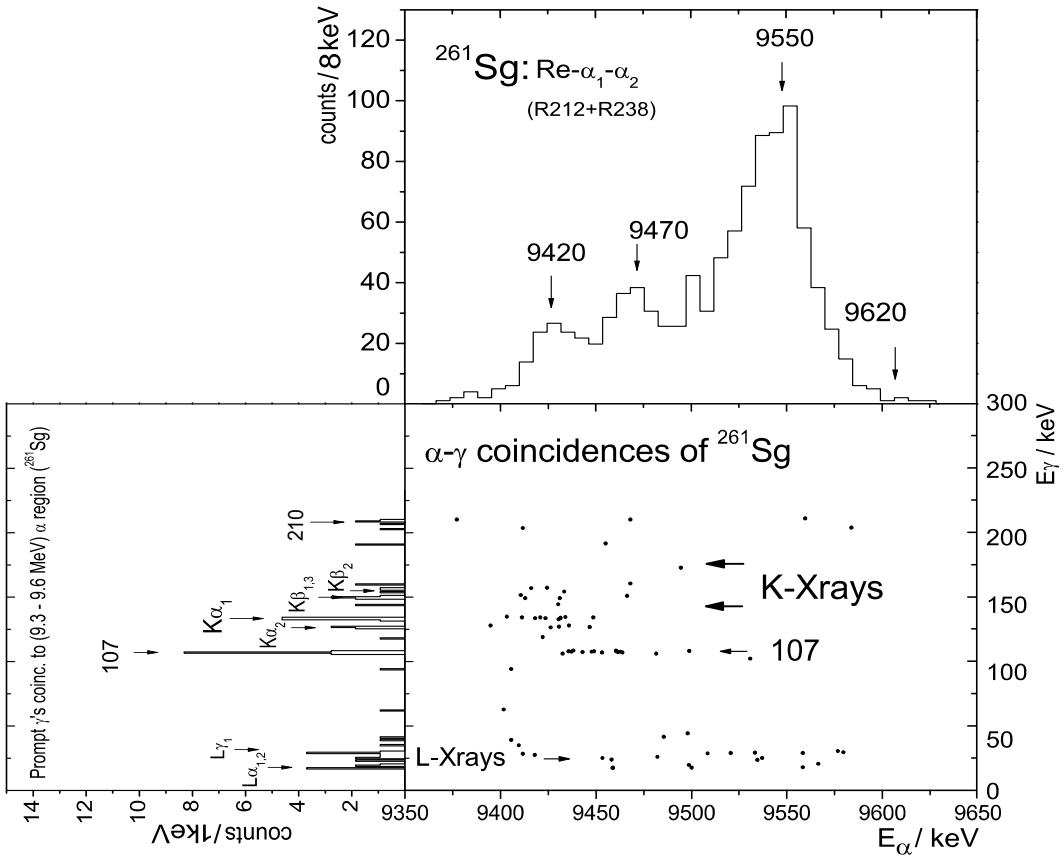

Figure 4.2: Two dimensional matrix (center) of prompt $\alpha - \gamma$ coincidences for ^{261}Sg region from both R-212 and R-238 using 4 μs time window. For the sake of lower background only pause coincidences were taken from R-212. The upper figure shows corresponding α-spectrum of ^{261}Sg taken from Re-α-α correlations. The figure on the left represents the projection of the prompt coincidences on the E_γ axis for E_α = 8.3-8.6 MeV and shows the γ-lines and conversion X-rays. In text its referred to as $2D_{E_\alpha - E_\gamma}$ plot.

spite large error of experimental result it can be concluded that theoretical value lies within 1σ interval of experimentally derived ratio. Although the CLOVER detector is not well suited to measure low energy γ-lines below some 40 keV, clear indication of L X-rays is also present. However, individual energies are not very well separable as in the case of K X-rays. This can be partly attributed to high γ-background in this energy region that might have produced some random α-γ coincidences. One more peculiarity needs to be yet pointed out. Taken the strongest L X-ray line Lα_1 with the calculated intensity of 20 % as a measure - consisting of 4 counts energetically aligned with predicted value within 0.5 keV - expected number of counts for Lγ_1 line would be less than 1. In fact eight counts that could be attributed to this line are observed. Three interpretations come to suggestion. One is already mentioned high γ-background in $E_\gamma \sim$ 0 - 50 keV region. Second

one is connected with the possible γ-transition at about 30 keV de-exciting very low-lying level in ^{257}Rf. However no further evidence for such line is found in the data. The last one exploits the fact that the exact total efficiency of the detector is unknown but steeply decreasing in this energy region (see Fig. 3.8). The observed discrepancy in the intensities of Lα_1 and Lγ_1 is about 13 which is predicted to be easily achievable in the decrease of 10 keV in the energy. This seams the most probable explanation. Finally, it can be concluded that rather broad peaks in the α-spectrum of 4.1 as well as the observation of X-rays suggest the strong influence of internal conversion in decay of ^{261}Sg.

Isotope		^{261}**Sg**		^{257}**Rf**	
X-ray	$i_{\text{theo.}}$ / %	$E_{\text{theo.}}$/ keV	$N_{\text{exp.}}$	$E_{\text{theo.}}$/ keV	$N_{\text{exp.}}$
Kα_1	44	133.4	11	127.4	26
Kα_2	29	126.3	5	121.0	41
Kβ_1	11	150.3	4	143.5	7
Kβ_2	4	154.5	1	147.5	2
Kβ_3	6	148.6	1	142.0	-
KO$_{2,3}$	1	155.9	1	148.9	-
Lα_1	20	17.9	4	17.1	2
Lα_2	2	17.6	-	16.8	1
Lβ_1	12	24.7	1	23.2	4
L$\beta_{2,15}$	6	21.7	-	20.7	1
Lγ_1	3	28.8	8	27.1	3

Table 4.3: The summary of K and L X-rays coming from isotope ^{257}Rf (in coincidence with α-decay of ^{261}Sg [left column]) and ^{253}No (in coincidence with α-decay of ^{257}Rf [right column]) taken in R-212 and R-238. Listed for comparison are those theoretical X-rays whose intensities are more then 1% except for L$_I$ for which no candidate was found in the data. Intensities i are common for both isotopes as they differ less than 1% for isotopes with ΔZ=2. Quantity N_{exp} denotes the number of found events in the data within $\pm$ 0.8 keV for particular energy. For ^{261}Sg only prompt $\alpha - \gamma$ coincidences are taken while for ^{257}Rf both prompt and delayed (Re-α_1-α_2-γ(Δt=110μs)) are added together.

Table 4.4 summarizes what was derived from the analysis concerning the $\alpha-\gamma$ coincidences leading towards the assignment of the decay scheme for ^{261}Sg. Namely, the γ-lines anticipated either from the simple α-energy difference or from α-γ coincidences and those actually found in Re-α_1 and/or Re-α_1-$\alpha_2(\gamma)$ correlations. Altogether 13 prompt coincidences of 107 keV γ-line with ^{261}Sg α-decays were found in R212 and R-238. It was also searched for γ-γ and/or γ-X-rays coincidences but there was no clear indication for γ-γ and/or γ-X-ray coincidences found for the γ-energy region 0 - 400 keV gated with coincident ^{261}Sg α-energy region 9250 - 9650 keV and gated on γ-energy 107 $\pm$ 2 keV. This is in line with the expectations based on acquired statistics of γ-events and estimated efficiency for γ-like event detection of $\varepsilon_{\rm tot} \sim 15\%$ in the energy range of interest 90 - 400 keV. For this reason it was not possible to assign any γ-γ and/or γ-X-ray cascade deexciting the nucleus ^{257}Rf being populated by α-decay of ^{261}Sg. There seems to be a good agreement between the energies of the observed levels and those predicted by Ćwiok *et al* [37]. in the isotope ^{261}Sg. Following discussion presents an overview of information derived from the data for individual α-lines of ^{261}Sg:

Isotope	E_γ / keV	$E_\alpha^{\rm coinc.}$ / keV	$T_{1/2}$ / μs	$N_{\alpha-\gamma}$	$N_{{\rm Re}-\alpha_1-\alpha_2(\gamma)}$	
^{261}Sg	107.3	9450	$\diamondsuit$	15	8	M1
	210*	-	-	3	0	-
	157*	-	-	2	0	-
^{257}Rf	90.7	9685	$\diamondsuit$	14	7	M1
	96.2*	8730	28^{+38}_{-10}	4	3	M2
	110.5*		$\diamondsuit$	6	3	-
	167.1	8780	22^{+30}_{-8}	10	5	M2
	283.4	8495	$\diamondsuit$	13	6	E1

Table 4.4: Summary of new γ-transitions observed in R-212 and R238 for ^{261}Sg and ^{257}Rf (see next section 4.1.3 for details). Lines * have only a tentative origin. Half-lives $\diamondsuit$ can not be determined, as these quanta are recorded within a single event and regarded as prompt with $\tau < 4\mu s$.

- **line 9345 keV:** The sign for the α-line at this energy was present in both R-212 and R-238. Broad width of about 70 keV suggests strong influence of internal conversion, although a double peak is also possible at present statistics. The decay from a higher levels of the rotational band can probably be excluded due to quite high hindrance factor of potential band-head (see table 4.2) of the potential band-head. Altogether 18 α decays for the energy interval E$\alpha \in$ 9280 - 9380 keV were observed. Two of these events were accompanied by K_{α_1}(K-L_3) and two by K_{β_1}(K-M_3) X-rays from ^{257}Rf in prompt coincidences. This is in line with the total of 3 expected coincidences for 18 counts considering maximum detector efficiency of $\varepsilon \sim 15\%$ for the

nobelium K X-ray energy region. No further indication for γ-line accompanying the α-decay of this energy was observed suggesting a highly converted transition.

- **line 9420 keV:** It can be seen from Fig. 4.2 that the main concentration of rutherfordium K X-rays is situated over the region assigned to 9420 keV α-line. The range of α-particles coincident to K_{α_1} X-rays is prolonged to about 9450 keV, but there are also a few K_{β_1} X-ray counts situated over 9466 keV α-region. This indicates that the transition of 9550 keV does not represent the g.s. to g.s. decay α-transition, because the total transition energy ΔE must be somewhat higher than the sum of K-shell binding energy for element Z = 104 which is 156.3 keV [70] and the α-energy, leaving the difference E_{e^-} = ΔE - $E^K_{bind.}$ to the free electron. This settles the g.s. to g.s. decay of ^{261}Sg to be situated not lower that 9600 to 9620 keV. It also indicates that the level populated by 9420 keV α-transition should decay to the level situated below the one populated by 9550 keV α-decays because difference 9550 - 9420 < $E^K_{bind.}$. There were 2 events with E_γ = 157 keV found coincident to 9420 $\pm$ 5 keV that could not be attributed to originate from ^{257}Rf K X-rays and thus might indicate a γ-transition. Additionally in γ-projection spectrum in Fig. 4.2 the clear indication of a γ-transition with $_\gamma$ = 210 keV can be seen. The coincident α-decays though have such a broad range that the assignment is not possible. Therefore these γ-transitions at present statistics remain only as speculations.

- **line 9470 keV:** It is evident from $2D_{E_\alpha - E_\gamma}$ plot that the α-peak at this energy is shifted to about 20 keV higher value than the location of α-decays coincident to 107 keV γ-line that appear at about 9450 keV. This effect is known as due to energy summing between conversion electrons and α-particles. If the sum E_α + E_γ (9450 + 107 keV) of coincident α-γ decays is considered than this would point to a decay into the level populated directly by 9550 keV α-transition. In total 15 events (see table 4.4) with the average energy of E_γ = 107.3 keV were found in Re-α_1-γ and 8 for Re-α_1-γ-α_2 correlations, respectively. Considering the level separation energy of 107 keV it is not possible for the associated nuclear level to undergo an internal conversion on the K-shell and only L-conversion takes place. This scenario is supported by observation of a few X-ray-events, namely $L_{\alpha_1}(L_3\text{-}M_5)$ = 17.9 keV and $L_{\alpha_2}(L_3\text{-}M_4)$ = 17.6 keV in this energy range that are coincident to 9420-9470 keV α-region. The calculated L-conversion coefficient for 107 keV γ-line is λ_L=3.0 $\pm$ 2.1. This number is closest to 9.9 value of total ICC on L subshell calculated for M1 transition of 107 keV in element Z = 104 [61] but also a mixing of E2 component is possible. Two events with Eγ = 107 keV from $2D_{E_\alpha - E_\gamma}$ plot are clearly separated from the main γ-group located over 9450 keV coincident α-range and corresponding α-decays are shifted

to about 30 keV higher energies. This could be an indication of a decay sequence $\gamma_{[107]}$-IC taking place in the ^{257}Rf daughter. Yet, another interpretation should be mentioned. If 107 keV γ-line is in fact M1 on the basis of 15 counts, than one can expect about $15\times\alpha_{\mathrm{L}}^{\mathrm{tot}}$ / $\varepsilon_{\mathrm{det}} \sim$ 1100 α-decays in total, populating such a level. If the transition energy of E = 107 keV is considered, binding energy on L-shel around $\mathrm{E_{bind}}$ = 30 keV and the average X-ray energy $\mathrm{E_x}$ = 17 keV, than the energy shift due to the conversion electron summing can be estimated as $\Delta\mathrm{E} \sim (\mathrm{E\text{-}E_{bind}}) + (\mathrm{E_{bind}\text{-}E_x}) = 83$ keV. Taking into account the recoil implantation depth of about 7 μm with electrons of such energy having about 40 μm range in Si, some 2/3 of them can be fully stopped. This would create a large 'peak' at 9470 keV + 80 keV $\sim$ 9550 keV.

- **line 9550 keV:** By approximately a factor of two broader width of this line than the detector resolution indicates that it is also influenced by summing from conversion electrons. In fact as can be seen from $2\mathrm{D}_{E_\alpha - E_\gamma}$ plot the most significant quantity of L X-rays is coincident to this energy region. By considering the unobserved γ-line deexciting this level that would exceed at least 3 times the background value, an lower limit on ICC on L shell of is $\alpha_{\mathrm{L}} \geq 2$ could be derived. Despite quite high uncertainty this value fits best to the transition of multipolarity M1 with $\alpha_{\mathrm{L}}^{\mathrm{tot}} \sim 90$, but also E2 is equally competing candidate with $\alpha_{\mathrm{L}}^{\mathrm{tot}} \sim 700$. Due to the reasons given in previous point it is still questionable, based on the present data if this 'peak' represents a real α-transition.

- **line 9620 keV:** The hindrance factor for this α-transition, defined as the ratio $\mathrm{T}_\alpha^{\mathrm{exp}}$ / $\mathrm{T}_\alpha^{\mathrm{theo}}$ with $\mathrm{T}_\alpha^{\mathrm{exp}} = \mathrm{T}_{1/2}$ / ($\mathrm{b}_\alpha\times$ i_α), where $\mathrm{T}_{1/2}$ and b_α denote the half-life and α-branching of the isotope of interest and i_α is the intensity of the transition relative to all α-transitions. The theoretical half-lives are calculated using the formula of Poenaru [15] with the parameter modification proposed by Rurarz [16]. Described procedure resulted in value of HF $\sim$ 325 for this α-energy that should represent the g.s. $\rightarrow$ g.s. transition between ^{261}Sg and ^{257}Rf. However highly hindered, it does not seem to lie below the observable, given these experimental conditions and as derived earlier from the sum of E_α + $\mathrm{E}_{\mathrm{bind.}}^{\mathrm{K}}$ it could be located around the energy region 9600 - 9620 keV. In fact it can be seen in embedded picture in Fig. 4.1 as clearly separated α-group at $\sim$ 9608 keV which is the value almost equal to 9610 taken as the average of the aforementioned interval. The value of HF suggests according to general consideration [62] that such transition would require the change in the parity of the final and initial states. According to the Table of Isotopes [70], the level in ^{257}Rf populated by 9560 keV (9550 keV in this work) decay should be located about 100 keV above the ground-state. This value is taken from the calculated systematics of Ćwiok *et al.* [37] however the assignment of $\mathrm{J}^\pi = 7/2^+$ for ground-state of ^{257}Rf is in conflict with [37]

and agrees with predictions of [79].

Realizing these features of acquired data from the analysis the first significant attempt to construct the nuclear decay scheme of the isotope ^{261}Sg can be undertaken. The first approximative level scheme of low-lying Nilsson levels in its daughter ^{257}Rf could be drawn as shown in Fig. 4.4. In the following the arguments based on the comparison of the data for ^{261}Sg decay chain with the systematics, calculations and other experimental data leading to this assignments are presented.

Taking into account the acquired statistics of $\sim$ 1600 α-decays for the isotope ^{261}Sg during the beam pause as well as several tens of α-γ and α-X-ray coincidences it is not possible to unambiguously assign the character of the transitions and J^{π} values of single particle nuclear levels. However estimates based on the conversion coefficients, decay energies, intensities and systematics can be made. Figure 4.5 presents the theoretical calculations for single-particle levels of isotones with N = 153. The source of such theoretical calculations is rather scarce for the region of transfermium elements to compare the experimental data against, cowering the range of single-particle levels with excitation energies up to about 2 MeV. There exist also theoretical calculations of Ref. [79] also listed in Fig.4.5 but only for the ground-states spins and parities of the isotones N = 155, 153. From the experimental point of view the acquired data on the α-decay of their mothers N = 155 isotones allowed on the basis of α-decay spectroscopy to construct to certain extent low-lying nuclear levels in N = 153 isotones [70]. The resulting level schemes of the isotopes ranging from ^{249}Cm to ^{255}No are shown in Fig. 4.3.

It needs to be pointed out that the most precise data exists for the nuclear level scheme of ^{251}Cf. They were taken from β^{+} and EC decay spectroscopy of ^{259}No and ^{255}Md respectively and β^{-} decay spectroscopy of ^{255}Es [64]. Every single-particle level shown in Fig. 4.3 represents a band-head of the rotational band (band members are not drawn for the sake of clarity) determined up to 3 to 5 levels within the band. It is a clear evidence for the deformation as theoretical calculations [79] predict for this region of nuclei. There is a severe information decrease when moving to next heavier N = 153 isotones of ^{253}Fm and ^{255}No.

In the process of assigning the J^{π} to individual levels in ^{257}Rf and also for the g.s. of ^{261}Sg, the general trend for N = 153 and N = 155 isotones taken from experimental data and the predictions of [37] were taken into account. The anchor point in this assignment is provided by the level scheme of ^{251}Cf as well as recently published data on decay of ^{257}No [65]. Direct comparison of Figs. 4.5 and 4.3 reveals that experimental data reproduce quite well the trend in decrease of $3/2^{+}$ level and increase of $7/2^{+}$ level moving to heavier N = 153 isotones. Although the experimental energies for $3/2^{+}$ sequence are lower and for $7/2^{+}$ sequence higher then than those predicted by calculations. The theory also predicts the existence of $11/2^{-}$ orbital steeply decreasing in the energy from light to heavy N = 153 isotones. The energy of E* $\sim$ 370 keV for single experimentally confirmed $11/2^{-}$ level in ^{251}Cf is in perfect agreement with the calculations.

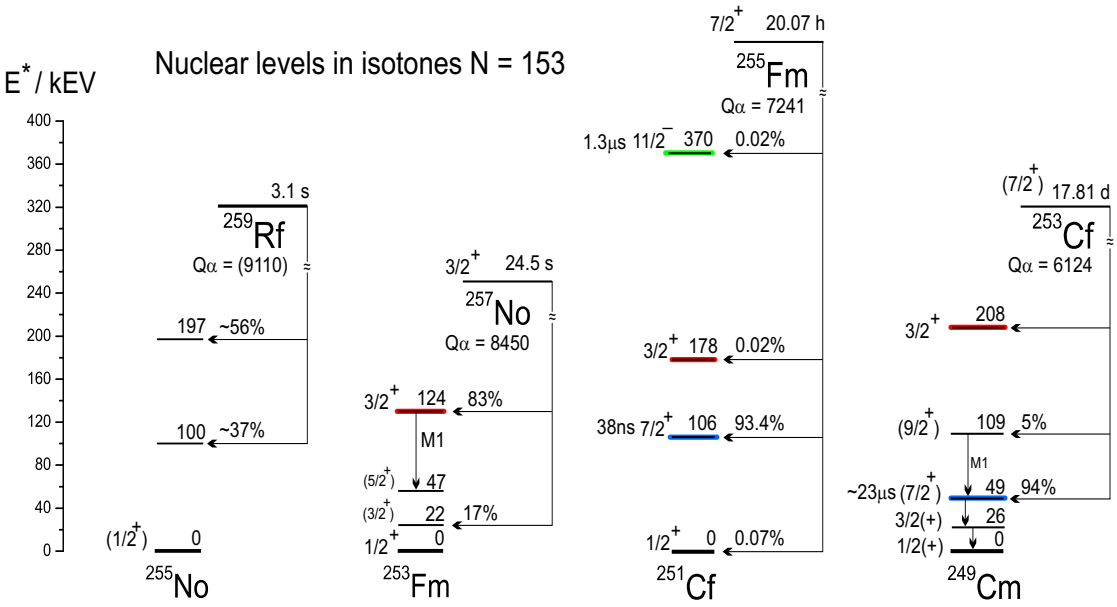

Figure 4.3: Experimental results on nuclear levels in isotones with N = 153 populated by α-decay of their mothers - isotones with N = 155. Data were taken from [70] and improved data for ^{257}No$\rightarrow^{253}$Fm were taken from recently published experimental results of Ref. [65] The levels significant to the discussion are depicted in color.

Another strongly enhanced and obvious feature of the experimental data is the observation of α-decay with the highest intensity populating the higher lying single-neutron orbital rather than the ground-state with one variation. On the basis of data from [65] the ground-state of ^{257}No was attributed to $3/2^+$ configuration which is different from $7/2^+$ for the lighter N = 155 isotones, ^{253}Cf and ^{255}Fm. For the last two mentioned isotopes the majority (more than 90%) of the α-decays proceeded via $7/2^+ \rightarrow 7/2^+$ transition while in ^{257}No this pattern has already changed. The change of the ground-state configuration in mothers N = 155 isotones starting from ^{257}No can be explained by the crossing of downsloping $3/2^+$ orbital and upsloping $7/2^+$ orbital. This crossing takes place in the daughter ^{253}Fm N = 153 isotone as suggested by the experimental data rather than in ^{249}Cm as predicted by the theory. Unfortunately the data for ^{255}No - closest N = 153 isotone to ^{257}Rf - are rather scarce with no J^π assignment for the single-particle levels and no γ-transitions yet known [70] in the de-excitation of ^{255}No after being populated by α-decay from its mothers. Also no g.s. to g.s. transition is observed and therefore the assignment of the level excitation energies is not unambiguous. After R-212 the $J^\pi = 7/2^+$ was tentatively assigned to the level in ^{257}Rf populated by the most intensive α-decay from ^{261}Sg and also to its ground-state in accordance with experimental systematics for lighter N =153 isotones. This level was also attributed an isomeric character based on predicted strongly hindered transition

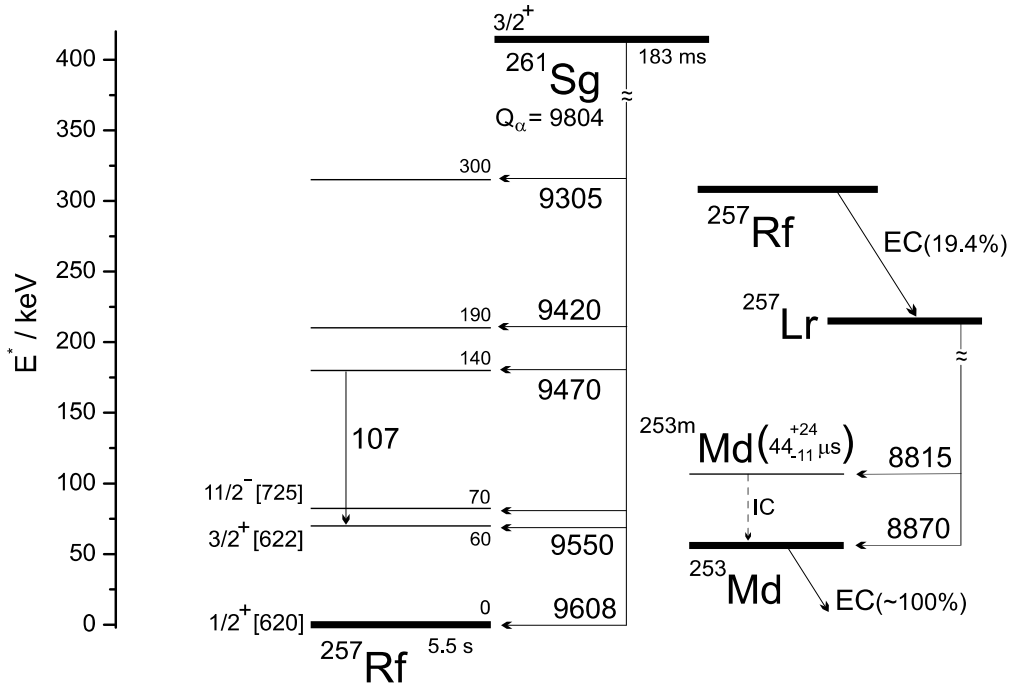

Figure 4.4: The first nuclear decay scheme of the isotope ^{261}Sg and low-lying Nilsson levels in ^{257}Rf constructed on the basis of two experiments (R-212, R-238) performed at velocity filter SHIP.

to $1/2^+$ ground-state and indication of enhancement of coincident rutherfordium L X-rays to 9550 keV α-decay when longer TAC value was used in coincidence search. This assumption however was not confirmed in R-238. Another difficulty with such assumption is connected with the observation of an isomeric-state present in the nucleus ^{257}Rf assigned as $11/2^-$ [48]. This finding is inline with the theoretical predictions of steeply decreasing $11/2^-$ level towards the heavier N = 153 isotones. On the other hand it was found to be located $\sim$ 70 keV above the ground-state from the difference of α-energies 9020 keV (^{257m}Rf - ^{253g}No) and 8950 keV (^{257g}Rf - ^{253g}No) derived in R-212 and R-238 (see next section 4.1.3). It is observed only in direct production of ^{257}Rf (^{50}Ti + ^{208}Pb $\rightarrow$ ^{257}Rf + 1n, ^{12}C + ^{249}Cf $\rightarrow$ ^{257}Rf + 4n) but not (or only with a very small branch) in the production via α-decay of ^{261}Sg. This scenario can hold only if $11/2^-$ is to be located below the $7/2^+$ level. Otherwise it would decay by M2 transition $11/2^- \rightarrow 7/2^+$ with a half-life of not longer than several tens of microseconds.

But the derived data indicate that the g.s. to g.s. transition in ^{261}Sg has an energy of 9608 keV. Even if one expects the 9550 keV transition to be influenced by the summing from the L conversion electrons and therefore to be shifted to higher energies the difference in energies would be close to 70 keV and therefore jeopardizing assumption about $11/2^-$ isomer. Moreover new data arose for the so far closest well studied N = 153 isotone ^{253}Fm as stated earlier that attributed the

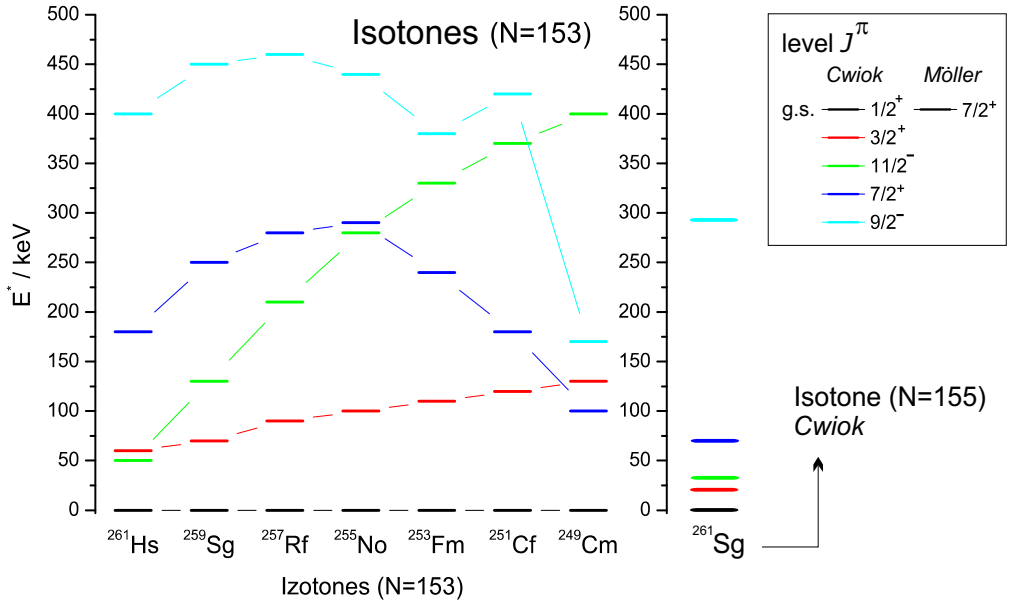

Figure 4.5: The calculated single particle nuclear levels for isotones with N = 153 taken from Ref. [37]. For the comparison also the same calculations for the levels for the mother of ^{257}Rf e.g. ^{261}Sg are shown. The grond state J^π values are also listed (same for N = 155 and N = 153 isotones) from Ref. [79].

ground-state of ^{257}No to $3/2^+$ state. Hence it is tempting to assign $3/2^+$ character also for the ground-state of ^{261}Sg and the level in ^{257}Rf situated at about 60 keV. The $11/2^-$ level could in such case still retain its isomeric character even if located above the $3/2^+$ level. This assumption yet has one drawback in predicting $J^\pi = 1/2^+$ [37] for the ground-state in ^{261}Sg that would result in the strongest intensity for the g.s. to g.s. transition which is not the case as experimental data prove in all known N = 153 isotones. Moreover these calculations predict the single-particle levels with the same J^π and their ordering for ^{261}Sg and its daughter ^{257}Rf as shown in Fig. 4.5. This would mean very similar nuclear structure for these isotopes differing by α-particle. It is quite unlikely with the experimentally observed highly hindered g.s. to g.s. transitions disproving this assumption. The $J^\pi = 7/2^+$ as derived as ground-state in ^{255}Fm is theoretically predicted as the ground-states for this isotope and also other N = 155 isotones using the model of Möller *et al.* [78]. But this prediction also suffers in serious drawback by predicting again the same value $7/2^+$ for the daughters's (N = 153 isotones) ground-states hence also the strongest g.s. to g.s. transitions. On the other hand the recent Hartree-Fock-Bogoliubov calculations with a Skyrme interaction succeeded in predicting the $3/2^+$ ground-state for ^{257}No [67], though they did not present the results for lighter N = 153 isotones. Nevertheless even Ćwiok *et al.* predict almost degenerate $3/2^+$ state situated only 0.01 to 0.02 MeV above the $1/2^-$ ground-state in all known N = 153 isotones. It is therefore quite justified to keep the assumption of

$3/2^+$ ground state starting from ^{257}No as experimental data suggest. One obstacle though still needs to be depicted. In the level scheme of ^{249}Cm the lightest N = 153 isotone there are three γ-transitions observed as seen in Fig. 4.3. One of these populates strongest α-fed $7/2^+$ level from above $9/2^+$ level by M1 transition with E2 component. In ^{253}Fm M1 transitions de-excite strongest α-fed $3/2^+$ level to either $1/2^+$ ground-state or one level in the collective band build upon the ground-state band-head. It is tempting to apply this pattern also to the case of the proposed ^{261}Sg decay scheme in Fig. 4.4. As stated earlier the only γ-transition of $E_\gamma = 107$ keV fits to be of M1 character with calculated $\alpha_L \sim 1.6$ with probable E2 component. By keeping the assignment of $3/2^+$ for the level at about 60 keV the M1 multipolarity would require for the above decaying level a spin difference of $\Delta I = 0,1$ and no change in parity. Consequently possible candidates would be either $1/2^+$, $3/2^+$ or $5/2^+$ levels. Theory though does not predict any of these level to exist in ^{257}Rf up to $E^* \sim 500$ keV. However our α_L conversion coefficient could be easily underestimated because of the low number of L-conversion X-rays observed and their not very clear identification and most importantly by unknown yet very small total detection efficiency of the CLOVER detector for this energy region. Therefore the assumption of possible E2 transition with $\alpha_L = 19.7$ for 107 keV γ-transition in rutherfordium nucleus can not be ruled out. This would allow the $3/2^+$ level to be populated from above lying $7/2^+$ level. Presented analysis would result in a sequence of levels in the nucleus ^{257}Rf:

$$1/2^+(\text{g.s.}),\quad 3/2^+,\quad 11/2^-,\quad 7/2^+$$

that is in complete agreement with the theoretical calculations [37] and also supportive for the experimental systematics of N = 153 isotones. It needs to be emphasized that this is only a tentative assignment derived on the basis of presented data. To disentangle this completely a new set of experiments would be required to unambiguously determine multipolarities of involved transitions hence only a hint for M1 character of 107 keV γ-line is given at this point. It was also sought by means of Re-$\gamma_{\text{del.}}$-α_1-α_2 correlations for the isomeric-state in mother nucleus ^{261}Sg that would de-excite by either γ-decay and/or internal conversion to the ground-state. No such indication could be found in the data of R-238 up to Re-$\gamma_{\text{del.}}$ times of 10 ms.

From the experimentally observed value of the E_α for the g.s. to g.s. transition it was possible to calculate the Q-value energy of $Q = 9804$ keV which is perfect agreement with the value of 9810 keV [70] derived from the systematics. It also agrees to the general Geiger-Nuttall trend as seen in Fig. 4.6 for the dependance of experimental Q-values on the half-lives as $\log T_\alpha = A + B/\sqrt{Q_\alpha}$ for N = 153 isotones. Although this relation is derived and generally used for even-even nuclei where isotopes with Z = *const.* form some sort of a line, parallel to other Z = *const.* lines. In presented figure the isotones with Z = 151, 153 and 155 form groups in dependance on Z. The scattered order of each group's members in Fig. 4.6 can be caused by not very precisely known α-branching ratios and g.s. to g.s. energies for these nuclei. A speculative slowing down of the decay half-lives can be

deduced from the stemming out the bottom part with isotopes of rutherfordium and seaborgium. This could indicate some structural changes happening during the decay of these isotones when crossing over Z = 104.

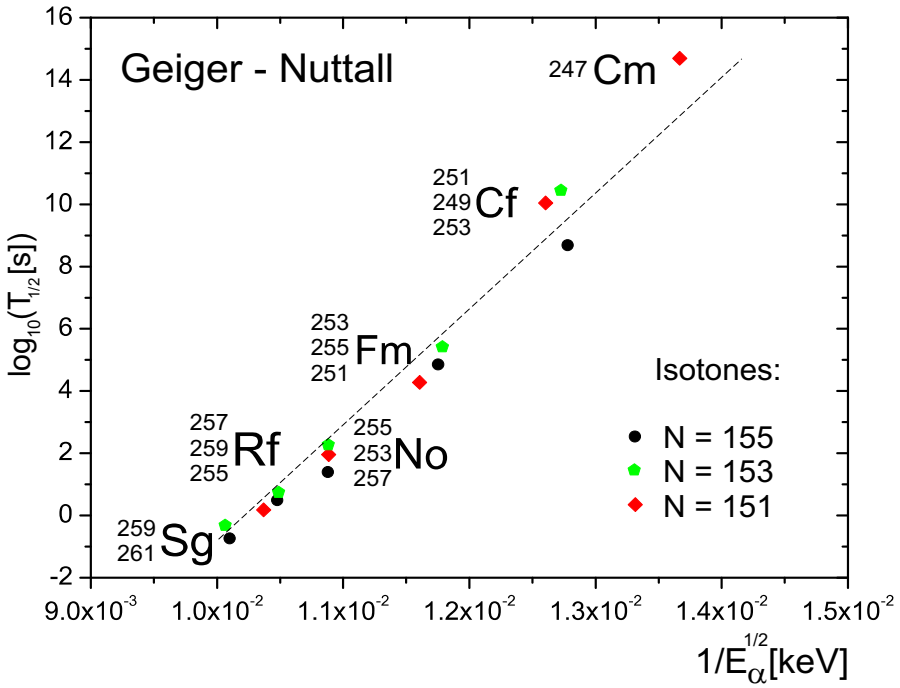

Figure 4.6: The Geiger-Nuttall like plot for isotones with N = 155, 153 and 151. The dashed line is to guide an eye.

Rather old and scarce data [32], [33] exist for ^{261}Db EC-decay product of ^{261}Sg. A careful analysis was done of possible decay through spontaneous fission and/or electron capture mode of ^{261}Sg. Two half-life components could be clearly identified in Re-SF correlations shorter one belonging to ^{261}Sg and longer to its EC-product ^{261}Db. These correlations were also compared against Re-α-SF correlations to exclude possible fault SF-events originating from the fission of ^{256,257}Rf. Also correlation search of the kind Re-$\alpha_1^{^{261}Db}$-$\alpha_2^{^{257}Lr}$ was performed to identify ^{261}Db through its α-branch. In total 11 SF-events and 4 α-events were found from both experiments that could be attributed to ^{261}Db resulting in EC-branch of b_{EC} = 1.3±0.3 % for ^{261}Sg and SF-branch of 73±29% for ^{261}Db. Ten SF-events were also assigned to come from ^{261}Sg with the SF-branch of b_{SF} = 0.6±0.2 %. The mean energy of ^{261}Db α-decays is 8927 keV in perfect agreements with previously measured value. The half-life on the other hand is $4.1^{+1.4}_{-0.8}$ s which is even with the inseparable contribution from the EC-decaying mother ^{261}Sg about a factor of two longer than results from [32] and [33].

The isotope ^{260}Sg was analyzed using only the data from R-212 where it was produced in order to measure 2n channel excitation function of ^{54}Cr + ^{208}Pb reaction. In total 120 events of the kind Re-SF and 35 events of Re-α_1-SF that

could be attributed to the decay of this isotope were observed. The data are summarized in table 4.2. In general a good agreement is observed with previously measured values of [43]. New α-line appears at the energy 9675 keV, but since two of three events for this line are in box its assignment is only tentative. For the other two lines the energies, half-lives and intensities are in line with previously published values. The half-life of $4.6^{+0.5}_{-0.4}$ ms derived from Re-SF correlations is also in perfect agreement. Concerning spontaneous fission branching a rather higher value of b_{SF}=76 ± 21 % was calculated, but the statistics acquired in R-212 for ^{260}Sg is about a factor of two higher than in [43] therefore present value is more reliable. Only one α-decay of ^{256}Rf was observed in correlation Re-$\alpha_1^{^{260}Sg}$(9749 keV, 3 ms)-$\alpha_2^{^{256}Rf}$(8786 keV, 10 ms) that is in perfect agreement with previously measured data. This leads to $b_{\mathrm{SF}} = 97^{+2}_{-6}$ % that also confirms previous results. The lowest hindrance factor in table 4.2 suggests the transition between like levels in ^{256}Rf and ^{252}No. Much more detail analysis of this isotope has been recently carried out at SHIP in R-228 to investigate potential existence of K-isomer in its decay. Complete analysis will be presented in [28].

4.1.3 Spectroscopy of ^{257}Rf

The first identification of the isotope ^{257}Rf and consequent study of single-particle levels in its daughter ^{253}No was performed by Ghiorso *et al.* [50] using the asymmetric reaction ^{12}C + ^{249}Cf. Later it was unambiguously assigned to element 104 by X-ray coincident measurement by Bemis *et al.* [51] using the same reaction. This also revealed an isomeric-state in the daughter nucleus ^{253}No with 31.3±4.1 μs half life. It was again produced in two separate experiments at SHIP by bombardment of ^{208}Pb with ^{50}Ti [52] as well as in indirect production [48] using the reaction ^{208}Pb(^{58}Fe,n)^{265}Hs$\rightarrow_{\alpha}^{261}Sg\rightarrow_{\alpha}^{257}$Rf. Although these experiments did not utilize the measurement of γ-rays and/or X-rays, they revealed a complex α-spectrum in the wide region E_α = (8.2-9.1) MeV influenced by IC-summing and also contribution from its EC-product ^{257}Lr. By comparing the structure of the α-spectra it was shown by F.P.Heßberger *et al.*, [48] that two high energy α-decays of approximately 8.97 and 9.02 MeV were completely missing in indirect production and identified as decays of the isomeric-state in ^{257}Rf. Exclusion of these two α-lines revealed expected similarities in decay patterns with its neighboring isotones ^{253}Fm and ^{255}No. Based on this the J^π of the isomer was proposed to be $5/2^+[622]$. The discrepancy however exists about the location of the aforementioned isomeric-state in ^{253}No. At first Bemis *et al.* assigned it to be located at 296 keV above the ground-state. This was derived from the energy difference of α-transitions attributed to decays in the ground-state of ^{253}No and the isomeric-state, respectively. Later it was corrected on the basis of results from SHIP [48], which proved the two α-lines at 8.97 and 9.02 MeV as decays from an isomeric-state ^{257m}Rf and the isomer $5/2^+[622]$ in ^{253}No was settled at 112 keV on the basis of the energy difference of α-transitions attributed to the decay into this level and the α-particles of highest energy (8903 keV) attributed to the decay of ^{257g}Rf. The problem aroused that

this is clearly below the K-binding energy of nobelium and therefore disagrees with the observation of delayed X-rays from ^{253}No in coincidence with the α-lines populating $5/2^+[622]$ level. This discrepancy needed to be clarified in yet another experiments whose analysis is presented here.

Further study of this isotope is a part of a long-time project carried out at SHIP aimed at investigation of nuclear levels systematics. Recent results include the study of ^{255}No [A9)] - member of N = 153 isotonic chain and analysis of ^{255}Rf$\rightarrow^{251}$No [55] [57] [A8)] - isotones with N = 151 and 149. Results presented here on isotope ^{257}Rf combine data from two different experimental runs R-212 and R-238 at SHIP both utilizing indirect production via the reaction ^{208}Pb(^{54}Cr,n)^{261}Sg$\rightarrow^{257}_{\alpha}$Rf. It was preferred over the reaction ^{208}Pb(^{50}Ti,n)^{257}Rf inspire of its about a factor of 6 to 7 higher cross section by two reasons. Firstly, the beam of ^{50}Ti can be presently run at UNILAC accelerator only from the penning source with the consumption of material about 1g/day giving the beam intensity only $\approx$ 300 pnA. On the other hand ECR source can deliver the beam of ^{54}Cr as high as 1pμA with low material consumption. Taken the the ratio $\sigma(^{257g}\mathrm{Rf})/\sigma(^{257m}\mathrm{Rf}) \approx 0.6$ observed in direct production of ^{257}Rf with $\sigma(^{257}\mathrm{Rf}) \approx$ 14 nb and the cross-section for ^{261}Sg production of $\sigma(^{261}\mathrm{Sg}) \approx 2$ nb, this means that lower cross section is just compensated with the higher beam. But the most importantly this reaction was chosen to suppress the production of ^{257m}Rf whose two most intensive lines of 8.97 and 9.02 MeV completely cover the energy range of expected ground state transition to ^{253}No.

It needs to be yet pointed out that in Ref. [70] γ-energies of 47.4, 63.2, 117.0 and 296 keV coincident to the decay of ^{257}Rf are listed. Supposedly they were derived from published work of [43] and [46] from experiments performed at SHIP. However, at that time also some γ-measurements were done, the efficiency was low at these experiments. Still couple of L X-rays were measured and one γ-event of 283 keV, but no conclusions were drawn. Therefore the source and reliability of these γ-energies is questionable with probable origin from private communications by Bemis *et al.* To stabilize the location of the ground-state transition in nucleus ^{253}No by α-decay plus to measure direct γ-transition from $5/2^+[622]$ isomer to the ground-state and clarify the situation about the γ-lines coincident to ^{257}Rf α-decays was the main goal of the experiment R-238.

As can be seen from Fig. 4.9 altogether thirteen α-peaks could be identified in the region $\mathrm{E}_\alpha \in 8.3 - 9.0$ MeV, some of them having only tentative character (see also table 4.2 for details). The total number of counts in α-spectrum 4.9 a) showing the second generation α_2 (^{257}Rf) taken from Re-α_1-α_2 correlation search is almost equal to what was collected for ^{257}Rf in its direct production in [48] (previous SHIP experiment R-166) but at that time derived only for two generation Re-α_1 correlation search. General agreement in α-line assignment exists between present work and [48] with small variations. In R-166 thick degrader foils were used in front of the detector that might have reduced EC-summing therefore causing some differences against R-238 in α-spectrum shape. The region around 8.44 MeV could not be disentangled in two separate peaks therefore only the mean value is

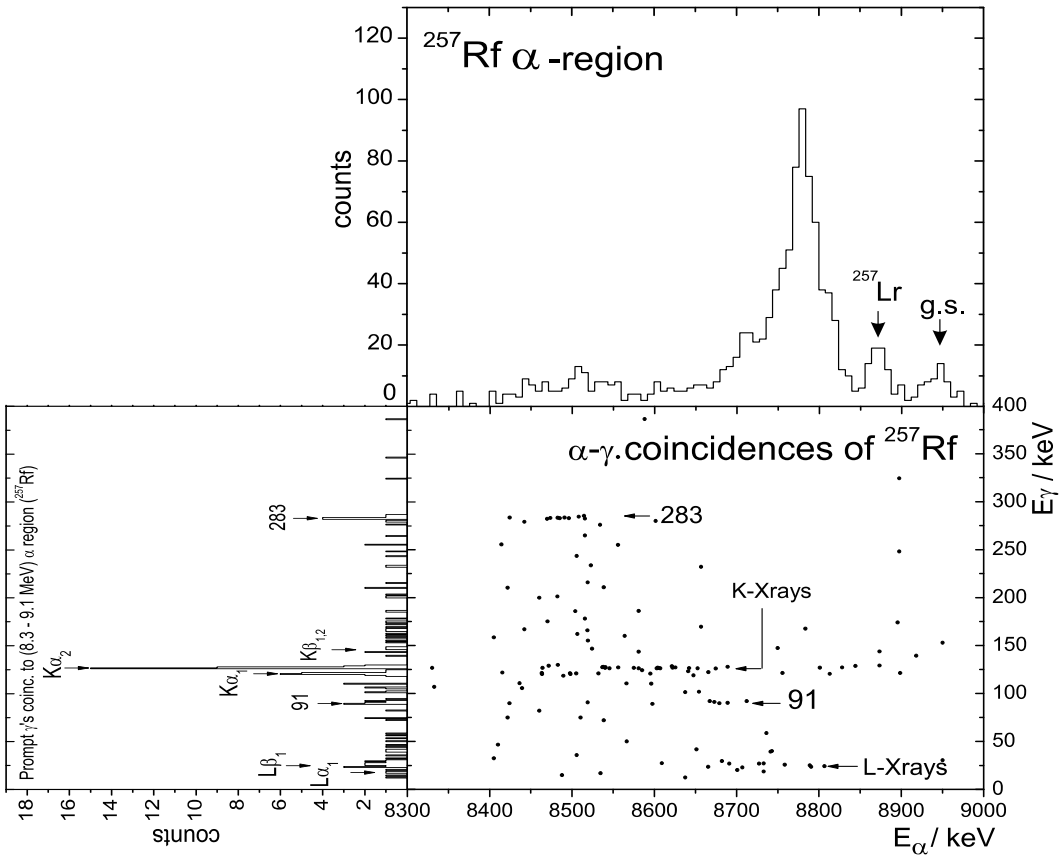

Figure 4.7: Two dimensional spectrum of α-events vs. γ-events taken from α-γ coincidences using 4 μs time window.

assigned. On the other hand in the regions of $\sim$ 8.55 MeV and 8.70 MeV fine structure appears in present data so in contrast to [48] two instead of one line are assigned. When the energy of double lines assigned to a single peak in the other experiment is averaged the general difference in α-energies is only ΔE = 5 keV which is less than systematic deviation caused by calibration uncertainties and detector resolution. The highest discrepancy ΔE = 47 keV is observed for the line corresponding to the ground-state decay. The last discrepancy concerning the α-spectrum of ^{257}Rf deals with the α-peaks around the energy 8283 kev reported with the relative intensity of $i = 4 \pm 1$ % in Ref. [48]. Although present analysis reveals an indication for α-peaks at the energies $E_\alpha \sim$ 8227 and 8257 keV in the pause α-spectrum in accordance to [59], but only one Re-α_1-α_2 correlation could be identified with the second α_2-generation from this region resulting in the upper limit for the intensity of $i \leq$ 0.1 %. This difference can not be explained by statistical fluctuation and can be viewed as another indication for the different population of ^{253}No levels in its direct and indirect production. Levels at the excitation energies of about $E^* \sim 0.7 - 0.8$ MeV are clearly observed in its direct production according to recent SHIP experiments. Based on present knowledge

this problem can not be addressed in more detail, but tentative levels at $E^* = 675$ and 725 are kept in ^{257}Rf level scheme in Fig. 4.13 with respect to the systematics as discussed later.

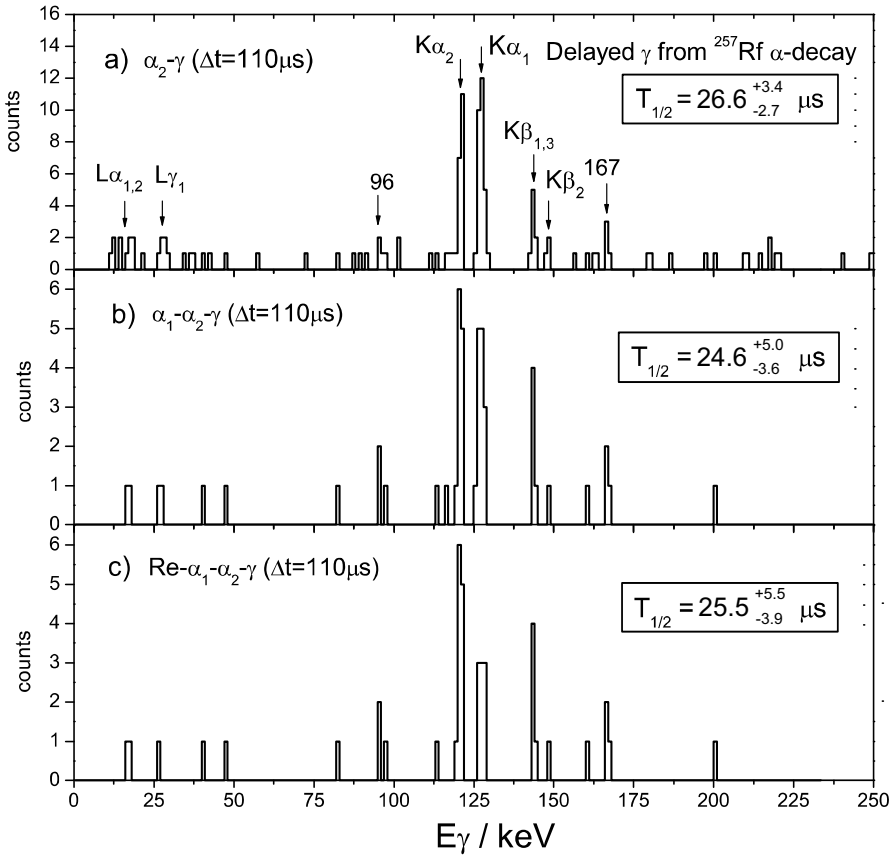

Figure 4.8: Spectra showing delayed γ-events correlated to second generation of α-decays (^{257}Rf) in the range $E_\alpha \in 8.3-9.0$ MeV from the reaction ^{208}Pb(^{54}Cr,n)^{261}Sg and for **a)** two **b)** three, and **c)** four members of correlation chain. The half-life in frames are calculated from time differences between ^{257}Rf α-decays and K X-rays taken from interval E$\in$ 118 − 150 keV.

Couple of γ-lines could be identified accompanying ^{257}Rf α-decays in prompt and/or delayed coincidences. The summary of information that could be derived from their analysis is overviewed in the following points:

- **90.7 keV**: Although a few coincidences are found for lower energy α's of ^{257}Rf the main group of events in Fig. 4.10 seems to originate from the level observed for the first time and populated by 8686 keV α-energy, even though the indication for this transition was already reported in [59]. This group is also visible in α-γ matrix in Fig. 4.7 from which is also evident the main concentration of L X-rays over this α-energy region. Internal conversion coefficient on L shell is $\alpha_L^{tot} = 8.4\pm4.2$ which fits to M1 multipolarity for

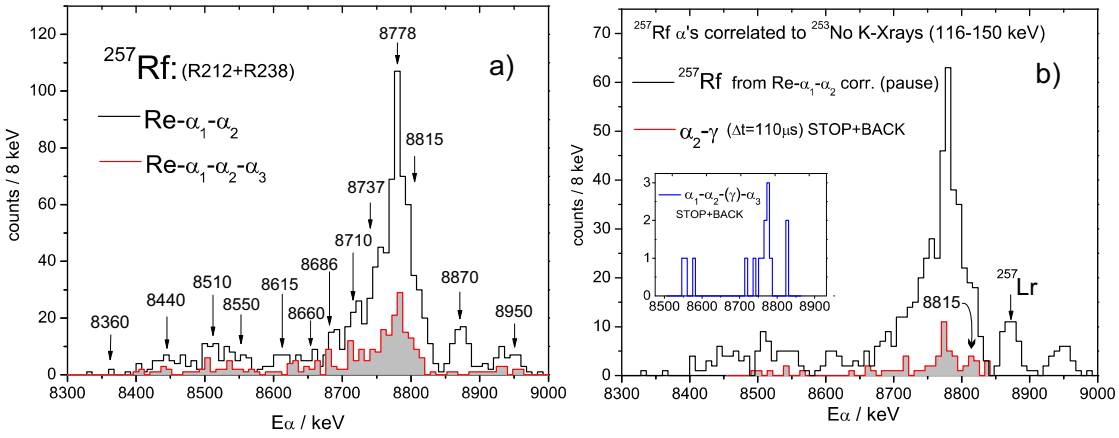

Figure 4.9: The summed ^{257}Rf α-spectrum from R-212 and R238 Re-α_1-α_2 correlations from the pause and superimposed over **a)** correlations to one more generation - ^{253}No and **b)** α-events correlated to delayed ^{253}No X-rays. Embedded blue spectrum shows the same α-generation as b) with additional α_3 generation.

this transition in nobelium. The energy difference between this level and the level $5/2^+[622]$ populated by the most intense α-line fits to the transition energy. Therefore 90.7 keV γ-transition can be assigned to populate $5/2^+[622]$ Nilsson level at E*=167 keV.

- **96.2 keV:** Indication for the γ-line at this energy can be seen in Fig. 4.8 for delayed $\alpha-\gamma$ coincidences with ^{257}Rf. Altogether four $\alpha-\gamma$ delayed coincidences were found of which three are part of Re-α_1-$\alpha_2(\gamma)$ correlation chains. The half-life for these delayed γ-events was calculated to be $T_{1/2}=28^{+38}_{-10}\mu$s which is in good agreement with the half-life for delayed coincidences between ^{257}Rf α-decays and ^{253}No X-rays. However one of the γ-events from Re-α_1-$\alpha_2(\gamma)$-α_3 correlations has an energy 97.4 keV which is on the edge of the detector resolution when compared with the mean γ-energy of the other two events and one coincident α-decay had quite low energy with the signal in the BOX detector. In Fig. 4.10 only those two events are shown with the α-coincident energy of $\sim$ 8730 keV. The upper limit for α_L^{tot} was also calculated for this transition as can be seen in Fig. 4.11. Unfortunately the scarce data does not allow for the definite identification of this γ-transition its multipolarity or the placement within the ^{253}No level scheme.

- **110.5 keV:** The γ-line at this energy was already tentatively assigned in [59]. In total 6 prompt and 1 delayed coincidences were found with the mean γ-energy E$_\gamma$=110.5 keV. The decay time of this single event is $\tau=38^{+180}_{-17}\mu$s which despite the big uncertainty is again in agreement with delayed α-X-rays coincidences. One peculiarity yet arises for the γ-energy of found coincidences in R-238 being about 1 keV higher than in R-212. Another

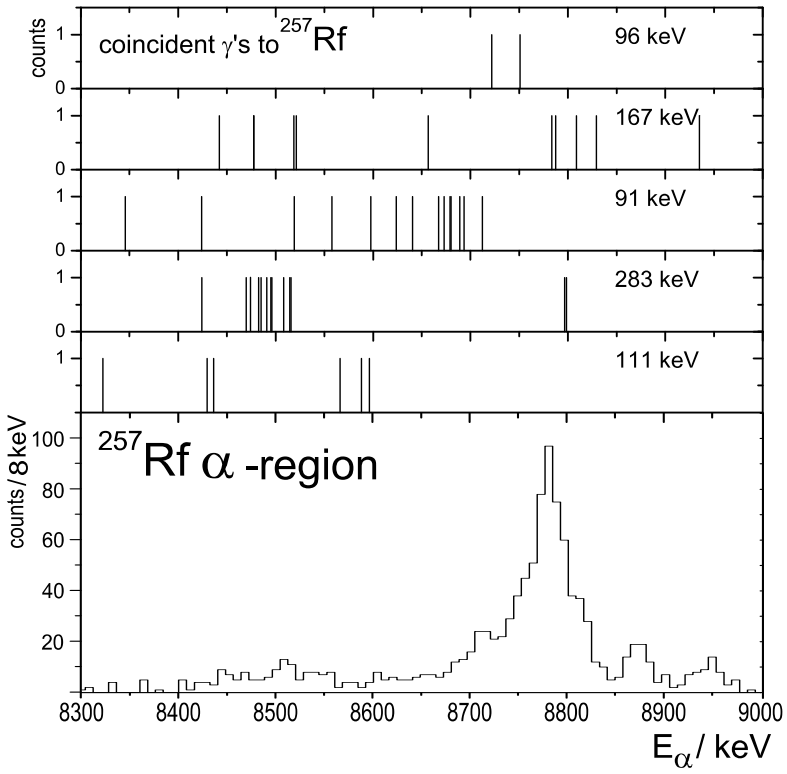

Figure 4.10: Gamma events found in prompt ($\tau < 4\mu s$) or delayed ($\Delta t = 110\mu s$) coincidences with ^{257}Rf α-decays in R-238 and R212.

drawback of the data for this line is that only 3 Re-α_1-$\alpha_2(\gamma)$ correlations were found with only one having the forth α_3 correlation. Most importantly all of these were found in R-212 which had about a factor of 3 lower statistics and the coincident α-decays have very large energy spread. In light of this evidence the origin of this line is still rather unclear.

- **166.7 keV:** One of the main purposes of R-238 was to measure the transition from predicted $5/2^+[622]$ level to the ground-state. Three delayed $\alpha - \gamma$ coincidences were found with the mean energy E_γ=166.7 keV. As seen from Fig. Fig. 4.8 all three delayed γs are members of complete Re-α_1-$\alpha_2(\gamma)$-α_3 correlation chains down to ^{253}No decay and therefore can be assumed as real. Calculated half-life of $T_{1/2}=22^{+30}_{-8}\mu$s is again equal to that of delayed α-X-ray coincidences. Besides these another eight prompt α_2-γ coincidences with the mean γ-energy 167.1 keV were found. Such high number of prompt coincidences found is unusual considering the 'prompt' interval of Δt = 4μs and calculated half-life for delayed events being quite apart and therefore hard to explain as a tail from the time distribution. Moreover only two of the prompt γs were part of Re-α_1-$\alpha_2(\gamma)$ correlation chains so their origin is somehow unclear. However, in recent SHIP experiment performed in April

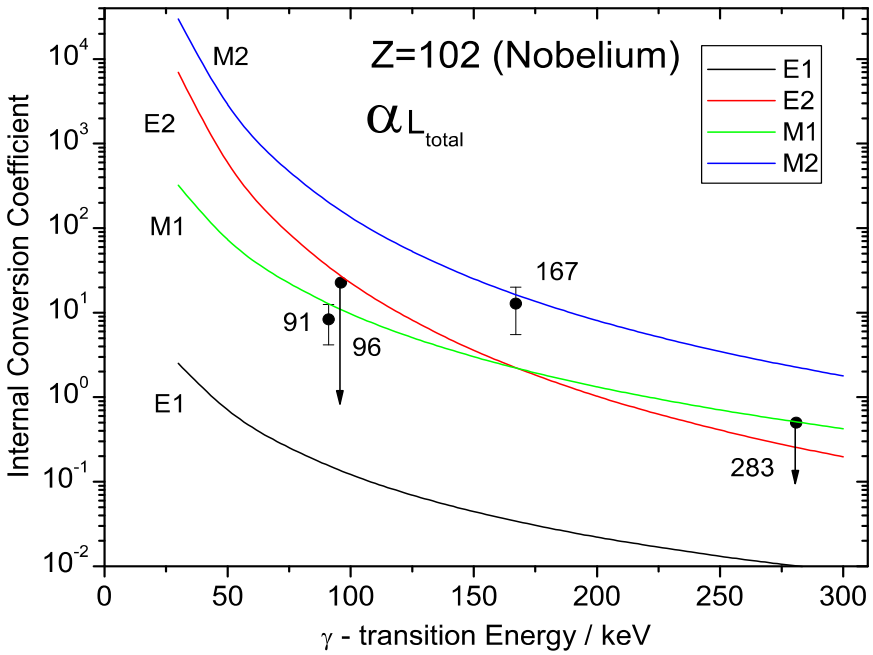

Figure 4.11: Internal conversion coefficients for transitions in ^{253}No calculated based on data from R-238. Theoretical curves for E1, E2, M1 and M2 transitions are based on calculations from Ref. [61].

2006 with direct production of ^{253}No the delayed γ-line at this energy was also observed. As plotted in Fig. 4.11 this transition would fit to M2 character with calculated coefficient $\alpha_L^{tot} = 12.8 \pm 7.2$. for IC on the L-shell. Theoreticaly derived value [61] for ICC at this γ-energy in nobelium is $\alpha_L^{tot} = 16.4$ for M2 multipolarity. The energy of this transition is also high enough to cause internal conversion on the K-shell considering $E_K^{bind} = 149$ keV in nobelium. The energy sum of α-energy feeding the supposed emitting level and the energy of this γ-transition is very close to the α-energy of proposed ground-state at ~ 8950 keV. If total number of observe K X-rays from α_2-γ coincidences is considered and number of γs with $E_\gamma = 166.7$ keV the calculated conversion coefficient $\alpha_K = 20.0 \pm 11.8$ can be taken as an ICC upper limit for this transition. This number is again in best agreement with theoretical value [61] $\alpha_K = 28.1$ for M2 multipolarity. Even though M1 multipolarity with $\alpha_K = 9.8$ could still be a candidate from the value point of view, its life-time of $\sim 10^{-11}$ s excludes it based on the delayed character of 166.7 keV transition.

- **283.4 keV:** This γ-transition was already observed in previous SHIP experiments [59] but no conclusions about its multipolarity were given. In total 13 α-γ coincidences could be assigned to this γ-group in present work. It is evident from Fig.s 4.7 and 4.10 that this line is in coincidence with the

α-energy interval around 8400 keV to 8520 keV. The upper limit of the internal conversion coefficient on the L-shell can be calculated from the number of L X-ray like events from the energy interval 14 - 30 keV from the data of both R-212 and R-238 and total number of 283 keV γs. The lines of 110 and 91 keV may also contribute to the L-shell conversion as their coincident αs are also found with energies from 8.4 - 8.5 MeV region. The value of $\alpha_{\mathrm{L}}^{\mathrm{tot}} \leqslant 0.5$ as an upper limit is in best agreement with E2 multipolarity as can be seen from Fig. 4.7. As for the ICC on the K-shell again an upper limit of $\alpha_{\mathrm{K}} = 0.6$ is in best agreement with E2 multipolarity as it is closest to the theoretical value [61] equals 0.1, while for E1 $\alpha_{\mathrm{K}} = 0.04$ and for M1 and M2 $\alpha_{\mathrm{K}} = 2.2$ and 5.4, respectively.

- **455.2 keV:** Another candidate for delayed γ-line consisting of three events with the mean energy E_γ=455.2 keV was found in $\alpha_2(\gamma)$-α_3 correlations. The calculated half-life is $\mathrm{T}_{1/2}=69^{+93}_{-25}\mu$s. Because of the low number of counts and therefore large half-life errors this value still agrees with those derived for delayed γ-lines 96.2 and 166.7 keV even though in absolute value this one is approximately by a factor of two higher than for the aforementioned lines. The mean energy of three correlated ^{253}No α-events is 8466 keV suggesting that it could be a de-excitation to the ground state located around the decay energy 8950 keV. Whether this line, if real, is an indication for yet another isomer in isotope ^{257}Rf or is a part of decay of current isomer needs to be checked for in future experiments and must be considered only as tentative indication.

Although Bemis *et al.* [51] assigned on the basis of delayed X-rays coincident to ^{257}Rf α-decays the presence of the isomer, he observed only 10 such events. In later indirect confirmation at SHIP (proposal U209) by observation of delayed X-rays coincident to ^{253}No evaporation residues in the reaction ^{207}Pb(^{48}Ca,2n)^{253}No it was not possible to investigate the structure of α-decays populating this isomer. In experiment R-238 the total number of 60 delayed K X-rays coincident to ^{257}Rf α-range could be assigned (see Fig. 4.8). The structure of coincident α-decays id shown in Fig. 4.9 b) superimposed over the pause spectrum. Based on this analysis it was possible to assign five α-lines coincident to delayed K X-rays. The line at 8660 has in general only tentative origin since it has intensity $< 3\%$. The correlations as seen in embedded picture in Fig. 4.9 b) (blue line) taken from α_1-α_2-(γ)-α_3 search provide rather strong evidence of the structure of α-decays of ^{257}Rf to the isomer in ^{253}No. Three lines at E_α = 8550, 8710 and 8778 keV could be clearly identified. One difficulty, however arises from α_1-α_2-(γ)-α_3 spectra. In α_2-(γ) delayed coincidences the α-line at E_α = 8815 keV (10 counts within the peak) is clearly separated from the previously identified isomeric transition of 8778 keV with the highest intensity, but already in four member correlation chain it is completely missing. According to statistical test [36] and stop detector efficiency this peak should consist of no less than 2 counts in α_1-α_2-(γ)-α_3 correlations. This points out to the fact that the isotope ^{253}No is not its generic daughter. The 8815

keV line was in [48] assigned with energy 8810 keV to the decay of ^{257}Lr the EC-product of ^{257}Rf. In present analysis this assignment is confirmed, but possible meaningful explanation for the mentioned discrepancy in correlation search is that this line is attributed as α-decay from ^{257}Lr populating so far unobserved isomer in ^{253}Md. The half-life for the isomer in ^{253}No was calculated[5] from time differences between ^{257}Rf α-decays and delayed X-rays from α_1-α_2(K X-rays) correlations to be $24.6^{+5.0}_{-3.6}$ μs which is in perfect agreement with the value 23±4 μs from recent SHIP experiments [59] and [60]. The K X-rays were considered from the interval $E_{X\text{-rays}} \in$ 118-150 keV. The value for the isomer in ^{253}Md was derived using the same correlation procedure with the second generation α_2 member from the interval $E_\alpha \in$ 8795-8830 keV to be $T_{1/2} = 44^{+24}_{-11}\mu$s. Due to low statistics it was not possible to distinguish the difference between the K X-rays originating from nobelium and those from mendelevium with the two separated in general by about 2 keV. The schematic level diagram for ^{257}Lr populating the isomer in ^{253}Md is shown in Fig. 4.4. It must be kept in mind that this assignment is only preliminary and needs to be checked in further experiments.

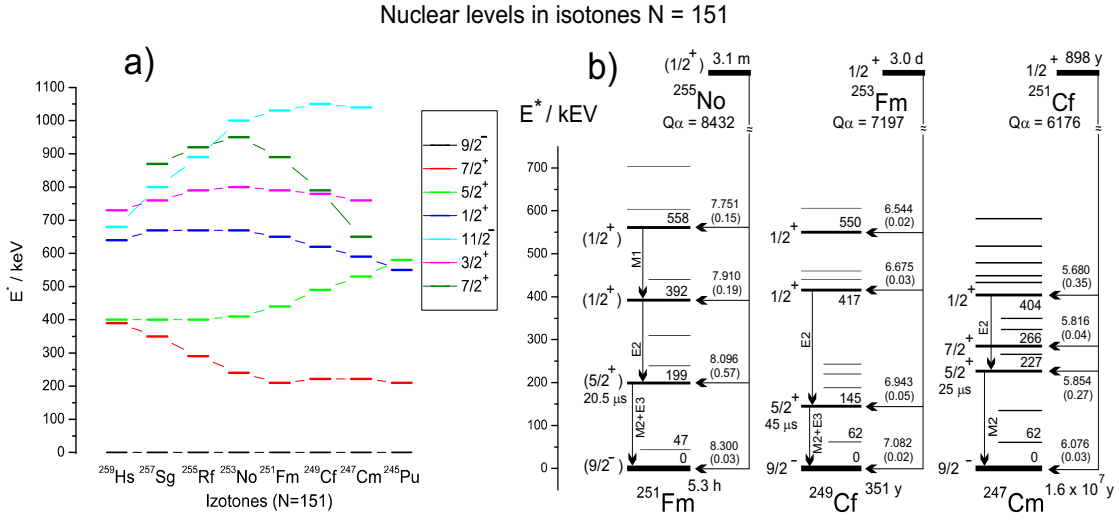

Figure 4.12: **a)**The calculated single-particle nuclear levels for isotones with N = 151 taken from Ref. [37]. **b)** Experimental results on nuclear levels in three best known isotones with N = 151 populated by α-decay of their mothers - isotones with N = 153. Data were taken from [70] and improved data for ^{255}No→^{251}Fm were taken from recent results [A9)] from SHIP.

Concerning the K X-rays in registered in prompt coincidence with ^{257}Rf α-decays these can be divided to be situated over several α-regions as seen from Fig. 4.7. First one is located over E_α = 8450 - 8500 keV. These K X-rays can be attributed to originate from the internal conversion coming from the same level as 283 keV γ-line. The second region seems to originate from the level populated by

[5] All values in μs region were corrected for the dead-time of the acquisition system of $\sim$ 15 μs.

8550 keV α-decays. Another coincident group has a wide spread over E_α = 8570 - 8700 keV. Levels connected with 110 and 91 keV γ-lines that also show a wide spread in coincident α-energies must contribute to these K X-rays events. However no definite conclusions about them can be derived based on the present data. The last coincident group of K X-rays can be located based on the Fig. 4.7 around the α-interval E_α = 8800 - 8900 keV. If these events originate from the conversion of the levels in ^{253}No than the g.s. to g.s. transition for ^{257}Rf$\rightarrow$ ^{253}No decay must be reaching a value more than the sum of $E_\alpha + E_K^{bind} \sim$ 8950 - 9050 keV. It is more natural to assign these events to originate from the conversion in ^{253}Md populated by ^{257}Lr whose main α-line of E_α = 8870 keV is situated exactly over this region.

As already stated in [59] the hint for observation of first excited states of the rotational bands build upon $9/2^-$ ground-state and $5/2^+$ isomeric-state could be identified in direct production of ^{257}Rf through the reaction ^{208}Pb + ^{50}Ti at SHIP. This assumption was based on the observation L X-rays that were coincident to slightly ($\sim 10 - 40$ keV) lower α-energies that would correspond to the α-decays into the band-heads. This scenario based on L X-ray observation could not be verified in present experiments due to several reasons. One is the usage of CLOVER detector instead of planar Ge-detector that has increased detection efficiency towards the energy region 90 keV - 1 MeV and rather low ($\sim$ 0.02) for L X-ray energy region. The second one is that the isomeric-state in ^{257}Rf was attributed to a low-lying $11/2^-[725]$ that is populated weakly while the bulk of the decays from ^{261}Sg populate the $3/2^+$ state single-particle orbital (see previous section 4.1.2). In other words the α-decays from the assumed $3/2^+$ ground-state of ^{261}Sg into $11/2^-$ isomer in ^{257}Rf are strongly hindered and have intensities below experimental sensitivity and consequently isomeric lines of 8.97 and 9.02 coming from this $11/2^-$ state of ^{257}Rf are not observed. The majority of L X-rays in the mentioned work of [59] are just connected with supposed conversion $11/2^- \xrightarrow{IC} 9/2^-$. In present analysis these L X-rays are not observed as seen in Fig. 4.7 that confirms a strong hindrance of the decay into $11/2^-$ level. However α-decays with energies 8737 and 8686 keV may be interpreted as populating the levels at E^* = 208 and 258 keV. The energy separation of these level fits to the pattern of the rotational levels $7/2^-$ and $9/2^-$ build upon the isomeric $5/2^-[622]$ single-particle Nilsson orbital as observed for lighter N = 151 isotones of ^{251}Fm, ^{249}Cf and ^{247}Cm. If this is the case, these levels would undergo M1 transitions to the band-head with half-lives in the order of ps so it is understandable to observe the α-decays populating these levels in delayed coincidences with K X-rays from $5/2^+$ isomeric level. In fact 91 keV γ-line is a good candidate for such transition de-exciting $9/2^+$ level by M1 transition to the $5/2^+$ band-head. Another working interpretation would be to assign it to $7/2^+[624]$ single-particle level, but this scenario has some difficulties (see also discussion below).

It was not possible despite twice the amount of recorded α-γ coincidences to unambiguously disentangle the situation about 283 keV transition. As already suspected in [59] two regions of concentration for coincident α-decays at E_α = 8440 and 8495 keV could be identified suggesting the intense feeding of the emitting

level at $E^* = 455$ keV from above 55 keV higher lying level. This is also supported here by rather broad and patternless distribution of α-decays from 8.4 - 8.5 MeV suggesting that principally several low-lying levels could be involved decaying predominantly by internal conversion. Unfortunately it could not be verified based on observation of coincident L X-rays shift. On the other hand the conversion coefficients for this transition suggest that it has E2 multipolarity instead of M1 as proposed in [59]. This further enhances the resemblance to lighter N = 151 isotones in which the two most intensive γ-transitions are the ones de-exciting and populating the isomeric $5/2^+[622]$ single-neutron orbital with multipolarities M2 or M2+E3 and E2, respectively. The α-region over which 283 keV γ-group is observed has the relative intensity of only ~ 6 % which represents another difficulty for M1 multipolarity since in such case most decays would undergo internal conversion with $\alpha_K = 2.2$ and would not create such intensive α-γ coincidence group. This also changes the situation about the J^π assignment of the emitting level. By keeping the level at $E^* = 167$ keV to be $5/2^+$ the E2 multipolarity would require the emitting level with J^π either $1/2^+$ or $9/2^+$. In accordance with neighboring isotone ^{251}Fm this level is also tentatively attributed to $1/2^+$ Nilsson orbital. Due to considerable lack of correlations with the third generation ^{253}No α-decays and no coincidences to delayed K X-rays from ^{257}Rf as shown in Fig. 4.9 the α-line at 8620 keV was tentatively assigned to originate from ^{257}Lr. New data from current analysis and also from recent experiments performed at SHIP with direct production of ^{253}No places another difficulty on the level assignment proposed in [59]. This stands out from the placement of $7/2^+[624]$ single-particle orbital. Two reasons against the placement of this orbital at $E^* = 355$ can be found. One of them is the E1 character of such transition that would bypass the $5/2^+$ isomeric level with M1 multipolarity and populate the $9/2^-$ ground-state, with both levels quite well established. The observation of the rotational band build upon $7/2^+[624]$ band-head was proposed in [66] from in-beam experiment performed at Argonne National Laboratory. This result is however in contrast with the in-beam data [30] taken at RITU separator in Jyväskylä that claimed the observation of the rotational band build on $9/2^-$ orbital. Both assignments were based on theoretically predicted value of intrinsic g-factor g_K. In light of recent SHIP experiment later corrected results published in Ref. [31] seems more reliable as the decay spectroscopy confirmed the observation of the γ-transitions expected in $7/2^+[624]$ rotational band. The problem arises that even γ-lines from the lowest M1 and E2 intraband transitions are being observed with high intensities. This places a severe argument against the placement of $7/2^+[624]$ orbital where multiple possibilities for the low-lying rotational levels to de-excite by E1 transitions exist. One more argument can be found in present data from the lack of α-transitions to the energy region around 8605 keV that would correspond to feeding of the supposed $7/2^+[624]$ level at $E^* = 355$ keV. If the in-beam data interpret the $7/2^+[624]$ level correctly this suggests that this band is highly populated and therefore can not exhibit such low α-transition into the band-head in decay spectroscopy data. However this analysis revealed an indication for 91 keV γ-transition with M1 mul-

tipolarity that would contrary fit to the assignment to originate from $7/2^+[624]$. This is again in conflict with non-observation of E1 transition into the ground state. The ratio according to the recent publication by Ahmad *et al.* [53] for E1:M1 to populate the ground-state vs. $5/2^+$ isomeric level is 50:1 in ^{247}Cm and similar case applies for other lighter N = 151 isotones. This issue therefore needs further investigation in nucleus ^{253}No.

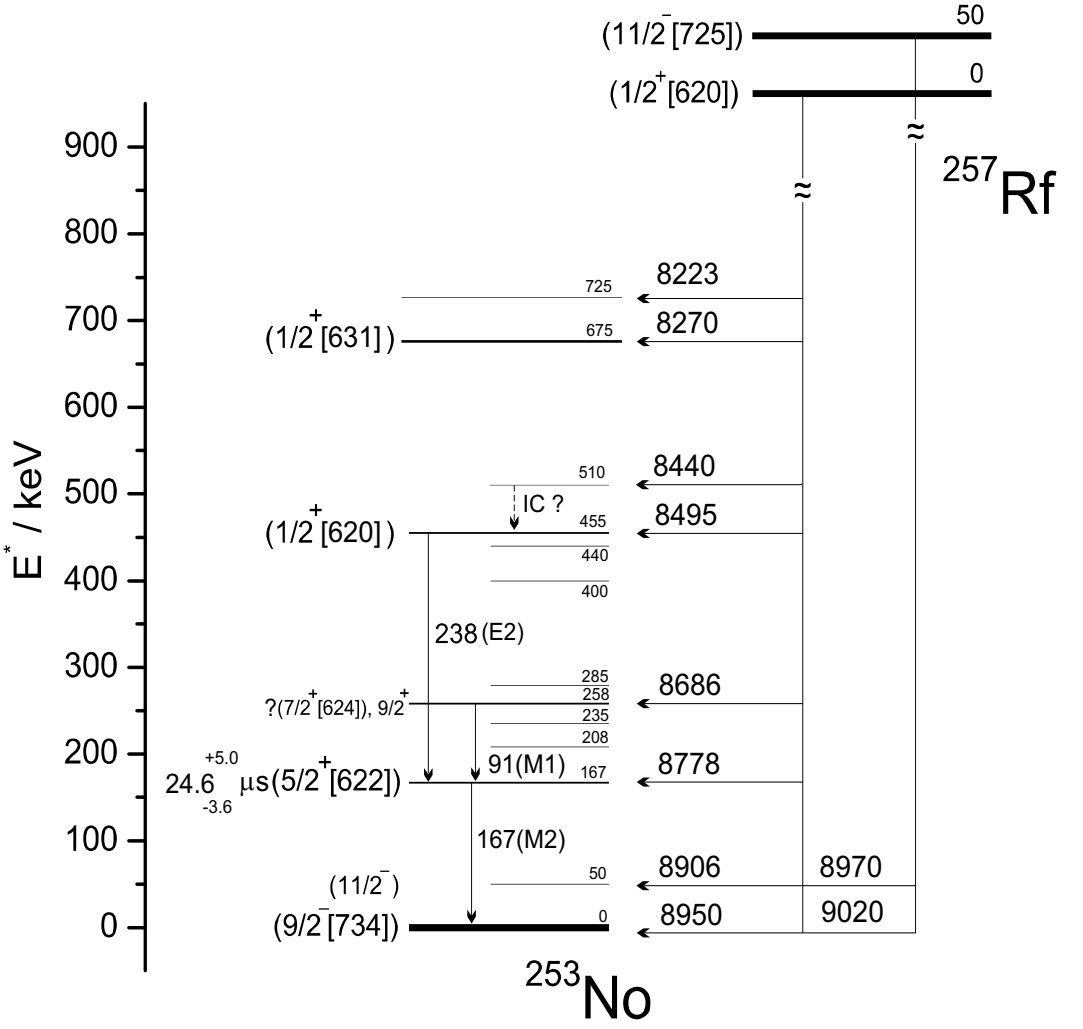

Figure 4.13: Proposed decay scheme for ^{257}Rf as deduced based on the experimental data acquired at SHIP in R-212 and R-238. Short lines represent levels of the rotational bands build upon single-neutron states.

The discussion about the systematics of experimentally observed single-neutron levels in N = 151 isotones and hence for ^{253}No - the heaviest so far studied in detail - relies first of all on well deduced spin and parity of $9/2^-[734]$ for their ground state from decay spectroscopy of ^{249}Cf and ^{247}Cm. Secondly it should complement to certain extent with theoretical predictions for the occurrence and behavior of

specific single neutron orbitals for odd-A, N = 151 isotones. Fig. 4.12a) shows these calculations taken from [37] up to energies close to 1.1 MeV for eight such isotones. Recently published work of Parkhomenko *et al.* [68] exhibits very similar pattern involving the same levels and is not plotted here. Experimentally deduced level schemes of lighter three N = 151 isotones, including the recent results from SHIP on ^{251}Fm are plotted in Fig. 4.12b) and all exhibit an existence of the isomeric $5/2^+$ level. Indeed this pattern is confirmed by SHIP data for ^{251}Fm [A9)] as well as for ^{253}No discussed in this work with similar excitation energies and half-lives of this isomer, indicating that the same nuclear levels are involved during the decay in mother and daughter nucleus. Couple of features resulting from the calculations as shown in 4.12a) are evident. Above all the theory does not predict the existence of isomer as the first two low-lying levels are interchanged in order $7/2^+$ and $5/2^+$, respectively while keeping the ground-state at $9/2^-$ and thus decaying as M1 and E1 transitions. Experiments including the presented results exhibit $5/2^+ \stackrel{M2}{\rightarrow} 9/2^-$ transition with measured half lives in order of few tens of microseconds as predicted by Weisskopf calculations. Another characteristic of the calculations is that first four levels exhibit rather flat behavior over the region of experimental interest from ^{247}Cm to ^{253}No with no predicted level crossings.

Proposed decay scheme for ^{257}Rf α-decay based on presented analysis is shown in Fig. 4.13. Its main contribution lays in the confirmation of the ground-state transition at 8950 keV and stabilization of $5/2^+$ isomeric level to be situated 167 keV above and decaying by M2 transition (with possible E3 component). Another step forward is tentative assignment of E2 character to 283 keV transition that confirms the experimental trend along with calculations predicting almost constant behavior of the levels in N = 151 isotones of our interest. Moreover current data put more emphasis on alternative assignment proposed in [A9)] with levels $1/2^+[620]$ and $1/2^+[631]$ existing in this order in neighboring nucleus ^{251}Fm. This way all N = 151 isotones from ^{247}Cm to ^{253}No would exhibit rather smooth variation of first three levels $5/2^+[622]$, $1/2^+[620]$ and $1/2^+[631]$. Initially proposed reversed order for $1/2^+[620]$ and $1/2^+[631]$ would result in either double crossing of these levels in ^{249}Cm$\rightarrow^{251}$Fm and again in ^{251}Fm$\rightarrow^{253}$No or crossing in ^{249}Cm$\rightarrow^{251}$Fm plus steep increase of $1/2^+[620]$ in ^{253}No and fluctuation of $1/2^+[631]$ going from ^{249}Cm to ^{253}No. This scenario would completely shatter the theoretically predicted systematic behavior of N = 151 isotones.

Fig. 4.14 taken from Ref. [70] shows an example of the Nilsson diagram calculated as described in Bengtsson and Ragnarsson [69] for the neutron region N > 126. The quadrupole deformation parameter ε_2 is scaled to the hexadecapole parameter ε_4 as $\varepsilon_4 = \varepsilon_2^2/6$. It needs to be emphasized that out of very few calculations for this region all of the available Nilsson diagrams even though calculated using different methods and potentials, they seem to predict the levels around shell closures at N = 150, 152 and 154 discussed here in the same order and similar shape as shown in Fig. 4.14. As already described the experimental data indicate that in N = 155 isotones starting from ^{257}No up to heavier ones the ground-state J^π changes from $1/2^+$ to $3/2^+$ and is also tentatively assigned to ^{261}Sg treated in

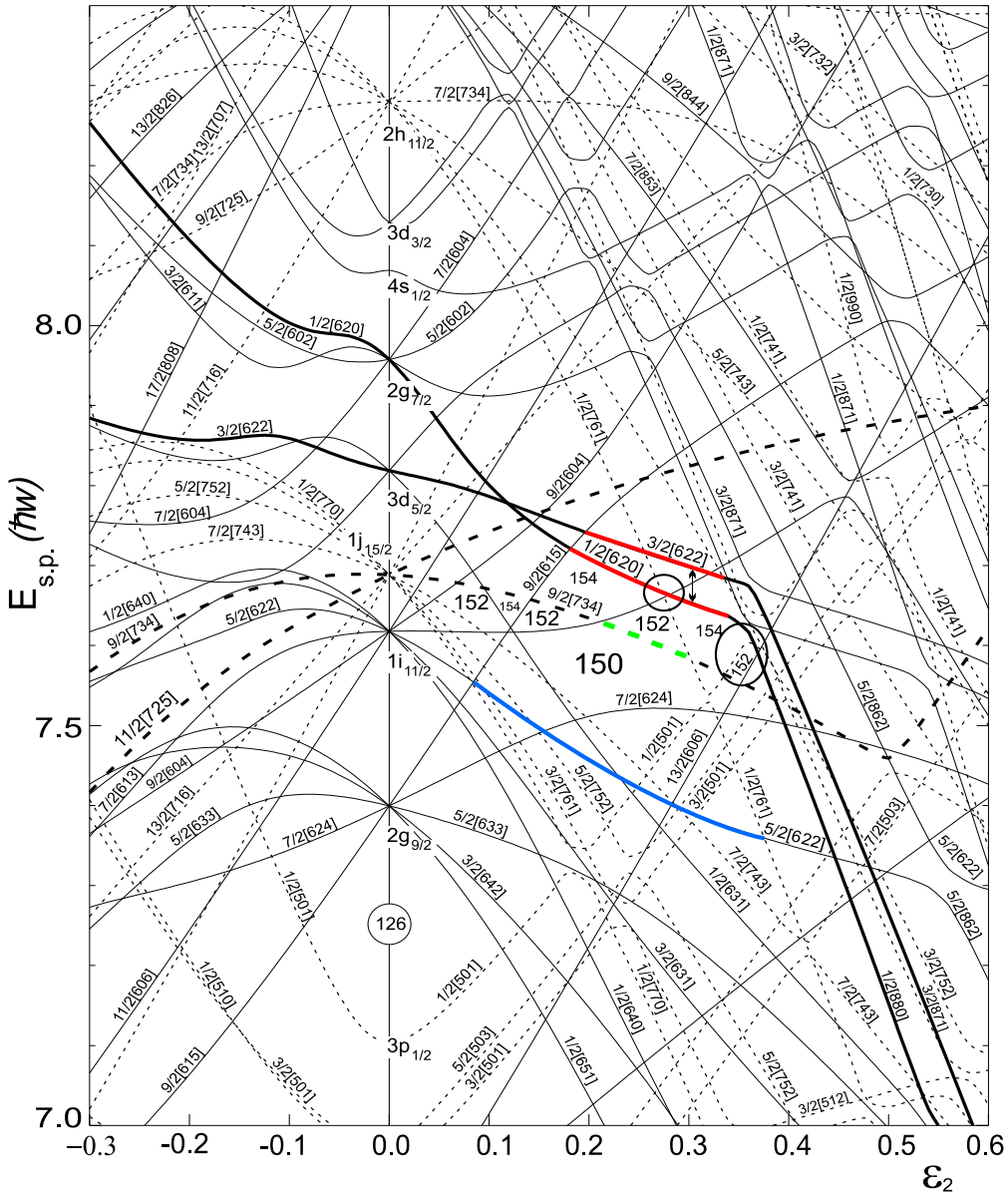

Figure 4.14: Nilsson diagram for the neutrons with N > 126. The single-particle energies are plotted in units of the oscillator frequency $\hbar\omega_0 = 41A^{-1/3}$[MeV].

this work. Confronting this experimental information with Nilsson diagram one sees that this scenario is possible if $3/2^+[622]$ orbital stemming from $3d_{5/2}$ neutron orbital gets under $1/2^+[620]$ level as shown in 4.14 by red lines at the region of $\varepsilon_2 \sim 1.8 - 3.5$. Thit does not seem unrealistic considering their relative closeness and similar dependance on the deformation. Yet another difficulty arises from keeping the ground-state for ^{257}Rf as $J^\pi = 1/2^+[620]$ like experimental data suggest for N = 153 isotones. This is possible over the 152 subshell closure at the regions marked by circles. Although situated over deformation region with $\varepsilon_2 = 0.2$ - 0.3 as

expected for transfermium elements [78] this would place the expected $11/2^-[725]$ (emphasized dotted line in Fig.4.14) isomeric level at much higher excitation energy as experimentally observed. The biggest discrepancy however exists between the experimentally well established systematics for the isomeric state of $5/2^+[622]$ observed in all N = 151 isotones and theoretical calculations. Even though the ground-state for ^{253}No can be found with $J^\pi = 9/2^-[734]$ indicated by green dotted line at roughly $\varepsilon_2 = 1.9$ - 2.8 over N = 150 subshell, the state $5/2^+[622]$ highlighted by blue line is way below the levels in question at expected deformation values. Moreover this level does not go over N = 150 subshell closers at positive deformation values as needed to become the candidate for level in ^{253}No. In conclusion can be stated that obvious discrepancy exists between the theory predicting the single particle levels and the experimental evidence. Concerning the present work this is most evidently pronounced for N = 151 isotones.

It should also be noted that R-238 lasted only a half of the time approved for investigation of ^{257}Rf via an indirect production. Some twelve days of beam time are still scheduled to take place during the year 2007 at SHIP. At good experimental conditions and beam intensities up to about 1000 pnA of ^{54}Cr it can be expected to more than double the acquired statistics for both ^{261}Sg and ^{257}Rf and hence clarify some unresolved problems as depicted in this work.

Detail study of the decay properties of the isotope ^{253}No was not performed within presented work. This is due to the existence of better quality data taken at different experiments using direct production of this nucleus via the reaction ^{207}Pb(^{48}Ca,2n)^{253}No [29] utilizing α-γ coincidence method at SHIP. In [29] also a decay scheme of the sequence ^{253}No$\rightarrow^{249}$Fm$\rightarrow^{245}$Cf is presented and the discussion linking these results to systematics of other N = 149, 147 isotones is given. However current experiments R-212 and R-238 also revealed a presence of γ-lines with energies E_γ = 280, 222 and 154 keV in prompt coincidences with ^{253}No α-decays from the region E_α = 8.0 - 8.8 MeV. No sign for spontaneous fission branch for this isotope was found in the data and the search for EC-branch is disabled due to 100 % EC-branch of ^{253}Md and unusably long decay time of 3 days for ^{253}Fm. The measured half-life of 1.5 $\pm$ 0.1 min for ^{253}No is in good agreement with previously reported data [29].

4.1.4 Excitation functions for ^{260,261}Sg

The trend of steeply decreasing fusion cross sections as measured at SHIP for both even and odd A isotopes is plotted in Fig. 4.15. On the left side the results are plotted as a function of excitation energy E^* calculated for the center-of-mass beam energy in the middle of the target thickness.

On the right side, the neutron binding energies according Myers and Ś̀wiatecki are subtracted. This results in 'free' reaction energy which equals to the sum of kinetic energy of evaporated neutrons and energy of emitted γ-quanta in de-excitation process. The arrows mark the position of E^* corresponding to the beam energy needed to reach the contact configuration according to the model of Bass.

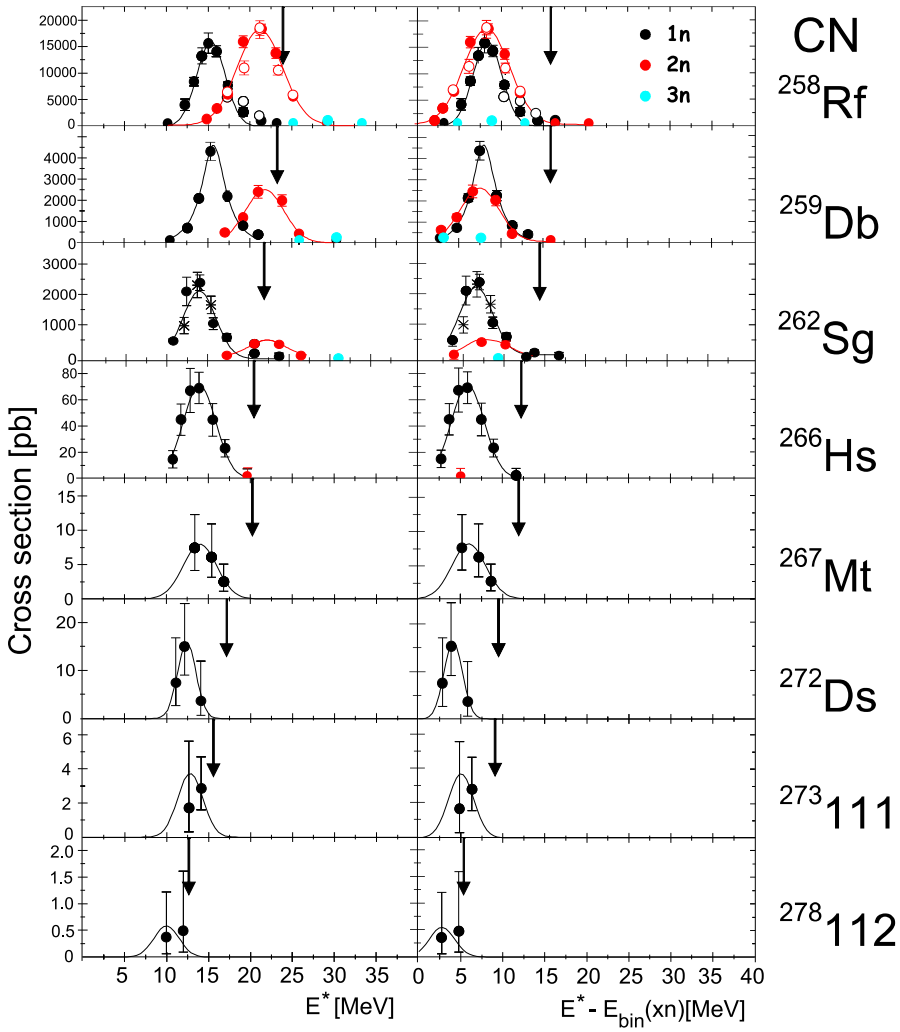

Figure 4.15: Systematics of production cross sections of 1-3n channels for heaviest elements of even and odd A. In case of overlapping points the error bars are not shown for the sake of clarity.

The excitation function in dependance on $E^* - E_{\mathrm{bin}}(\mathrm{xn})$ show that the cross section maxima is for every isotope centered between the zero and the Bass energy. One of the goals behind the experiment R-212 at SHIP was to precisely measure excitation functions for 1n and 2n de-excitation channels of reaction ^{54}Cr + ^{208}Pb leading to compound nucleus ^{262}Sg (this result is also a part of Fig.4.15). Another task was to test the application of chemical compounds such as PbS with higher melting points as targets which is needed as the pursuit for even heavier elements requires higher beam intensities.

Targets from two different materials were used for the reaction leading to the compound nucleus ^{262}Sg in R-212. One of them was a metallic lead that showed positive results with average thickness of 453 μg/cm^2 Pb evaporated on 38 μg/cm^2

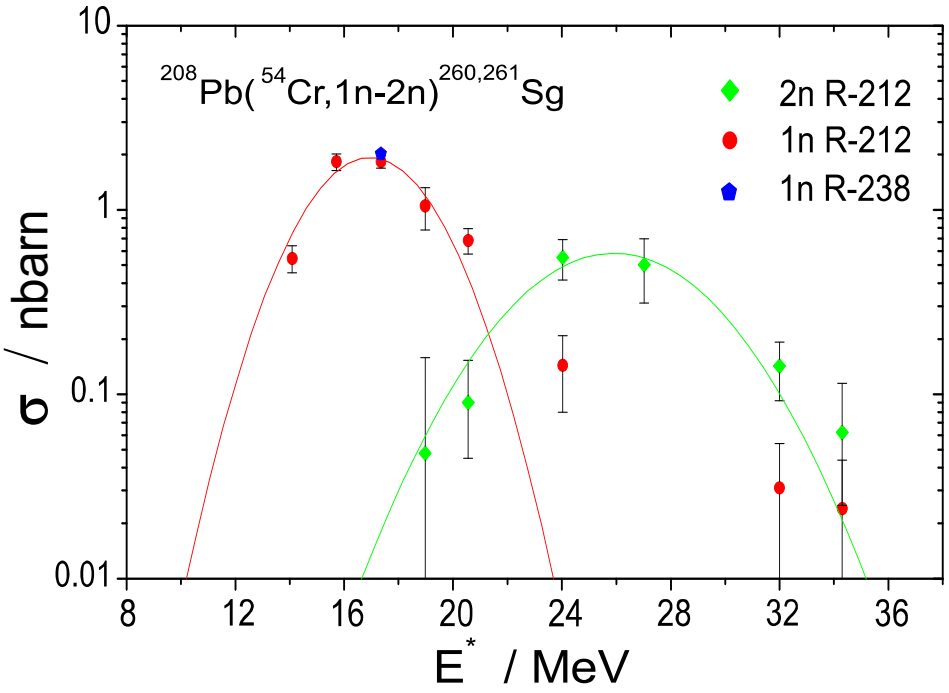

Figure 4.16: Measured excitation functions in R-238 for ^{260,261}Sg produced in reaction ^{54}Cr + ^{208}Pb using metallic ^{208}Pb targets. One point from R-238 is also added.

of carbon backing and covered with 10 $\mu g/cm^2$ of carbon layer which purpose was to reduce the bursting out of the target material caused by impinging projectiles and to improve radiative cooling as well. The excitation functions for 1n and 2n channels measured in reactions with this type of target are shown in the Fig. 4.16.

Isotope	σ/nb	$E_{\mathrm{lab}}/\mathrm{AMeV}$	Run	Target	Reaction	Ref.
^{260}Sg	0.69 ± 0.17	4.97	212	Pb	^{54}Cr + ^{208}Pb	This work
	0.28 ± 0.05	4.92	212	Pb	^{54}Cr + ^{208}Pb	[43]
	$0.022^{+0.050}_{-0.018}$	4.90	212	Pb	^{54}Cr + ^{207}Pb	[43]
^{261}Sg	2.02 ± 0.06	4.77	238	PbS	^{54}Cr + ^{208}Pb	This work
	2.19 ± 0.20	4.76	212	Pb	^{54}Cr + ^{208}Pb	This work
	0.50 ± 0.14	4.85	212	Pb	^{54}Cr + ^{208}Pb	[43]

Table 4.5: Comparison of cross sections measured in this work for isotopes ^{260,261}Sg with experimental data from [43].

In R-212 experiment the position of the maximum of the excitation function for reaction ^{208}Pb(^{54}Cr,n)^{261}Sg was found to lie close to 4.76 AMeV, corresponding to cross section of 2.19 ± 0.20 nb. Previous result 0.5 ± 0.14 nb [43] at 4.85 AMeV for production of ^{261}Sg through 1n channel corresponds well within experimental

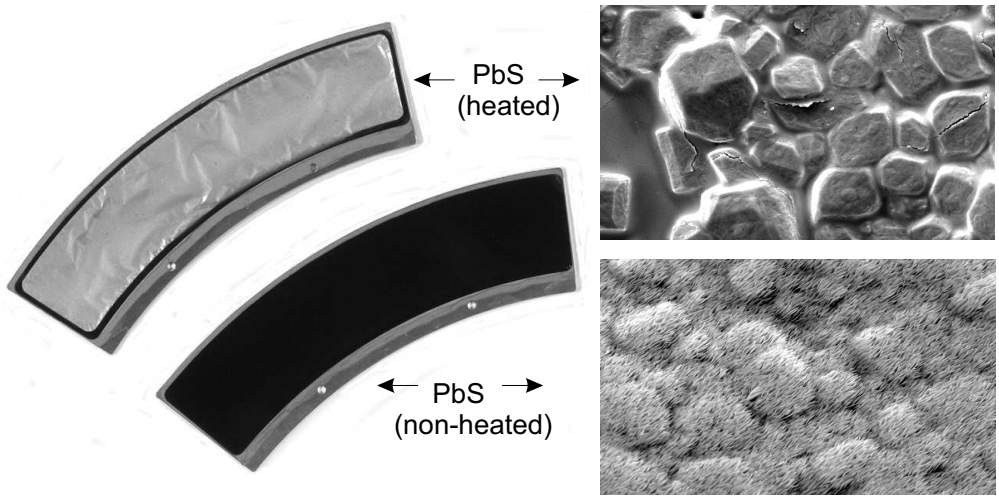

Figure 4.17: Pictures on the right show surface structure of different PbS targets made by a Scanning Electron Microscope with the same magnification. Both pictures are taken from samples that were not irradiated. The left picture represents the macroscopic appearance of these types of targets with evident color difference.

errors to our value of 0.45 ± 0.12 nb derived from the gaussian fit at this energy.

For the same reaction the targets produced of lead sulfide (PbS) were used. The average thickness of PbS was 455 μg/cm^2 with effective thickness of the lead itself 418 $\mu g/cm^2$. It was also evaporated on 40 μg/cm^2 of carbon backing and covered with 10 μg/cm^2 of carbon. The GSI target laboratories had been working for several years on the compound PbS and it was used prior to R-212 in several test experiments. Reaction products were found but there were some hints that the microstructure of the material might cause a problem for the narrow excitation functions [27]. This was in fact proven in R-212 where on the contrary to the metallic lead, this type of compound target from the first production cycle showed very poor results in reproducing the production cross section, as can be seen on the Fig. 4.18 (black squares). The difference with the metallic Pb is apparent. The excitation function is broad without a pronounced maximum.

These targets were labelled "black" because of their color appearance. They were produced by a method of thermal evaporation and showed very rough and sin-like surface structure with the period of approximately 1 μm as shown on scanning electron microscope picture in Fig. 4.17. The material consist of plates standing in vertical rows. This structure provided very different conditions for the fusion since heavy ion impinging on such non-uniform surface had to traverse either the full thickness of the target or a void with almost no interacting material. Such significant differences in energy loses of the incoming projectiles and very different conditions for the fusion process confirmed the expectation that the target microstructure strongly influences their performance in the experiment.

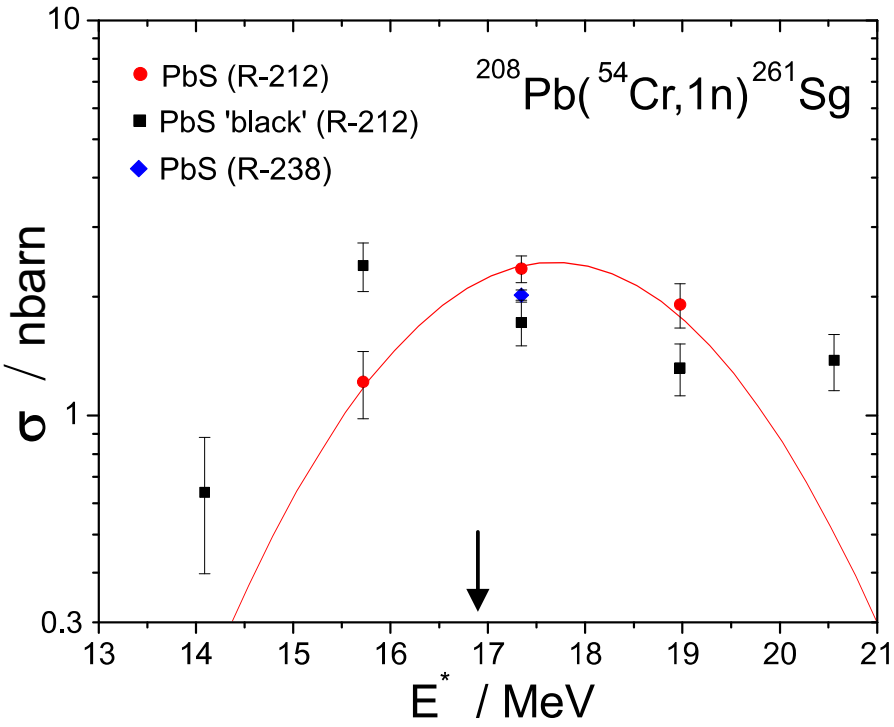

Figure 4.18: Measured excitation functions in R-212 for ^{261}Sg produced in reaction ^{54}Cr + ^{208}Pb using PbS and PbS-black targets. Also point from R-238 is plotted and the arrow marks the position of the maximum of the excitation function for metallic lead target.

In later production stages the carbon backing was heated during the evaporation process with a quartz lamp to about 570 K. As can be seen from the second scanning electron microscope picture in Fig. 4.17 this process completely removed the rough surface structure. The only visible structure comes from the imprint of the grainy betain-sucrose profile that was used as interlayer in the production of the carbon backing. These targets thus resemble much closely the metallic material. This was proven already in R-212 by measuring three points at E* ~15.7, 17.3 and 19.0 AMeV. The production cross section as plotted in Fig. 4.18 resembles much better the excitation function for the metallic Pb targets. The only notable difference is the shift of the PbS excitation function to a bit higher energy of E_{lab}=4.77 AMeV. This beam energy was also chosen for the production of ^{261}Sg in the same reaction in R-238 using the compound PbS targets. As can be seen from both Fig. 4.16 and Fig. 4.18 the cross section value agrees quite well with the maximum from the experiment R-212.

For production of ^{260}Sg in R-212 we measured total cross section of 0.69 ± 0.17 nb at 4.97 AMeV. The result on the Gaussian fit at energy 4.92 is 0.56 ± 0.15 nb which is about a factor of two higher that the value reported in [43] for this energy. The excitation function from present experiment is fixed at six different

energies instead of three as in [43], therefore our value should be more reliable. In R-238 we expect based on the measured excitation functions for in R-212 the ratio ^{261}Sg/^{260}Sg $\sim 10^2$ which means to expect about 11 decays of ^{260}Sg in pause spectrum. Taking into account about 50% fission branch for ^{260}Sg our finding of 5 α-decays and 3 SF-events attributed to this isotope in energy region 9.7-9.8 MeV is in line with the expectations.

4.2 Isotope ^{262}Bh

At the end of experimental run R-212 (see section 4.1.1 for details) the target was switched from ^{208}Pb to ^{209}Bi, aiming at production of odd-odd isotope ^{262}Bh using 1n channel of the reaction ^{209}Bi(^{54}Cr,1n)^{262}Bh. It served also as another opportunity to test the compound targets. Two different types of compound targets were used, namely Bi_2O_3 and BiF_3. The first one was irradiated using the beam energy of 4.828 AMeV and the second with beam energies of 4.828 and 4.865 AMeV, respectively. Total dose delivered to the targets was approximately 2.03×10^{18} projectiles.

The first evidence for the synthesis of isotopes with Z = 107 was reported by Oganessian *et al.* [73]. Later production of odd-odd nucleus ^{262}Bh was performed at SHIP and published in [74] and [75]. The complex α-spectrum was described with two well separated time components assigned to the decay of the ground-state and isomeric-state configurations, respectively. The same decay properties were also confirmed in its indirect production via the decay of ^{266}Mt (see [58] and references therein). Most recently the isotope ^{262}Bh was studied at LBNL using the reaction ^{208}Pb + ^{55}Mn [76]. Even though in older SHIP experiments also γ-events were registered no attempt to use α-γ spectroscopy methods was yet employed to investigate in more detail the nuclear structure of its daughter ^{258}Db until the experiment discussed here.

Present analysis revealed even more complex pattern for α-decay spectrum of ^{262}Bh as shown in Fig. 4.25 than those reported in [75] or [76]. Present data provide the most reliable information since the statistics acquired in R-212 is about six times higher than either one of [75] or [76] where at most five counts were recorded for each separate α-group. Despite the higher statistics, some of the α-peaks (see table 4.6) assigned in the present work retain only tentative character.

The production cross section for reaction ^{209}Bi(^{54}Cr,n)^{262}Bh was found to be 0.29 ± 0.03 nb at the beam energy 4.828 AMeV. Due to only two values of the beam energy it was not possible to construct an excitation function for production of ^{262}Bh. Therefore it is difficult to compare present results to the maximum cross-section value of 0.16 ± 0.03 nb at 4.94 AMeV as reported in [75] using the same reaction, even though in Ref. [75] four different beam energies were used. It can be tentatively deduced from Fig. 4.19 that values from both experiments follow decreasing trend at the right side of the excitation function. This is however in conflict with [75] where decrease in cross-section was found at the lower beam

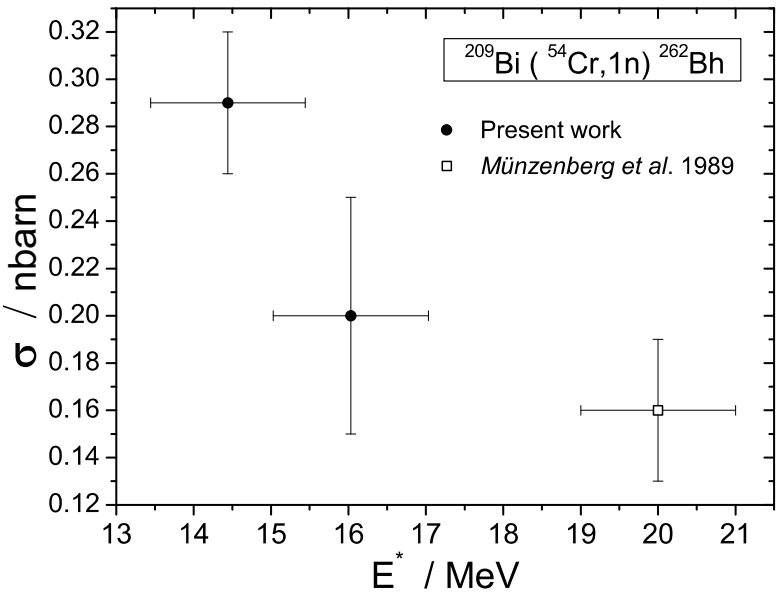

Figure 4.19: Two values of production cross section for ^{262}Bh isotope from reaction ^{209}Bi(^{54}Cr,1n) using BiF_3 targets. Maximum value of 0.29 ± 0.03 nb was derived for the beam energy of 4.828 AMeV($E^* = 16$ MeV). The beam energy uncertainty of $\pm$20 AkeV is considered. For comparison, cross section from Ref. [75] is also shown.

energy of 4.87 AMeV. Recently, the isotope ^{262}Bh was produced utilizing the reaction ^{208}Pb + ^{55}Mn [76]. Three points of the corresponding excitation function were measured giving the maximum value of $\sigma = 0.54^{+0.18}_{-0.15}$ nb which is almost by a factor of two higher than the value presented here for ^{209}Bi + ^{54}Cr. Although Ref. [76] uses only the beam energies in the center of the target, their energy for the maximum of the excitation function $E_{cot} = 264$ MeV should correspond to the excitation energy of $E^* = 14.5$ MeV. The use of different reaction having somewhat different Q-value and also different barrier results, that E^* for maximum of the cross-sections cannot be simply compared. Assuming however that both reactions utilized 1n evaporation channels the maximum of the excitation functions should be quite close to each other. This is in line with presented findings of the highest cross section for almost equal energy of $E^* = 14.4$ MeV and the assumption of the right side of the excitation function in Fig. 4.19 despite the missing points below $E^* = 14$ MeV seems to be justified.

It was also sought for the trace of 2n channel leading to ^{261}Bh. The identification based on the third α-generation from Re-α_1-α_2-α_3 correlation analysis had to be employed since ^{261,262}Bh isotopes can not be reliably distinguished due to similar α-energies and half-lives. This is also valid for their daughters ^{257,258}Db. Three candidate correlation chains that proved to be in fact correlations of ^{262}Bh$\rightarrow \ldots$ could be found. This assignment was evident by comparing the analysis outputs for ^{262}Bh decay chains and assumed chains for ^{261}Bh. It was further supported

by the half life 3.4 s of "^{261}Bh" daughter, which fits more to ^{258}Db half life of 4.4 s. Also the α-energies for the mother decays E_α = 9979, 9998 and 10190 keV are more in-line with the most intensive α-groups of ^{262}Bh. Therefore it can be concluded, that the isotope ^{261}Bh, if produced in the presented reaction is below the observable for given experimental conditions with the calculated upper limit of $\sigma_{(^{261}\mathrm{Bh})} < 1.7$ nb.

Altogether 65 spontaneous fission events could be identified within the energy interval of 120 -220 MeV. The correlations of the kind Re-α_1-SF were analyzed and assigned to originate from the isotope ^{258}Rf produced by EC-decay of ^{258}Db. There were five SF-events found in Re-SF correlations that could not be attributed to ^{258}Rf due to missing preceding α-decay of ^{262}Bh neither found in stop or box detector within 700 ms time window and $\pm$ 2 mm position window after the recoil implantation. These events can originate either from ^{262}Bh or its possible EC-decay product ^{262}Sg. The calculated half-life for mentioned five SF-events is $T_{1/2} = 133^{+107}_{-41}$ ms. This value is compatible with the half-life of ^{262g}Bh component. However, according to the half-life systematics for lighter even-even isotones with N = 156 and also measured value $T_{1/2} \sim 7$ ms [77] for ^{262}Sg discovered at SHIP and decaying predominantly by spontaneous fission it is not possible to clearly distinguish between the two cases. In analogy with the isotope ^{261}Sg discussed in section 4.1.2 also for ^{262}Bh, differing by one neutron, small fission branch of $b_{SF} = 2 \pm 1$ % could be found in present data which should be taken as an upper limit. One decay chain of the kind Re-α-SF was also found with the E_α = 9388 keV, τ_α = 70 ms and τ_{SF} = 56 ms. This can be assumed based on the observed decay times and α-energy to originate from EC-decay of ^{262}Bh and subsequent α-decay of ^{262}Sg, ending in fission at ^{258}Rf. Due to the lack of experimental evidence supporting this interpretation this must be taken as tentative even though the the probability of $P_{\mathrm{err}} \sim 10^{-3}$ of random origin of such chain can be calculated [36]. From the given number of described correlations an upper limit of $b_{EC} = 3 \pm 1$ % for EC-branch of ^{262}Bh can be calculated.

By comparing the analysis of the decay path $^{262}\mathrm{Bh} \xrightarrow{\alpha} {}^{258}\mathrm{Db} \xrightarrow{\alpha}$ together with $^{262}\mathrm{Bh} \xrightarrow{\alpha} {}^{258}\mathrm{Db} \xrightarrow{EC} {}^{258}\mathrm{Rf} \xrightarrow{SF}$ decay mode, it was possible to assign EC-branching ratio for ^{258}Db to be $b_{EC} = 36 \pm 11\%$, which agrees well with the value 33^{+9}_{-5} reported in [70]. By means of Re-α_1-α_2 correlations the half-lives of 3.81 ± 0.56 s and 15.8 ± 3.5 s could be assigned to ^{258}Db and ^{254}Lr, respectively. These values are consistent with values of $3.0^{+0.8}_{-0.6}$ s and $10.0^{+4.5}_{-2.4}$ s reported in [75] as well as the values of $4.4^{+0.9}_{-0.6}$ s and 13^{+3}_{-2} s presented in [52]. Mentioned isotopes were also produced in different experiments at SHIP and are treated in more detail in the next section 4.3. The link between the decay scheme of ^{262}Bh and theses isotopes will be given there as well.

Two time components consistent with the previous measurements could be reproduced in present experiment giving the improved values for the ground-state $T_{1/2} = 135^{+15}_{-12}$ ms and the isomeric-state $T_{1/2} = 13.2^{+1.2}_{-1.0}$ ms as seen from Fig. 4.20. The upper part of the spectrum in Fig. 4.20b) above $E_\alpha \sim 10190$ keV clearly lacks the long time component. The α-group at 9812 keV not observed in

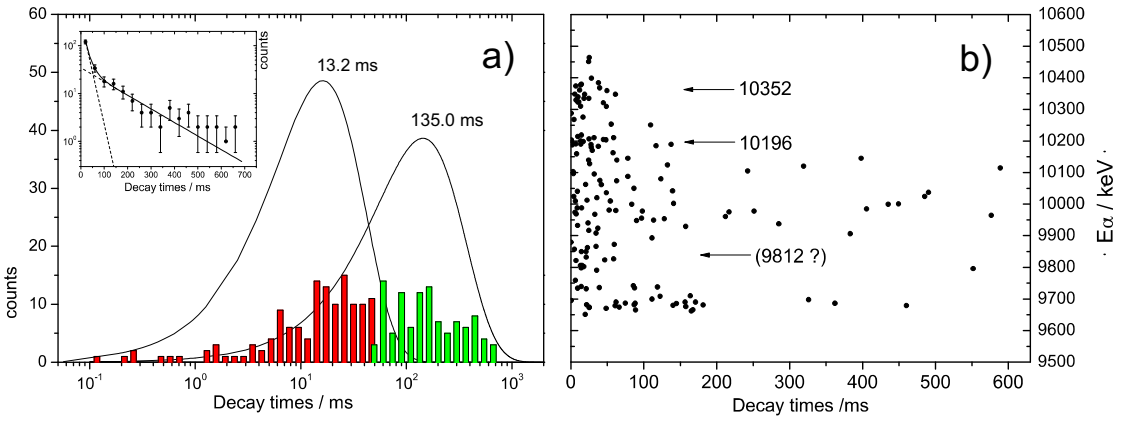

Figure 4.20: **a)** Time distribution of ^{262}Bh decays for both isomeric-state (red histogram) and the ground-state (green histogram). The curves represent the density distribution of counts in a radioactive decay on a logarithmic time scale [36]. The embedded picture represents the decay curve for ^{262}Bh constructed from Re-α_1 correlations with two component fit. **b)** Plotted decay times for ^{262}Bh α-region 9.6 - 10.5 MeV taken from Re-α_1 correlations showing three components representing short living isomer.

E_α/keV	i_α/%	$T_{1/2}$/ms	b_{EC}/%	b_{SF}/%
9684	16.7±3.5	135^{+15}_{-12}	< 3.0±1.0	2.1±1.0
9737 ^{t}	4.9±1.8			
9812	7.4±2.2			
9865 ^{t}	4.3±1.7			
9980	21.6±4.0			
10044	3.1±1.4			
10100	9.9±2.6			
10140 ^{t}	1.9±1.1			
^{m}10196	13.0±3.0	$13.2^{+1.2}_{-1.0}$	-	-
^{m}10267 ^{t}	3.1±1.4			
^{m}10352	14.2±3.2			

Table 4.6: List of spectroscopic information derived for the isotope ^{262}Bh. Three last lines abbreviated ^{m} represent isomeric-state in ^{262}Bh and those marked by ^{t} have only tentative assignment. Coefficients b_{EC} and b_{SF} are common for both states.

[75] but reported in [76] on the basis of three counts also seems to lack the time component above 70 ms, however to assign it to the isomeric state would be still preliminary based on this data.

It must be emphasized that a few hundred decays recorded for ^{262}Bh in the

pause spectrum is far from the sufficient statistics to perform spectroscopy with the purpose of spin and parity assignment for individual levels in the decay scheme for this heavy odd-odd nucleus. Nevertheless it represents the best quality data so far acquired for this isotope in R-212 experiment. Its purpose laid in the check of feasible usage of the targets based on the oxide and/or fluoride compounds and evaluation of possibilities for in-depth investigation by means of decay α-γ spectroscopy in future longer irradiations. However, taking into account the enhanced quality of the data, some possible decay scenarios are discussed here.

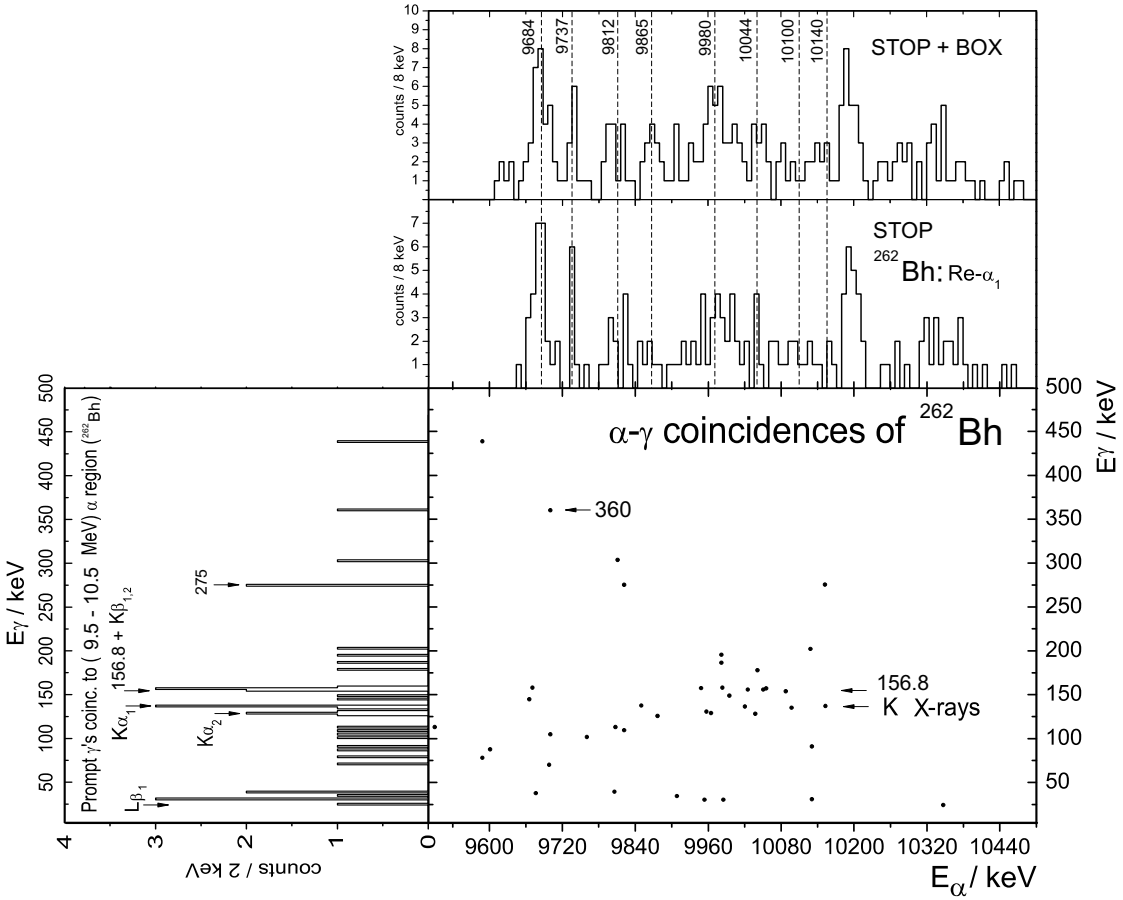

Figure 4.21: Two dimensional matrix (center) of prompt $\alpha - \gamma$ coincidences for ^{262}Bh α-region. The upper two figures show corresponding α-spectra of ^{262}Bh taken from Re-α_1 correlations. One represents stop detector events only and the second one having added the events with the summed energy $E_{STOP+BOX}$. The figure on the left represents the projection of the prompt coincidences on the E_γ axis for α-region E_α = 9.5 - 10.5 MeV.

Concerning the spectroscopic data derived for ^{262}Bh, relatively good agreement can be found in energies of individual peaks as well as the overalls decay pattern with the previous work of Ref. [75] and also recent work of Ref. [76]. Although

the appearance of some lines listed in table 4.6 can be due to summing of lower energy α-particles and conversion electrons which at present state can not be clearly distinguished. For the two most pronounced α-lines at 9684 keV and 10196 keV belonging to the ground-state and isomeric-state, respectively, the measured FWHM values are 24 and 32 keV. This suggests that these α-decays populate the levels in the daughter ^{258}Db not de-exciting by internal conversion but rather by γ-transitions. Acquired statistics is unfortunately not sufficient to measure these γ-lines in respect to collected number of α-decays in these peaks and total efficiency for α-γ coincidences at most 16 % giving the values for expected number of α-γ coincidences 3^{+11}_{-3} and 4^{+12}_{-3}, respectively. On the other hand it is also possible that lifetimes of the levels populated by these α-decays may be some μs (or longer); then CE will not add up with α-particles and γ/X-rays will be delayed. This has to be clarified in future synthesis of ^{262}Bh and its daughter ^{258}Db with possibility to correlate recoils and αs with delayed γs and/or X-rays.

Needed piece of information to stabilize the decay path of ^{262}Bh is the observation of such α-γ coincidences that would stabilize the relative position of isomer and ground state. If the isomeric-state observed to decay by α-particle emission with the half-life of $13.2^{+1.2}_{-1.0}$ ms is considered to lay above the ground state, than the competing γ-decay into this ground state would need to have the half-life of comparable or longer value. If its placement is taken speculatively to be located about 0.1 - 0.3 MeV above the ground-state and decay time to be of the order of $\geq 10^{-3}$ s, than the multipolarity of such transition would be expected to be either one of M3, E3 or higher. Unfortunately free data collection mode when γ-signals can trigger the event acquisition was not used in R-212 therefore it was not possible to search for delayed Re-γ correlations and this question needs to be solved in later measurements.

The α-γ matrix for prompt coincidences shown in Fig. 4.25 reveals the presence of K X-rays from the de-excitation of levels in the daughter nucleus ^{258}Db. Namely two peaks at 136.5 and 129.2 keV corresponding to K_{α_1} and K_{α_2} X-rays respectively are clearly separated. The collected number of four counts in each of these peaks is within the statistical uncertainty and agrees with calculated relative intensities of 43.6 and 29.2 % [70]. The line at $E_\gamma = 156.8$ keV consisting of six counts can have a contribution from K_{β_1} and K_{β_2} X-ray components with energies of 153.7 and 158.0 keV, respectively with summed intensity of 15.4 %. The observed intensity in this line, however can not be attributed to the statistical fluctuation according to [36] with overestimated number for contributing K X-rays of $2^{+2.6}_{-1.3}$. Consequently it can be assigned to contain a real γ-transition. Another assumption that can be drawn from Fig. 4.25 is that the even the highest energy α-line at $\sim$ 10140 keV can not represent the g.s. to g.s transition. This is evident from the observation of K X-rays over the α-region 8950 - 10150 keV. Taking into account the binding energy $E_K^{bind} = 160$ keV on the K-shell for Z=105 and the conservative estimate that the lowest emitting level is populated by 10044 keV α-decays, resulting g.s. to g.s. transition should have the energy not lower than $\sim$ 10200 keV + E_{e^-}. Non observation of such decays suggests that this transition is strongly hindered below

the experimental sensitivity. Concerning the assumed 157 keV γ-transition, quite broad distribution of coincident α-decays from 9950 to 10085 keV suggests that the emitting level, tentatively assigned to be populated by 9980 keV transition, is either strongly fed by IC from the higher level or it is followed by IC to to the lower level. Assuming the strong internal conversion on the K-shell from the level fed by 9865 transition to the level fed by 10100 α-decays, resulting $E_{e^-} \sim 85$ keV for the maximum EC-summing would have a major contribution to the peak at 9980 keV. This would be however somehow in contrast to the number of observed γ-decay of 157 keV, so more probably this alternative would have to come from the L(M)-shell conversion. Another scenario is to attribute the strongly IC-decaying level to the one populated by 157 keV transition. At the present quality of the data this question can not be answered satisfactorily.

The line at $E_\alpha = 9684$ keV has two interesting γ-events coincident to it. One is located at $E_\gamma = 360$ keV which would point to the total Q-value of about 10040 keV. The α-line at this energy is also observed as seen in the spectrum 4.25. Together with small width of 9684 keV α-line, this could indicate a possible E1 transition. Another coincident γ-event has the same energy of 157 keV as the events discussed in previous paragraph, that could indicate another transition into the level emitting 157 keV γs. However, at present statistics these observations must be taken only as a speculations.

Possible future synthesis of ^{262}Bh at SHIP should try to utilize the reaction ^{208}Pb + ^{55}Mn with about two times higher cross section [76] for $E^* = 14.5$ MeV than for the reaction used in R-212. Doubling the present statistics should be sufficient to unambiguously resolve the possible γ-transitions from the levels populated by α-decays with $E_\alpha = 9684$ and 10196 keV. The expected number of measured coincident γs should be 6$\pm$3 considering internal conversion less that 20 % for both transition which seems reasonable taking into account the width of these lines observed in the present analysis. The situation about $E_\gamma = 157$ keV transition would also be clarified at such conditions.

4.3 Isotope ^{258}Db and its decay products

4.3.1 Experiment

The experimental run R-218[6] was performed at SHIP in GSI Darmstadt from 14.4. 2004 till 27.4. 2004 and was aimed at the production of isotopes ^{258}Db and ^{255}Rf through the reactions ^{209}Bi(^{50}Ti,1n-2n)^{257,258}Db and ^{207}Pb(^{50}Ti,2n)^{255}Rf, respectively. This work concentrates on the analysis of the first mention reaction. As a beam, enriched material of ^{50}Ti was used, which was diluted in gold. The total amount of ^{50}Ti in the electrode was $\sim$ 15 % giving the current of $\sim 6.2 \times 10^{11}$ particles/s. Based on a positive experience from previous beam-times the targets

[6]This run was the first one performed at SHIP that used new UNILAC accelerator beam line that reduced the background.

were produced from Bi_2O_3 compound to withstand higher temperatures and having the average thickness of $\sim 430\mu g/cm^2$. Transmission efficiency through the velocity filter SHIP was estimated to be ~ 40 % for the fusion products and detection efficiency for the stop detector alone ~ 47 % and $\sim$ 85% for the combination stop + box detectors. The compound system of ^{259}Db was leaving the target with the energy of ~ 42 MeV if fusion at the middle of the target was considered. The total amount of projectiles that impinged on the target was $\sim 2.7 \times 10^{20}$ during the irradiation of ^{209}Bi targets.

The first part of the experiment was dedicated to production of ^{258}Db so the energy of titanium beam in the laboratory frame was chosen to 235.5 MeV, which should correspond to the maximum of 1n channel. Considering the energy losses in the upstream carbon layer of about $\sim 40\mu g/cm^2$ and in 1/2 of the bismuth target final excitation energy E* of the compound nucleus was close to 15.5 MeV at the moment of fusion, which corresponds to production cross section of ~ 4 nb for ^{258}Db and $\sim 7{\times}10^{-2}$ nb for ^{257}Db according to HIVAP calculations. It was also sought for ^{257}Db produced by 2n channel from the reaction ^{50}Ti + ^{207}Pb by looking for $\alpha_1 \rightarrow \alpha_2 \rightarrow$ correlations using also box detectors and anticoincidence condition on α-signals. With these conditions there were 14 correlation candidates for ^{257}Db$\rightarrow^{253}$Lr $\rightarrow$ found. With total detector efficiency close to 90% and α-branching $b_\alpha = 0.75$ for ^{249}Md one could expect to find ~ 8 decay chains ^{257}Db$\rightarrow^{253}$Lr$\rightarrow^{249}$Md$\rightarrow$. There were five such chains found. Even though one chain of ^{257}Db$\rightarrow^{253}$Lr$\rightarrow^{249}$Fm$\rightarrow$ could be expected based on $b_\alpha = 0.15$ for ^{249}Fm, none was actually found. Taking into account about 170 $\alpha_1 \rightarrow \alpha_2 \rightarrow$ correlations found for ^{258}Db, the production ratio ^{257}Db/^{258}Db is $\sim 8\%$, which is a bit contrary to the ratio of about 2 % resulting from the HIVAP calculations. However, if we consider the fusion to take place in 1/4 of the target thickness, the resulting E* is close to 16.8 MeV and for the ratio ^{257}Db/^{258}Db we obtain $\sim 8\%$. If one accounts also for the HIVAP systematic error that can reach up to one order of magnitude, the predicted and measured production rates for ^{257}Db agree within the uncertainty of the excitation energy of the compound system. From the total number of 14 correlations ^{257}Db$\rightarrow^{253}$Lr$\rightarrow$ and 4 correlations ^{257}Db$\rightarrow^{253}$Lr$\rightarrow^{249}$Md$\rightarrow$ it was possible to extract half lives calculated using procedure described in [36]. These values agree with previously reported numbers [34]. No γs were observed with α-decays assigned to ^{253}Lr. One gamma event with the energy 254 keV (103.2+150.2) was observed in coincidence with 8040 keV α-decay of ^{249}Md which confirms the previously measured data (for more information on ^{257}Db see section 4.4).

4.3.2 Calibrations

For the purpose of the test reaction as well as α-energy calibration of the stop and box detectors, the reaction ^{170}Er(^{50}Ti,4n)^{216}Th was chosen. The final α-spectrum taken between the beam pulses is shown in Fig. 4.22. In order to shift the production cross section closer to the maximum of the excitation function for ^{216}Th, a degrader foil from old Pb and Bi targets was placed in front of the

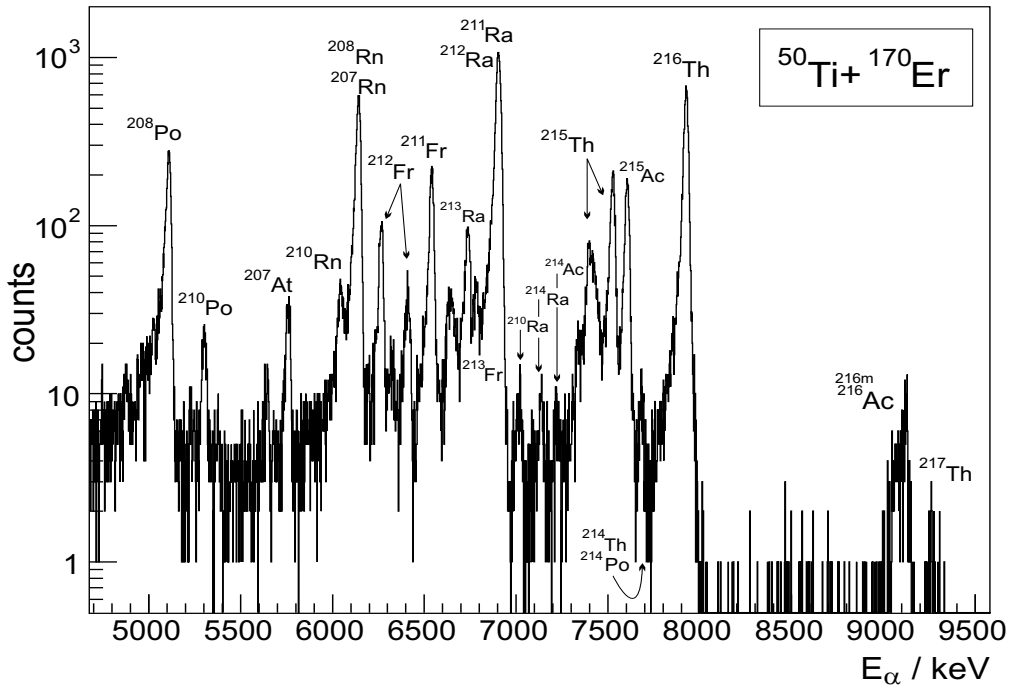

Figure 4.22: The pause α-spectrum from the reaction ^{170}Er(^{50}Ti,3-5n)^{215,216,217}Th used for the calibration of PSSD and BOX detectors.

^{170}Er target, however, both isotopes ^{216}Th as well as ^{215}Th were produced in ratio ^{216,216m}Th/^{215}Th ~ 2.7 given by HIVAP calculations and $\sim 2.8 \pm 0.2$ derived from the experimental values. For the α-calibration purposes three α-lines were used - namely ^{216}Th, ^{211,212}Ra and ^{217,208}Rn. For the dublet lines, the average energy weighted over experimental intensities was used. Final resolution for PSSD was FWHM = 28 and 26 keV for two lines of 7921 keV (^{216}Th) and 7604 keV (^{215}Ac), respectively. The resolution for the box detector was estimated for the same ^{216}Th α-line to be 52 keV FWHM. Also a rough fission calibration was done using pause spectra from the high energy branch and three most intensive α-lines of ^{217,208}Rn, ^{211,212}Ra and ^{216}Th.

The calibration of four clover detectors was done using sources of ^{133}Ba and ^{152}Eu. The precision of gamma calibration was influenced by nonlinearity of one of the clovers, however the introduction of third order polynomial fit over the calibration values helped to diminish this drawback. Total resolution for two lines of 121.78 keV (^{152}Eu) and 356.02 keV (^{133}Ba) was FWHM = 2 keV which is the same value within the errors of the fitting procedure as FWHM for the individual CLOVER crystals.

4.3.3 Spectroscopy of ^{258}Db

It was found in production of ^{262}Bh from the experiment R-212 using the ^{209}Bi target discussed in previous section 4.2, that the both states of the mother isotope ^{262m,g}Bh are linked through α-α correlations with the same α-energy region of ^{258}Db. This means that despite the fact that certainly different states in ^{258}Db are populated by α-decay of ^{262}Bh (complex α-spectrum), but only α-decay from one state (probably ground-state) in ^{258}Db is being observed. This could also indicate, that the level structure of ^{258}Db is different than that of its mother ^{262m,g}Bh. Such a verdict is not surprising on the other hand as there is no eminent reason for the level structures to bear resemblances as in odd-odd nuclei the low-lying states (including the ground-state) are made by vector coupling of unpaired proton and neutron spins. This is further supported by very different α-pattern of ^{258}Db compared to its mother. Nevertheless some qualitative information about the level structure of these isotopes can be derived from recent experiments. The summary concerning detail α-γ analysis of ^{258}Db is presented in the following points:

- As seen from Fig.4.24 nice narrow α-γ coincident group of E_γ = 220.6 keV depopulating an excited level in ^{254}Lr is connected with the ^{258}Db α-decays of E_α = 9085 keV. Taking into account experimentally observed number of counts listed in table 4.8 and the K-shell binding energy in Z = 103 of $E^K_{bind.}$ = 153 keV, the upper limit for the conversion coefficient of this γ-transition can be estimated to be $\alpha_K \leq 3$. This basically excludes all magnetic transitions for which $\alpha_K \geq 4.9$ are predicted [61] for Z =103 and E_γ =221 keV, but is not decisive about the multipolarity of the electric transition. However it can be reasoned that only E1 or E2 candidates are possible since the γs are observed as prompt and secondly the α-transition to ^{254}Lr ground-state must have energy at least 9305 keV.

- On the other hand the γ-group at E_γ = 156.9 keV is spread over the α-region of 9000 to 9150 keV, indicating that the level connected with this transition is either fed by or is decaying into the level de-exciting by internal conversion.

- Compiled information in data table [70] lists the existence of 95 keV γ-line with M1 multipolarity deexciting the level in ^{254}Lr. In recent experiments there was only one γ-event accompanying the first alpha in Re-$\alpha_1(\gamma)$-α_2 correlation chain observed with this energy. Even though the energy differences of assumed α-peaks are in favor of such γ-transition, there is no indication in Fig. 4.24 for a separate γ-group at this energy. Based on present data with clear indication for two separate γ-lines de-exciting the levels in daughter nucleus ^{254}Lr assignment and origin of 95 keV γ-line is rather questionable.

In previous ship experiment [45] it was observed by searching for the isomeric state in ^{258}Db that its α-spectrum showed different pattern when correlated to ^{254}Lr compared to correlations to EC-product ^{254}No. Specifically in correlations to ^{254}No the α-line of ^{258}Db at E_α = 9160 keV observed with the intensity of about

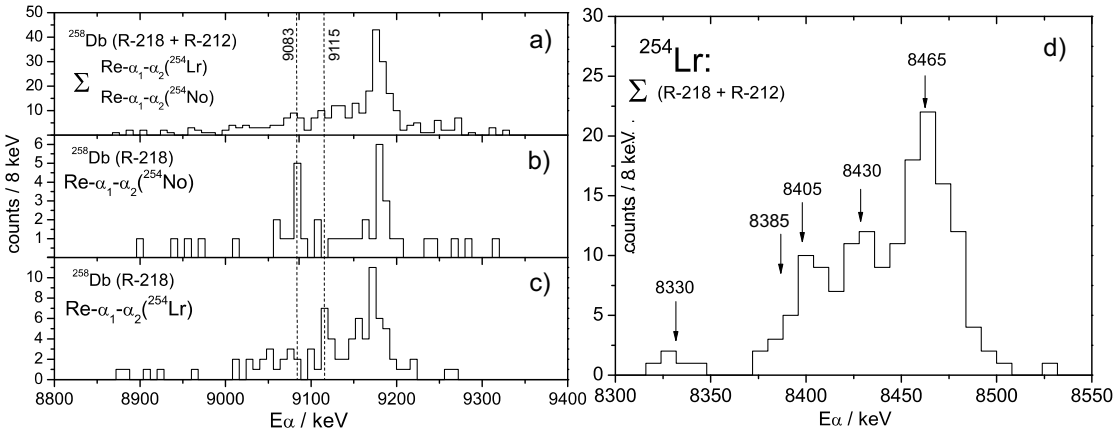

Figure 4.23: Spectrum of ^{258}Db taken from **a)** the sum of experiments R-218 and R-212 and from correlations to both ^{254}Lr and ^{254}No. **b)** from R-218 and correlations to ^{254}No α-region. **c)** from R-218 and correlations only to ^{254}Lr α-region.**d)** α-region of ^{254}Lr summed from correlations of both R-218 and R-212. It should be kept in mind that this spectrum can not be directly compared against the number of found α-γ coincidences shown in Fig. 4.24.

20 % when correlated to ^{254}Lr was highly suppressed. Such a deviation could be interpreted in two ways:

1. The decays of ^{258m}Db going through $^{258m}\mathrm{Db}\xrightarrow{\alpha}\ ^{254m}\mathrm{Lr}\xrightarrow{EC}\ ^{254}\mathrm{No}\xrightarrow{\alpha}$ and those decaying like $^{258g}\mathrm{Db}\xrightarrow{\alpha}\ ^{254g}\mathrm{Lr}\xrightarrow{EC}\ ^{254}\mathrm{No}\xrightarrow{\alpha}$ have different α-energies of ^{258g}Db and ^{258m}Db, and very similar α-energies for ^{254g}Lr and ^{254m}Lr, yet different EC-branching rations for ^{254g}Lr and ^{254m}Lr,
   or

2. the decays of ^{258}Db proceed via three paths. One populates ^{250}Md through $^{1)}\ ^{258}\mathrm{Db}\xrightarrow{\alpha}\ ^{254}\mathrm{Lr}\xrightarrow{\alpha}$. And remaining ones $^{2)}\ ^{258}\mathrm{Db}\xrightarrow{\alpha}\ ^{254}\mathrm{Lr}\xrightarrow{EC}\ ^{254}\mathrm{No}\xrightarrow{\alpha}$ and $^{3)}\ ^{258}\mathrm{Db}\xrightarrow{EC}\ ^{258}\mathrm{Rf}\xrightarrow{\alpha}\ ^{254}\mathrm{No}\xrightarrow{\alpha}$, both feed ^{254}Lr. This means that α-spectrum of ^{258}Db correlated to the decay of ^{254}Lr would be due to sequence $^{1)}$, while the alpha-spectrum correlated to the decay of ^{254}No would be due to sequences $^{2)}$ and $^{3)}$.

The observation of α-line correlated only to ^{254}No which would be missing in correlations to^{254}Lr could represent so far unmeasured α-branch in ^{258}Rf. Despite the higher statistics in recent experiments compared to older results of [52] these issues could not be unambiguously disentangled. The spectra shown in Figs. 4.24 b) and c) represent the α-region of ^{258}Db derived in R-218 from the correlations of the kind Re-α_1-α_2 and Re-α_1-$\alpha_2^{'}$, respectively. They show the mentioned deviation in ^{258}Db α-pattern as indicated in previous SHIP experiments. However

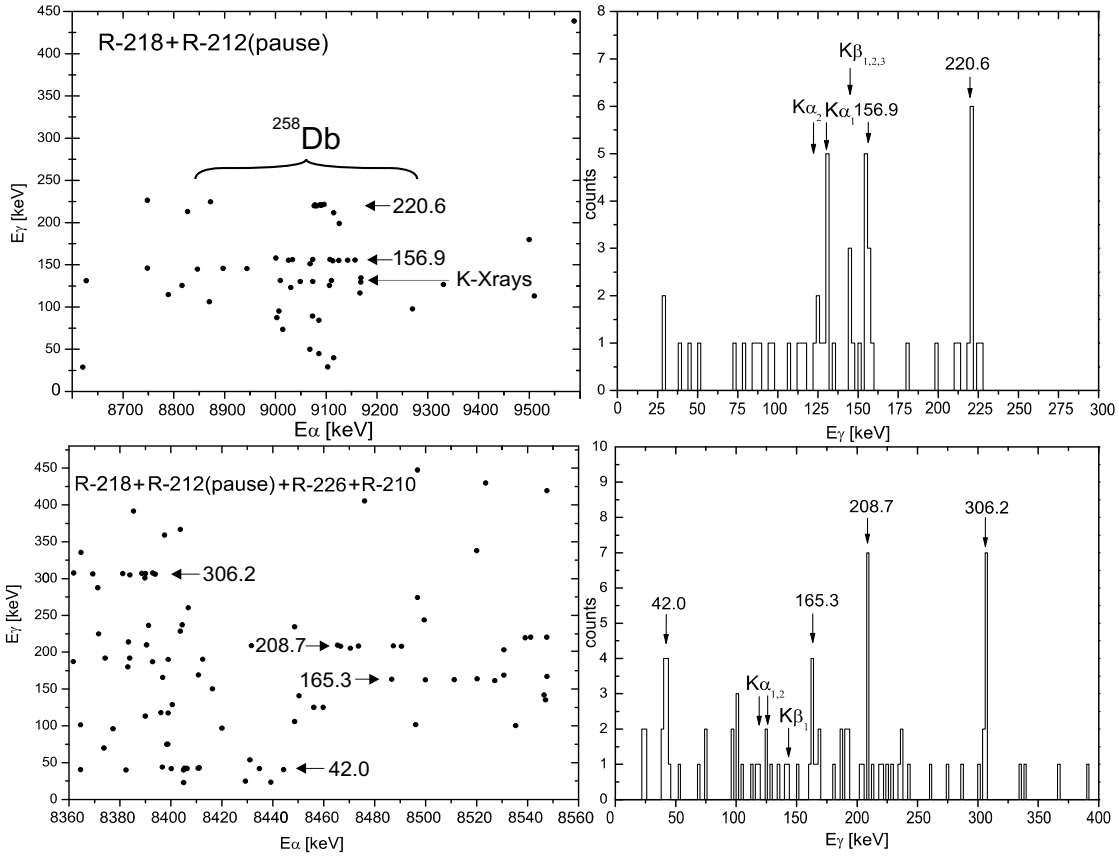

Figure 4.24: Upper two pictures show two dimensional α-γ matrix (left spectrum) for ^{258}Db and its projection to y axis (right spectrum). The data were added from experimental runs R-218 and R-212. Lower spectra represent the same situation for isotope ^{254}Lr and in this case data are the sum of the runs R-218, R-212, R-210 and R-226.

in present case different α-energy of suppressed peak Eα = 9115 keV was measured in correlations to ^{254}No in present data together with enhanced peak at Eα = 9083 keV. The energy of enhanced peak, if indeed originating from ^{258}Rf and representing the transition to the ground-state with Q_α = 9226 keV would reproduce well the Q-value of 9250 keV taken from systematics and reported in Ref. [70]. Nevertheless, in R-212 where ^{258}Db was produced as the α-daughter of ^{262}Bh the above mentioned differences in ^{258}Db α-spectrum could not be confirmed. Although in respect to direct vs. indirect production of specific isotope, different ratio of ground-state and isomeric-state can be expected. This is again in contrast to general agreement in ^{258}Db α-spectrum pattern measured in R-212 and R-218. This observations therefore require more precise measurements. The best way to disentangle this issue would be to measure ^{258}Rf directly, for example utilizing reaction ^{238}U(^{24}Mg,4n)^{258}Rf and to get more precise data with at least ten times higher statistics for the isotope ^{258}Db.

As seen from table 4.7 the hindrance factors for ^{258}Db are considerably higher than those of its daughter ^{254}Lr or the neighboring isotope ^{257}Db discussed in the next section 4.4. It might indicate that the ground state transition is even below the level populated by E_α = 9306 keV and thus the decays into the higher lying levels is suppressed by unfavorably small Q-value. This behavior is also observed for other N = 153 odd-odd nucleus ^{252}Es. Its role must also play the crossing of closed neutron subshell N=152 by the α-decay. Hindrance factors > 1000 indicate that this crossing causes major reorganization of the nucleons when α-particle is emitted. It also means that the parity change takes place during the decay and the spin projections of the initial and final states should be antiparallel.

4.3.4 Spectroscopy of ^{254}Lr

Compared to previous experiment described in and [54] aimed at direct production of ^{254}Lr utilizing the reaction ^{48}Ca + ^{209}Bi, in our experiment the isotope ^{254}Lr was produced indirectly as a decay product of ^{258}Db either in reaction ^{209}Bi(^{50}Ti,1n-2n)^{257,258}Db or ^{209}Bi(^{54}Cr,1n)^{262}Bh and altogether about 166 and 71 of its decays, respectively were detected in the pause spectrum. In order to improve the knowledge on nuclear structure of this isotope all statistics for α-γ coincidences for α-energy region from 8360 to 8560 keV, was summed from the experiments utilizing both, direct and indirect production in experimental runs R-210, R-212, R-218 and R-226. The resulting α-γ matrix and the γ-projection are shown in lower spectra of Fig. 4.24. The interpretation of these results ca be summarized as follows:

- Two alpha lines reported in [52] agree with present lines of 8405 and 8465 keV as shown in Fig. 4.23 while in [54] the α-structure could not be disentangled in separate lines. In addition two other α-lines of 8330 keV and 8430 keV appear in present analysis. It should be also noted that Re-α-α correlations with ^{254}Lr being the third generation, with energies up to 8.7 MeV could be found. Relative intensities and half lives are summarized in table 4.7. Considering the value of $T_{1/2} = 13.4^{+4.2}_{-2.2}$ s for its half life derived in present analysis, one can conclude excellent agreement with previously measured data.

- The electron capture branching of ^{254}Lr was calculated by comparison of Re-^{258}Db$\overset{\alpha_1}{\rightarrow}$ ^{254}Lr$\overset{\alpha_2}{\rightarrow}$ and Re-^{258}Db$\overset{\alpha_1}{\rightarrow}$ ^{254}Lr$\overset{EC}{\rightarrow}$ ^{254}No$\overset{\alpha_2}{\rightarrow}$ decay paths. The value of $b_\alpha = 72 \pm 3$ % corrected for the known SF and EC branches of ^{254}No is again in good agreement with older measurements. However only one possible candidate was found, resulting in $b_{\rm SF} < 0.8$ % for ^{254}Lr.

- In present measurement two γ-lines reported in [54] could be reproduced with the improved energies of 306.2 keV and 208.7 keV and tentatively assigned [54] line at unusually low energy of 42.0 keV was unambiguously identified as seen from Fig. 4.24. Despite the drawback of a higher α-γ background it is

Isotope	E_α / keV	i / %	$T_{1/2}$ / s	HF	b_{EC}/ %	b_{SF}/ %
^{258}Db	8905	2.2±1.1	$4.7^{+4.6}_{-1.6}$	323	30±3	-
	9022	12.9±2.9	$6.0^{+1.6}_{-1.0}$	169		
	9085	12.3±2.8	$3.9^{+1.1}_{-0.7}$	177		
	9128	24.2±4.1	$3.1^{+0.6}_{-0.4}$	98		
	9173	42.7±5.9	2.6±0.3	61		
	9261	4.5±1.6	$5.9^{+3.2}_{-1.5}$	2400		
	9306	1.1±0.8	$3.5^{+8.3}_{-1.4}$	8100		
^{254}Lr	8330	2.1±0.9	$13.3^{+10.6}_{-4.1}$	76	28±3	<0.8
	8385	6.8±3.6	$13.1^{+2.7}_{-2.0}$	29		
	8405	7.9±2.8	$13.3^{+2.6}_{-1.9}$	21		
	8430	13.2±2.5	$12.0^{+2.6}_{-1.8}$	23		
	8465	70.0±7.0	$15.1^{+1.2}_{-1.1}$	7		

Table 4.7: Summarized basic spectroscopic properties of ^{258}Db and its decay product ^{254}Lr as deduced from experiments R-218 and R-212. As the situation concerning the α-branch of ^{258}Rf can not be unambiguously solved at present, all intensities and branchings are calculated as if all decays from 8.8 to 9.4 MeV originate from ^{258}Db.

possible, due to improved statistics to already draw some conclusions about the levels being populated in the daughter product ^{250}Md. Even though the binding energy on the K-shell for the element with Z = 101 is $E^{K}_{bind.}$ = 146.5 keV and so the transitions 306.2 keV and 208.7 keV could be K-converted, the K X-rays are quite subtle as seen in γ-projection spectrum of Fig. 4.24. Indeed, the transitions with the energies 306 and 209 keV must be only weakly converted based on non-observation of the summing effect with the conversion electron that would produce α-summing energy 'lines' at around 8530 - 8550 keV for K-shell conversion for these two transitions and at 8640 - 8660 keV for L-shell conversion. This means that the bulk of the internal conversion that evidently influences the α-spectrum of ^{254}Lr as seen from Fig. 4.23 b) most probably proceeds through the conversion on the L(M)-shells from other levels that those populated by 8385 and 8465 keV transitions. It must be however kept in mind that different decay paths, i.e. for example, the 306.2 keV transition from the level populated by the 8385 keV α-decay must not necessarily be the only decay path of this level. This is certainly true for the level populated by 8405 keV α-decay and emitting 42 keV γs. As seen in lower spectra in Fig. 4.24 the major group of 42 keV events is concentrated over 8405 keV α-region. But two counts at lower α-energy of $\sim$ 8370 keV and also two at the higher energy of $\sim$ 8440 keV are present as well. This suggests that this level populated by 8405 keV α-transition is fed from above by converted transition, plus 42 keV γ-decay populates level that is also converted. The level itself, emitting 42 keV γs is

^{258}Db						
X-ray	E / keV	i / %	$N_{\mathrm{count}}^{\mathrm{exp}}$	γ-line	E / keV	$N_{\mathrm{count}}^{\mathrm{exp}}$
$K_{\alpha 1}$	130.6	44	6	γ_1	220.6	7
$K_{\alpha 2}$	123.9	29	4	γ_2	156.9	10
$K_{\beta 1}$	147.1	11	3			
^{254}Lr						
X-ray	E / keV	i / %	$N_{\mathrm{count}}^{\mathrm{exp}}$	γ-line	E / keV	$N_{\mathrm{count}}^{\mathrm{exp}}$
$K_{\alpha 1}$	125.2	44	2	γ_1	306.2	9
$K_{\alpha 2}$	119.2	29	1	γ_2	208.7	7
$K_{\beta 1}$	141.1	11	1	γ_2	165.3	6
				γ_2	42.0	11

Table 4.8: Summary of theoretical energies and intensities of the most intensive K X-rays for Z = 103 and 101 taken from Ref. [70] and experimentally observed number of counts at these energies from decay of ^{258}Db and ^{254}Lr. Also listed are γ-lines de-exciting levels in these isotopes. The quantity $N_{\mathrm{count}}^{\mathrm{exp}}$ denotes the number of experimental events counted in $\pm$ 2 keV interval around the mean γ and/or X-ray energy.

most probably converted only weakly for two reasons. Due to low detection efficiency of about $\varepsilon_{\mathrm{det}} \sim 5\%$ at this energy region, majority of transitions must proceed through γ-radiation. Secondly the width of $\sim$ 25 keV of the corresponding α-γ group represents the PSSD resolution. This can be also used as an argument that the α-line at about 8430 keV is real since if 42 keV transition would be heavily converted the peak representing the total energy summing would reach at about 8425 keV and therefore contributing heavily to this α-region. This however does not seem to be the case.

- As the characteristic K X-rays are not precisely located over any of above mentioned γ-transitions capable of conversion on the K-shell, only upper limits can be evaluated. Calculated values for 306 and 209 keV transitions are $\alpha_{\mathrm{K}} < 0.9$ and $\alpha_{\mathrm{K}} < 1.2$, respectively. This finding excludes all magnetic transitions. From the electric ones the choice is narrowed down to only E1 and E2, which are possible due to their life-times below μs region, as 306 and 209 keV γs are observed in prompt coincidences. Based on the present data however, it is not possible to decide between the two.

- The agreement between the sums of α-γ coincident groups of 8385 + 306 keV and 8465 + 209 keV indicates that they might populate the same state in the daughter ^{250}Md. It is also likely that this summed energies represent the total Q-value of the decay from ^{254}Lr to ^{250}Md. Hence the ground-state transition should be situated around $\sim$ 8685 keV.

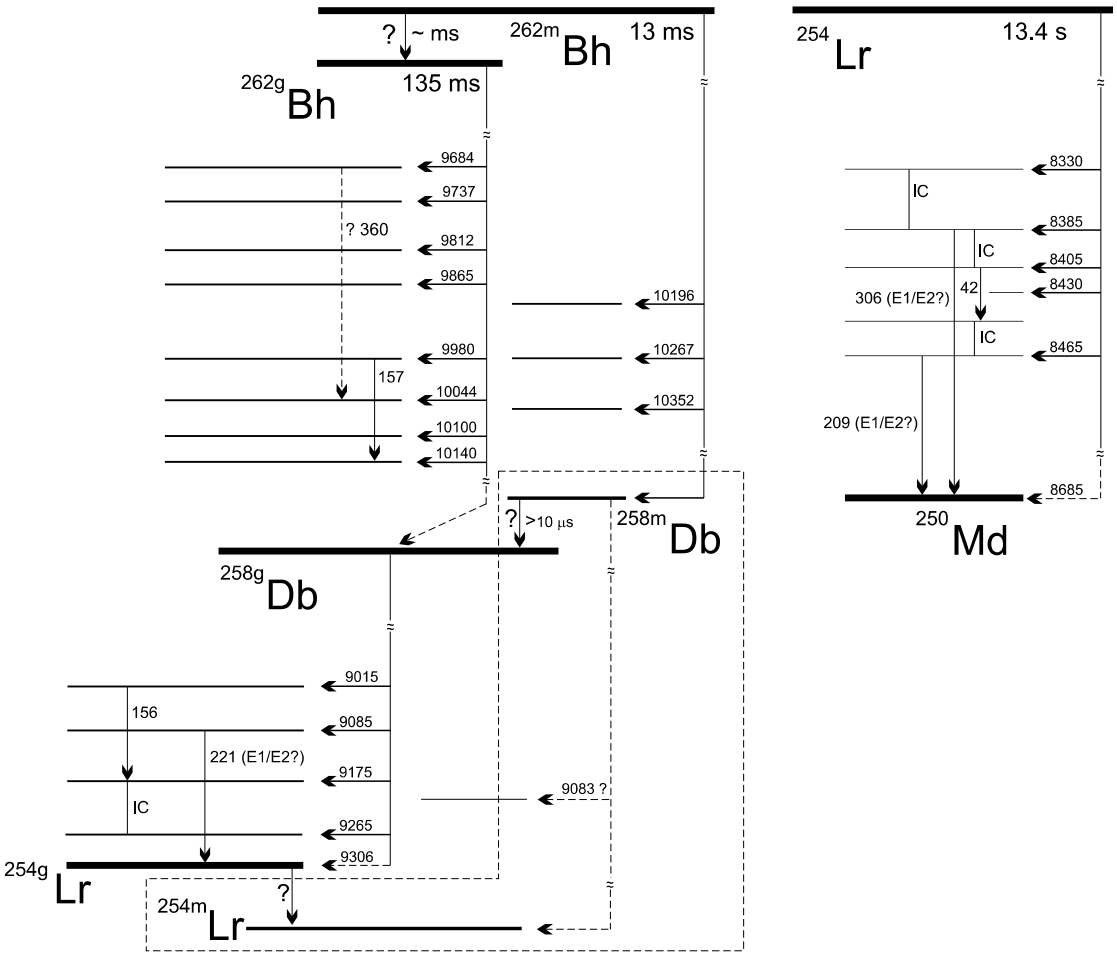

Figure 4.25: The level scheme for the decay sequence ^{262}Bh→ ^{258}Db→ ^{254}Lr→. Assignment is based on the data analysis discussed in sections 4.2, 4.3.3 and 4.3.4. Placement of ^{258m}Db and ^{254m}Lr must be viewed only as a working hypothesis.

- There is an indication for yet another γ-group in Fig. 4.24 with the energy close to 190 keV located over 8370 - 8420 keV α-region, suggesting an influence with conversion electrons. Nevertheless at this stage it remains only a hint to the future experiments.

- Two more coincident γ-groups can be located over the α-region from 8490 to 8550 keV. Unambiguously identified γ-transition of E_γ = 165.3 keV has a large spread in coincident α-energy. If the emitting level is taken to be populated by 8520 keV α-decays than the sum energy would again point to about 8685 keV transition. This would however require strong population of such level from above by most probably L-converted transition This is in contrast with the shape of ^{254}Lr α-spectrum which does not show significant contribution above 8.5 MeV region. Origin of this transition other than from the decay of ^{254}Lr seems justified. This is supported by the fact that in [54]

this line was completely missing, despite its almost equal intensity with other γ-lines observed in present work. It is possible that it comes from the decay of one of the isotopes ^{255,256}Lr that were also produced with considerable intensity in R-226 and whose α-regions overlap with that of ^{254}Lr. This is also true for γ-group at $\sim$ 220 keV located over 8545 keV α-region having however only tentative character at this statistics.

Similar as in the case of its mother ^{258}Db, no sign of unambiguous identification for the isomeric state in ^{254}Lr could be found in the data. Due to the low collected statistics for the isotope ^{250}Md or its EC-product ^{250}Fm, these isotopes were not the object for spectroscopic studies within the scope of this work.

4.4 Spectroscopy of ^{257}Db and its decay products

As a part of experiment R-218, in four days of irradiating a bismuth target with titanium beam with the maximum intensity of $\sim$ 350 pnA, approximately 7.6 $\times 10^{17}$ projectiles were delivered to the target. PIG source was used with enriched material ($\sim$ 15% of ^{50}Ti) dissolved in gold. Delivered beam had the energy of E_{beam} = 4.85 AMeV. Two target wheels, first made from metallic bismuth and the other one from the compound of Bi_2O_3 were used for irradiation with average thickness of 450 and 422 μg/cm^2, respectively. Considering that the fusion takes place in the middle of the target and taking into account the energy losses, the calculated excitation energy of the compound nucleus was E^*=22 MeV. This energy should correspond to the maximum of 2n channel for reaction ^{209}Bi + ^{50}Ti $\rightarrow$ ^{257}Db with the value for the crossection $\sigma \sim 3$ nb [34].

The recent experiment gave the value[7] of $\sigma = 2.12 \pm 0.10$ nb which, considering approximately by a factor of 2 times higher number of synthesized nuclei of ^{257}Db should be more accurate number. On the other hand the crossection calculation can vary by the factor of 2 resulting from systematic error formed mainly by the uncertainty in separation efficiency. Therefore the values are consistent to each other. At this excitation energy also the isotope ^{258}Db is produced through the 1n channel. Based on the amount of produced daughter isotopes ^{254}Lr and ^{253}Lr the estimated ratio of ^{258}Db/^{257}Db was 0.29 $\pm$ 0.05, which should correspond to a crossection for 1n channel of $\sim$ 0.5 - 0.6 nb. The energy of the ERs after they have been separated by SHIP was calculated to be up to 35 MeV at the moment of implantation. This calculation was done assuming they originated from the fusion in the middle of the target and lost the energy passing through the target, its carbon backing and six TOF foils using the computer code SRIM [44]. Their range in silicon at this energy should be $\sim$ 6 μm from which detection efficiency of the stop detector was calculated to be ε_{det} $\sim$ 53 %.

[7] Only statistical error was taken into account.

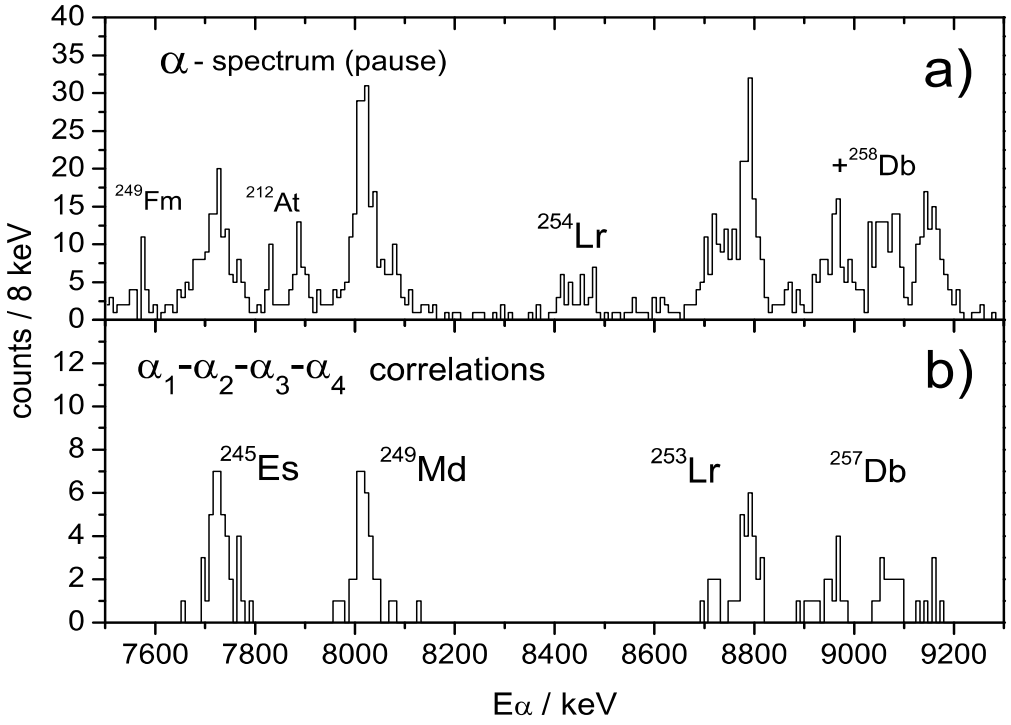

Figure 4.26: **a)** Total α-spectrum taken from the pause of the experiment R-218. **b)** α_1-α_2-α_3-α_4 correlations spectrum showing the members of ^{257}Db decay chain.

The experimental run R-218 at SHIP was the first one using new wider UNILAC accelerator beam line to suppress the background caused by interaction of beam halo with the pipe's wall. Unfortunately there were a couple of problems connected with this experimental run. Only one TOF detector of the time of flight system out of three was working properly. The efficiency of TOF was estimated to be $\varepsilon_{\mathrm{TOF}} \sim 99.0\%$. The TOF signal was taken from the time difference between the signal of one TOF detector and the signal from the implantation into the PSSD. Resulting TOF resolution was not sufficient to use TOF vs. $\mathrm{E_{MeV}}$ method to unambiguously distinguish between ER and scattered target like nuclei and/or transfer events in Re-α correlation search. Another reduction of correlation procedure efficiency came from the fact that about 30 % of all α-decay signals in the box detectors had no position, what further reduced the number of found α_1-α_2 correlations. Also worth mentioning is the fact that one of the strips of the box detector was not working and one of four clover detector segments had nonlinear characteristic. The last restriction is the resolution of the stop detector which was estimated on the basis of the resolution for individual strips from noncalibrated spectra. The average resolution (FWHM) of all 16 strips was 29 keV. The resolution for the worst 6 strips was 38 keV while for the rest it was measured to be about 24 keV.

Already known energies as well as relative intensities and half lives (see table 4.9) for observed α-lines of ^{257}Db, ^{253}Lr and ^{249}Md shown in fig. 4.26 agree within

Isotope	E_α / keV	FWHM	i / %	$T_{1/2}$ / s	HF	b_{EC}	b_{SF}
^{257}Db	8874	30	4	$3.43^{+2.34}_{-0.99}$	88	< 0.03	≤ 0.11
	8965	38	40	2.32 ± 0.16	10		≤ 0.05
	9066	56	37	2.32 ± 0.16	23		
	9155	25	19	0.67 ± 0.07	25		≤ 0.12
^{253}Lr	8620	50	5	$1.08^{+0.86}_{-0.33}$	16	< 0.02	
	8719	25	28	1.32 ± 0.14	8		0.12 ± 0.03
	8786	28	67	0.67 ± 0.06	3		0.01 ± 0.006
^{249}Md	7970	-	1	$22.4^{+13.5}_{-6.1}$	1		
	8022	26	78	22.2 ± 1.6	8		
	8080	30	19	22.2 ± 1.6	202		
	8280	-	2	$12.5^{+8.5}_{-3.6}$	63		

Table 4.9: Table summarizing basic spectroscopic properties of ^{257}Db and its decay products as deduced from this experiment.

the error bars with the values of previous SHIP experiment [34]. The uncertainties of all α-lines based on the stop detector resolution are $\pm$ 15 keV, not taking into account the uncertainty of the α-calibration whose precision deteriorates in the region of the interest (8-10 MeV) by $\sim$ 10 keV due to the absence of α-lines used for detector calibration from this high energy region.

Standard spectroscopic methods described in previous sections were used to analyze these data. Next few paragraphs describe the acquired information and new results:

- One new line of ^{253}Lr at E_α = 8620 keV could be unambiguously identified on the basis of correlation analysis. In total there were five chains of the kind Re-α_1-α_2 found with the second generation α_2 from this α-peak. Two of these chains were further correlated to another event from the decay path as can be seen from the table 4.10. Four chains originated from 9155 keV peak of ^{257}Db and one from 8965 keV peak of the same isotope. The half life of these four events of ^{257}Db is $0.47^{+0.46}_{-0.15}$ s and for the one from 8965 keV peak is $1.19^{+5.70}_{-0.54}$ s.

  These values agree well with reported values [34] for the isomeric-state and ground-state half-lives of ^{257}Db, respectively. The half-life of all ^{253}Lr events is $1.55^{+1.24}_{-0.48}$ s, which agrees with the known half life of ^{253}Lr isomeric-state [34]. Its tempting to think about two lines, because three events were located around the energy 8603 $\pm$ 2 keV and two remaining events at 8636 $\pm$ 2 keV. The difference of 33 keV is greater than the stop detector resolution suggesting in other case summing effect from the conversion electrons. But considering the low number of counts and not the best detector resolution in this experiment, this new line of ^{253}Lr is tentatively assigned at the average energy of 8620 $\pm$ 20 keV.

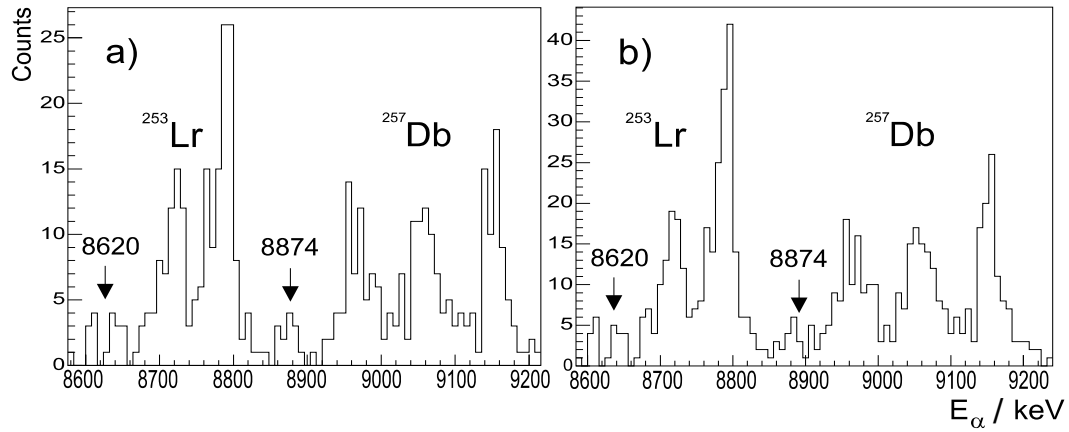

Figure 4.27: New α-lines of ^{253}Lr (8620 kev) and ^{257}Db (8874 keV). The Fig.s **a)** and **b)** represent the antiTOF spectra summed from seven and eleven best strips, respectively.

Gen.	E_α/keV	Δt/s	δx^t_{lh}/mm	δx^b_{lh}/mm
Re	-	-	-	-
^{257}Db	9143	0.55	0.79	0.73
^{253}Lr	8605	2.85	1.14	-
^{245}Es	7773	33	1.05	-
Re	-	-	-	-
^{257}Db	9144	0.57	-0.49	-0.10
^{253}Lr	8603	3.06	0.03	0.03
^{249}Fm	7578	211	-0.25	0.07

Table 4.10: The example of basic spectroscopic data for two decay chains going through a new line of ^{253}Lr. The first chain is of a kind Re→ ^{257}Db→^{253}Lr→(escaped alpha from ^{249}Md)→^{245}Es→ and the second one is Re→ ^{257}Db→^{253}Lr→(EC-decay of ^{249}Md)→^{249}Fm→. The symbols δx^t_{lh} and δx^b_{lh} denote the position differences between consecutive generation of decays as 'seen' by high and low energy branch of electronics from the top and bottom of the strip, respectively.

As far as the cases like this one deal with the low statistics, the probability $P_{\rm err}$ was calculated based on the procedure of [36], that the observed number of correlation chains n_m (in this case - five Re-α_1-α_2, i.e. triple correlation chains) are result of a random fluctuation of the background. Based on the experimental values of total time of the measurement T $\sim 3\times10^5$ s, number of counts in three consecutive groups $n_{Re} = 7\times10^5$, $n_{\alpha_1} = 480$, $n_{\alpha_2} = 420$ in antiTOF spectra and two correlation time windows of $\Delta t_{1,2} = 18$ s, $\Delta t_{2,3} = 15$ s, than for number of chains $n_m = 3$ the value of $\sim 2\times10^{-24}$ can be

calculated (see table 4.11). Based on this value it can be concluded that five observed chains belong to real correlations going through E_{α_2} = 8620 keV α-line of ^{253}Lr.

Moreover, the maximum correlation time was estimated that would produce a random correlation in the energy region of the interest ($\sim$ 9 MeV). In order to do so, it was sought for α_1-α_2 correlations between two most energetic α-lines of ^{257}Db that should not have any generic relationship. The first random correlation came after some 22 minutes which is more than 60 times longer than the time used in correlation search between first and second generation alpha Δt = 20 s. This value further justifies the reliability of the α-α correlation method.

Another candidate, this time for a new α-line of ^{257}Db appears at 8874 keV as shown in Fig. 4.27. Indication of a group of events at this energy can also be seen in Fig. 4.28 b) and c). In order to emphasize the line better, the events from the strips with the best resolution and lowest background were summed with the result displayed in Fig. 4.27. Four Re-α_1-α_2 correlation chains were found for the seven best strips and six for all strips, respectively. Followed by third generation alpha were two of these chains for the best strips and four for all strips, respectively.

n_m	Re-α_1	Re-α_1-α_2	Re-α_1-α_2-α_3	α_1-α_2	α_1-α_2-α_3
1	0.37	2×10^{-8}	4×10^{-15}	1×10^{-4}	2×10^{-8}
2	0.08	2×10^{-16}	7×10^{-30}	8×10^{-9}	2×10^{-16}
3	0.01	2×10^{-24}	8×10^{-45}	4×10^{-13}	2×10^{-24}

Table 4.11: Probabilities P_{err} representing an error interpretation of observed number n_m of different kinds of correlation chains calculated as described in [36]. The parameters used in calculations consist of number of events in individual groups: $n_{Re} = 7\times10^5$, $n_{\alpha_1} = 480$, $n_{\alpha_2} = 420$, $n_{\alpha_3} = 330$, total time of the measurement $T \sim 3 \times10^5$ s and time windows $\Delta t_{1,2} = 18$ s, $\Delta t_{2,3} = 15$ s and $\Delta t_{3,4} = 150$ s, respectively. Counting rates defined as $\lambda_i = n_i/T$ needed to be yet divided by number of subdetectors $\sim$ 280 representing the position resolution of PSSD.

Based on these observed correlations it seems that the 8874 keV line decays through both ground and isomeric-state of ^{253}Lr. The half-life for this α-line deduced from the Re-α_1-α_2 correlations (all strips $\rightarrow$ 6 events) and from Re-α_1-α_2-α_3 (all strips $\rightarrow$ 4 events) is $3.43^{+2.34}_{-0.99}$ s and $4.76^{+4.70}_{-1.58}$ s, respectively. The half-lives were calculated according to the procedure for the low statistics described in [36]. This somewhat higher value than for the remaining ^{257}Db α-lines might indicates other (perhaps isomeric) origin of this level in ^{257}Db. The probability to get a random three member decay chain is similar than in the previous case of a new α-line in ^{253}Lr.

Careful analysis revealed yet two more candidates for new α-lines observed

in ^{249}Md at the energies 8280 keV and 7970 keV which will be discussed in more detail in section 4.4.1.

- In previous SHIP experiment dedicated to ^{257}Db the construction of decay scheme for this isotope was based on nonobservation of the crosscorrelations between the most energetic α-lines of ^{257}Db and ^{253}Lr and between two low energy α-lines of ^{257}Db and low energy α-line of ^{253}Lr [34]. The probability limits for these crosscorrelations were ≤ 0.02 and ≤ 0.01, respectively. In present experiment we could confirm the value for the first type of correlations (high energy lines), but different situation was found for the low energy α-lines.

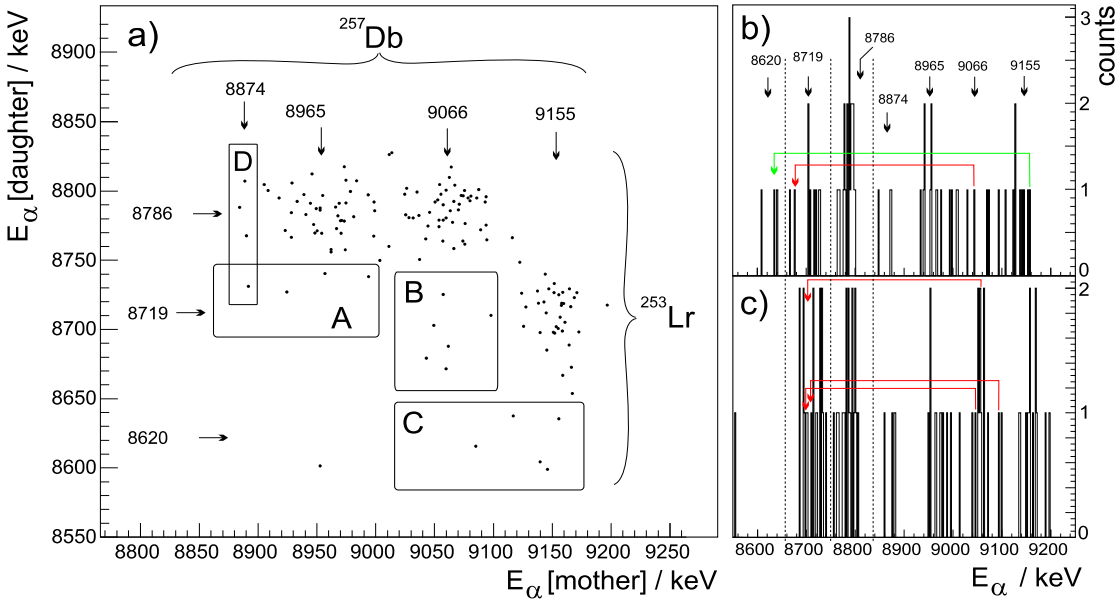

Figure 4.28: **a)** Two dimensional energy spectrum of α_{Mother} vs. α_{Daughter} correlations from the stop detector. Groups of events in rectangles A and B represent the crosscorrelation events not observed before between two low energy α-groups of ^{257}Db and low energy α-group of ^{253}Lr. Events in rectangle C represent a new α-line of ^{253}Lr. **b)** and **c)** Alpha spectra for strips number 7 and 8, respectively. Red arrows show examples of correlations between 9066 keV peak of ^{257}Db and 8719 keV peak of ^{253}Lr. It is evident that these correlations are not caused by poor calibration or detector resolution. All of them were preceded by recoil and majority were followed by third generation α-event. Green arrow shows the energy position of the correlation going to a new α-line of ^{253}Lr with the same conditions.

It can be seen in Fig. 4.28 a) that in fact there are correlations between 8965 keV α-line of ^{257}Db and 8719 keV α-line of ^{253}Lr (4 events in rectangle A), and between 9066 keV α-line of ^{257}Db and 8719 keV α-line of ^{253}Lr (6 events in rectangle B). Careful analysis within each strip of PSSD was performed for

these correlation events. All of them were preceded by recoil event. Further, 3 out of 4 events in rectangle A and 5 out of 6 events in rectangle B were followed by third generation alpha (either ^{249}Md (6), ^{249}Fm (1) or ^{245}Es (1)). Three events in area A have signals in box detector, therefore, considering also their placement close to 8786 keV line of ^{253}Lr, they could be interpreted as escaped αs from this line. On the other hand, all events in the area B originate from the stop detector solely so based on the evidence given, they could be considered as previously not observed real crosscorelations. On the basis of present data it can be concluded that the probability for the 9066 keV line to decay through the 8719 keV line is $\sim 0.11 \pm 0.5$. The events in the rectangles C and D represent the crosscorelations of new α-lines 8620 keV (^{253}Lr) and 8874 keV (^{257}Db), respectively. It seems that 9620 keV line is correlated mainly with 9155 keV line of ^{257}Db and 8874 keV line to 8786 keV line of ^{253}Lr, respectively. However, on the basis of present statistics no definite conclusions can be drawn.

The aforementioned evidence for new α-lines in ^{257}Db and ^{253}Lr and the appearance of yet unobserved crosscorrelation between already known α-lines of ^{257}Db has some influence on the decay scheme proposed in [34] as will be discussed in section 4.4.1.

- By means of Re-α-SF correlation search the fission branch could be identified for ground and isomeric-state of the isotope ^{253}Lr. In total 14 such correlations were observed, two of them having originated in 8965 keV and 9066 keV peaks respectively and twelve in isomeric peak of 9155 keV of ^{257}Db. The acquired values of $b_{SF(^{g253}Lr)} = 0.01 \pm 0.006$ and $b_{SF(^{m253}Lr)} = 0.12 \pm 0.03$ agree within the error bars with the previously measured values of Ref. [34]. The neighboring odd-odd isotopes ^{256}Db and ^{258}Db should have even higher barrier against spontaneous fission than odd-even isotope ^{257}Db. According to the HIVAP calculations [45] at the excitation energy of E^*=22 MeV the contribution from ^{256}Db should be negligible and as stated earlier the contribution of ^{258}Db deduced from the observed number of its daughter product ^{254}Lr is about 29 $\pm$ 5 %. The total number of the events in the high energy branch in the region from 80 to 220 MeV that could be attributed to spontaneous fission was 90. Fourteen of these events were assigned as originated from the fission of ground or isomeric-state of ^{253}Lr. Based on the production ratio ^{258}Db/^{257}Db it was estimated that there should be roughly 65 decays to ^{258}Rf and by considering almost 100 % fission branch of this isotope it points to eleven events that could have originated in spontaneous fission of ^{257}Db. It is not possible to assign them to the fission of ground or isomeric-states due to very similar half lives and small statistics. Therefore an upper limits based on the observed number of αs in relevant peaks could be calculated leading to the values of $b_{SF(^{g257}Db)} \leq 0.05$ and $b_{SF(^{m257}Db)} \leq 0.12$. These values also agree with the limit estimations of Ref. [34].

  It was difficult to search for EC-decay branch in both ^{257}Db and ^{253}Lr due

to similar half-lives of ^{257}Db and ^{257}Rf ($T_{1/2} \sim 1$s) as well as overlapping α-energy regions for ^{253}Lr - ^{257}Rf ($E_\alpha \sim 8.8$ MeV) and for ^{249}Md - ^{253}No ($E_\alpha \sim 8.01$ MeV). In the correlation search of the kind: Re-(^{257}Db$_{[\text{EC-decay}]}$)-^{257}Rf→ ^{253}No→, the time window for ^{253}No was set to Δt = (170 - 600 s) in order to eliminate the false correlation with overlapping ^{249}Md of which less then 0.8 % should survive past 170 s time interval. In total 8 correlations were found that could be attributed to EC-decay of ^{257}Db. By correcting the number of found correlations to full correlation time, subtracting the number of correlations that could be explained by the decay via long lived tail of ^{249}Md and comparing it to the number of found chains of the kind Re→^{257}Db→^{253}Lr→ it gives the upper limit $b_{EC} < 0.03$ for ^{257}Db.

Similar procedure was used to estimate EC-branch of ^{253}Lr. This time it was sought for Re-^{257}Db→ (^{253}Lr$_{[\text{EC-decay}]}$)-^{253}No→^{249}Fm→ correlations in comparison with the straight decay path going through ^{249}Md. After correcting for EC-branching of ^{253}No and ^{249}Fm the upper limit estimate of $b_{EC} < 0.02$ for electron capture branch of ^{253}Lr was estimated.

4.4.1 Decay scheme of ^{257}Db and nuclear structure in odd A odd Z = 99 - 105 region

The discussion about the decay scheme of ^{257}Db needs to be based upon previous results for this isotope [34], long term investigation of the region of odd A odd Z = 99 - 105 isotopes (see Ref. [A7)]) and the new information introduced by this work. The main goal of present experiment was to localize the isomeric decay branch ^{257m}Db → ^{253m}Lr relative to the path going through the g.s.-g.s. decay, search for the isomeric-state in the granddaughter ^{249}Md and to establish evidence for definite assignment of J^π values to the ground-states, isomeric-states and proton one-quasiparticle states in these nuclei. One difficulty of the decay scheme suggested in [34] to hold lies in explaining previously unobserved crosscorrelation group between 9066 keV line of Db and 8719 keV line of ^{253}Lr as already discussed and placement of new possible α-lines being part of decay sequences explained in preceding section. In previously suggested level scheme such decay path was not energetically possible. Moreover the evidence still holds for non-observation of decay of isomeric line 9155 keV in ^{257}Db through 8786 keV line in ^{253}Lr with the probability limit < 0.01. This could be attributed again to energetic forbiddance or to high dismatch of J^π values in isomeric and ground-state in ^{253}Lr. The properties of proposed decay scheme for the isotope ^{257}Db and its decay products as shown in fig. 4.30 can be justified as explained in the following steps:

- Keeping the J^π assignment as proposed in [34], the appearance of crosscorrelations suggests to lower the isomeric $1/2^-[521]$ state bellow the $9/2^+[624]$ ground-state in ^{257}Db. This would however interfere with the systematics as scratched in [A7)] for neighboring Lr and Es odd A isotopes. Possible solution would be to place the isomer ^{253m}Lr between $7/2^-[514]$ and first excited

$9/2^+[624]$ level in ^{253g}Lr. This way the decay path Db(8965 keV)→ Lr^m(8719 keV) would be possible. This is however of no such importance, because as discussed in previous section these crosscorelations could by fake caused by escaped α-particles. Moreover it would require either M4 or one of the sequences of M2-M1-M1/E3-M1 with all these cases highly hindered. But the scenario still energetically forbids the crosscorrelation group Db(9066 keV)→ Lr^m(8719 keV) that seems to be real to occur. The group of events at E ∼ 9060 keV in Fig. 4.28 can then be explained as a fine structure decay of the isomeric $1/2^-[521]$ state in ^{257m}Db. This assignment would fix the placement of isomer in ^{253}Lr between 0 - 100 keV above its ground-state and the isomer in ^{257}Db between 90 - 190 keV above the ground-state. Non-observation of the transition between the isomeric and ground-state level in ^{257}Db can be attributed to M4 character of such decay.

- If one wants to follow the theoretical predictions of [37] and [38] for the ground-states for ^{257}Db and ^{253}Lr being $9/2^+[624]$ and $7/2^-[514]$, respectively, it was difficult to explain the summing with conversion electrons as far as the transition $9/2^+ \rightarrow 7/2^-$ in ^{253}Lr is of E1 character with conversion coefficient $\alpha_L \sim 0.1$. By placing the isomer between $7/2^-[514]$ and first excited $9/2^+[624]$ level in ^{253}Lr it is possible for $9/2^+[624]$ level to undergo a series of decays of M2-M1-M1/E3-M1 or M2-E2 character onto the $1/2^-[521]$ isomer through the rotational band build upon it[8]. However either one of these would be highly hindered compared to the straight E1 path into $7/2^-[514]$ level.

- By assigning 8874 keV line to α-decay of $9/2^+[624]$ ground-state of ^{257}Db it is possible for it to decay through both - ground and isomeric-state path in ^{253}Lr but Re-α_1-α_2 correlations suggest that the first path takes place. Calculated hindrance factor for this line is ∼ 88 therefore suggesting the decay into the level with different J^π. Therefore it can be tentatively assigned to decay into $5/2^-[512]$ level in ^{253}Lr located ∼ 190 keV above the ground-state. The level with such J^π is also predicted by calculations [37] and [38], but to be located in 670 and 560 keV energy region, respectively.

- New α-line in ^{253}Lr with E_α = 8620 keV can be attributed to the decay of $1/2^-[521]$ isomeric-state of this isotope. Four of the Re-α_1-α_2 correlations going through this line originated in 9155 keV decay of ^{257m}Db and one in 8965 keV line of ^{257}Db, which is only one from the g.s.-g.s. decay branch and for which this path is also energetically allowed. Even though HF ∼ 16 doesn't suggest unhindered decay it is way too small for populating either $7/2^+[633]$ or $9/2^+[624]$ levels that are predicted by theory to exist in the nucleus ^{249}Md. Decay into rotational level $3/2^-$build upon the $1/2^-[521]$

[8]This depends on how many levels of the rotational band build upon $1/2^-[521]$ isomeric-state in ^{253}Lr would fit below $9/2^+[624]$ level of ^{253}Lr ground-state branch. In this case $3/2^-$ and $5/2^-$ rotational levels are considered.

state in ^{249}Md would explain this line being influenced by summing (FWHM $\sim$ 50 keV) with conversion electrons as the de-excitation would go through M1 highly converted transition with $\alpha_{\mathrm{L}} \sim 10$.

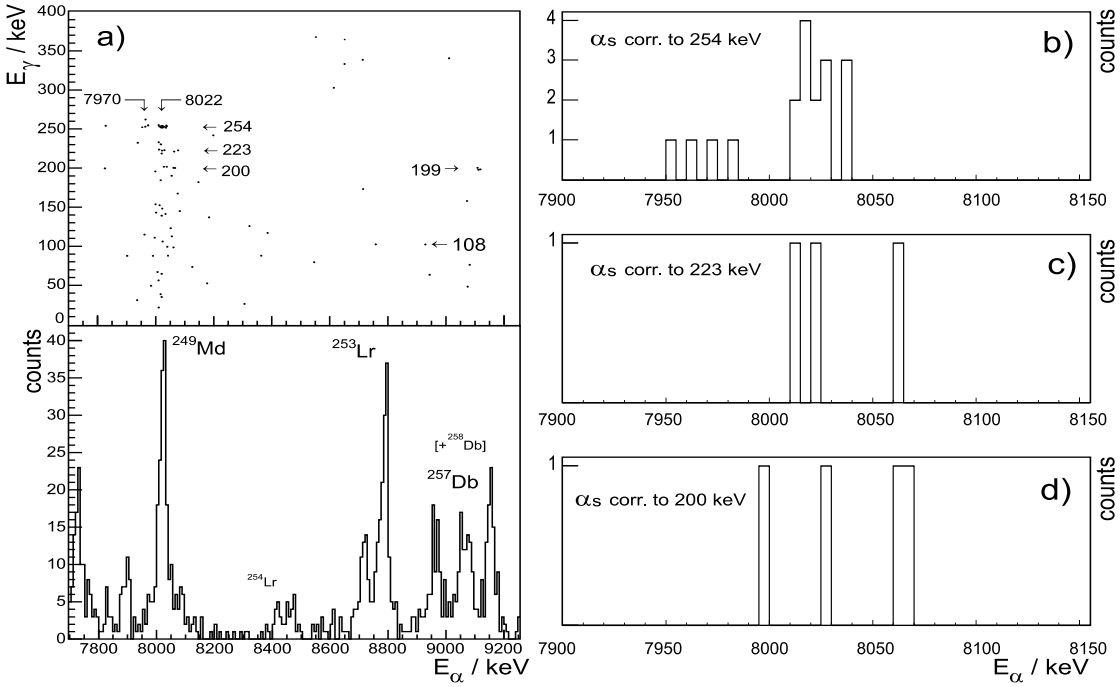

Figure 4.29: **a)** The spectrum showing γ-events in coincidence within 4 μs with the alpha energy region for ^{257}Db, ^{253}Lr and ^{249}Md isotopes. **b)**, **c)** and **d)** represent α-decays of ^{249}Md in prompt coincidence with 254, 223 and 200 keV γ-transitions.

- One γ-event with the energy of Eγ = 102.1 keV was found accompanying the 8965 keV α-line of ^{257}Db in nice Re(23 MeV)-α_1(8.93 MeV)-α_2(8.77 MeV)-α_3(7.99 MeV) correlation. This γ-energy fits perfectly the energy difference between α-lines 9066 - 8965 keV = 101 keV. However it is very unlikely that this transition really represents E1 character of this decay, because for about 140 events in 8965 keV peak and the clover detection efficiency for 100 keV region of $\varepsilon_\gamma \sim 15\%$, about 17 such γ-events can be expected to be registered. To clarify this question, further measurements are necessary.

- A group of three events with $E_\gamma \sim 199$ keV can be seen in fig. 4.30 over the 9150 keV α-region. This would however require the ground-state of ^{257}Db to be shifted about 200 keV down which would than require to make some major changes in the so far proposed decay scheme as for example to shift $1/2^-[521]$ level under the $7/2^-[514]$ level in ^{253}Lr. The group of α-events with approximate energy of 9350 keV can be observed in low energy spectra but

it was not possible to prove or disprove its ground state origin be correlation search so it remains an unanswered question.

- There are two decay paths observed feeding the ground-state in ^{249}Md - once directly by 8786 keV g.s. to g.s. decay from ^{253}Lr and also from $1/2^-[521]$ level in ^{249}Md. The reason that the 8719 keV line is not influenced by IC summing can be found in M3 character of $1/2^-[521] \rightarrow 7/2^-[514]$ transition with expected half-life of $\sim$1 s which disables the α-signal and IC-signal to be recorded as a single event. In fact, slightly different half-lives were measured for 8719$\rightarrow$8022 keV decay path ($24.1^{+4.5}_{-3.3}$ s) and for 8786$\rightarrow$8022 keV decay path ($20.7^{+2.3}_{-1.9}$ s). Although there is an indication for the hindrance in the first case, these intervals overlap and the difference in absolute values can be attributed to more than a factor of two lower statistics in 8719 keV peak. Nevertheless, it is very probable that $1/2^-[521]$ state in ^{249}Md represents an isomer, that needs to be checked in future experiments by coincidences with delayed γs and/or X-rays from this state.

- Two differences in decay properties of ^{249}Md being preceded by either 8719 or 8786 keV were scatched in [34]. In current measurement the difference could be verified in the width of 8022 keV α-line being preceded by either 8768 keV line of ^{253}Lr (FWHM $\sim$ 35 keV) or 8719 keV line (FWHM $\sim$ 19 keV). One way to explain this would be to assign $1/2^-[521]$ level in ^{249}Md to the isomer that decays with very similar energy $\sim$ 8022 keV that is not effected by IC summing. On the other hand the assumption of shorter ($\sim$ 1.5 s) half-life could not be verified for ^{249}Md in the energy region above 8060 keV. Based on observed number of 17 α_1-α_2-α_3 correlation chains it can be concluded that the half-life of $16.1^{+5.1}_{-3.1}$ s which, taking into account the small statistics is equal within the error bars to the collective half-life.

- As can be seen from figs. 4.29 b) - d) the γ-lines of 223 and 200 keV coincide with both 8022 and 8080 keV α-lines of ^{249}Md whereas 254 keV γ-line coincides with 8022 keV α-decay. The γ-transitions 223 and 200 keV cannot be however assigned to originate from the level populated directly by 8080 keV α-decay for two reasons. Most importantly this would shatter well established systematics of the low-lying single particle levels described in [A7)]. Secondly, also α-decays of 8022 keV seem to be coincident to 200 keV γs which would require high feeding of the level populated by 8080 keV α-decays from above lying $7/2^-[514]$ level by internal conversion. This is however in conflict with the assumed E1 character of 254 keV transition. The coincidences of 200 keV γ-decays with α-events of about 8080 keV can be presently explained by assumed K-conversion of 200 keV transition which would leave the maximum energy for the conversion electron of $\sim$ 56 keV pointing towards 8080 keV region. It would be supported by M1 character of this transition if population of the first excited rotational level $5/2^-$ build upon $3/2^-[521]$ ground-state is assumed [A7)].

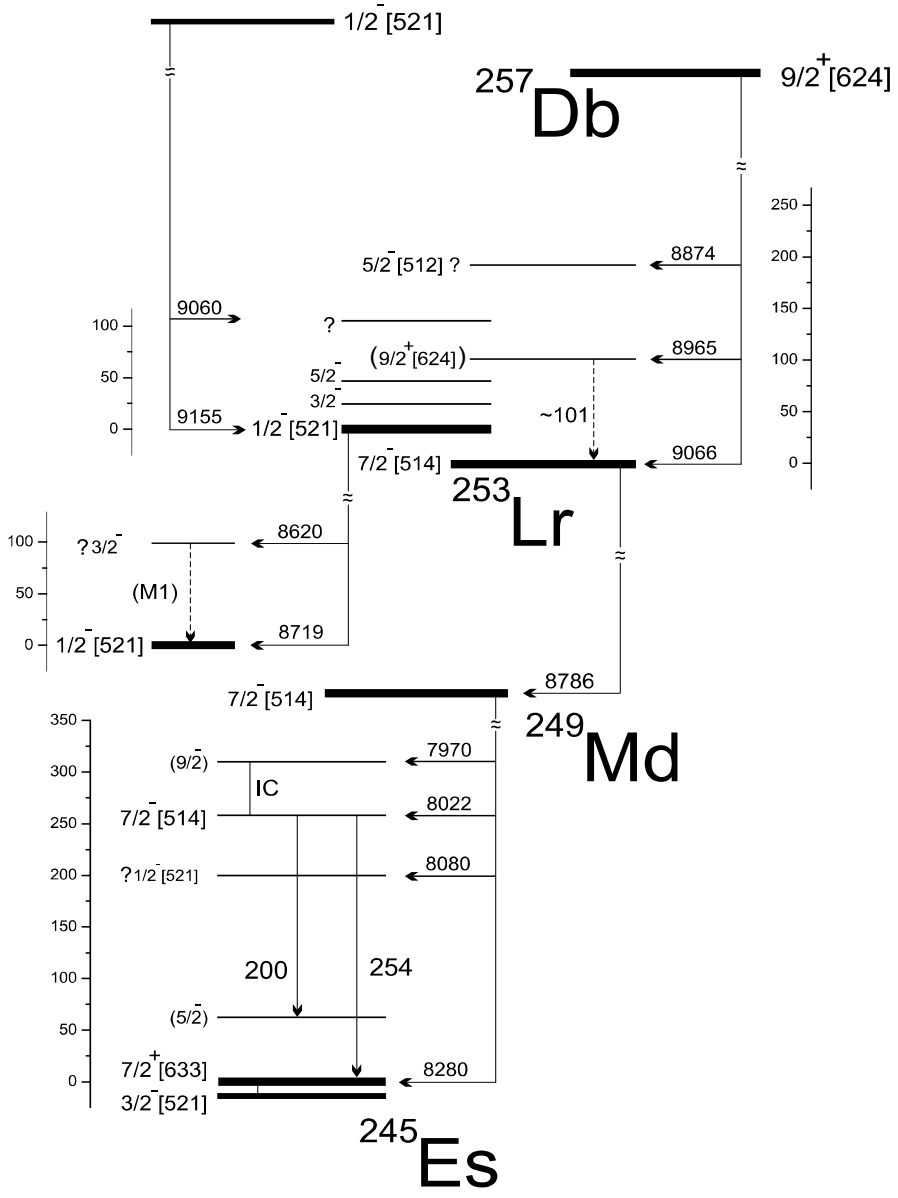

Figure 4.30: Proposed decay scheme for the isotope ^{257}Db and its decay products ^{253}Lr,^{249}Md and ^{245}Es.

The candidate for new α-line in ^{249}Md with the energy $\sim$ 8280 keV also populating $7/2^+[633]$ level fits energetically with decay path of 8022 keV + 254 keV = 8276 keV $\sim$ 8080 keV to the same level. Although the evidence for 8280 keV α-transition is still quite vague and it may represent the result of summing the 8022 keV line with conversion electrons. The α-events coincident to 254 keV γ-line also display a group at $\sim$ 7970 keV as seen from Fig. 4.29b). These coincidences can be presently explained by conversion of the level fed by 7970 keV decay into $7/2^-[514]$ level.

- The nature of 223 keV γ-line measured together with the α-decays of ^{249}Md is nor very clear so far. The γ-line with approximately the same energy and highest intensity [29] was also observed in coincidence with the decay of ^{253}No whose energy overlaps with that of ^{249}Md, a member of potential EC-decay chain from mother nucleus ^{257}Db.

  Also uncertain remains the assignment of the ground-state J^{π} for ^{245}Es. As can be seen from Fig. 4.32 and the discussion in the [A7)] the assignment of $3/2^{-}$ is tentatively given to be located below $7/2^{+}$ for odd einsteinium isotopes $^{243-249}$Es. It was so far unambiguously assigned only in ^{251}Es [80].

- It can be seen from α-γ coincidence spectrum in fig. 4.29 a) as well as α-spectrum coincident to 254 keV γ-line in fig. 4.29 b) that there is another α-line at $\sim$ 7970 keV clearly separated from the main 8022 keV α-line by the energy difference of 52 keV. Alike energy difference of 53 keV can be found in ^{251}Es decay scheme between α-transition populating $7/2^{-}[514]$ single particle orbital and lower energy α-transition. Therefore in analogy with ^{251}Es level scheme and well established systematics in $^{243-251}$Es isotopes [A7)] the level populated by this 7970 keV transition can be tentatively assigned as a first level $9/2^{-}$ of the rotational band build upon the $7/2^{-}[514]$ single particle orbital.

The decay scheme for ^{257}Db shown in Fig. 4.30 is constructed on the basis of [34], theoretical calculations displayed in Fig. 4.31 and data analysis presented in preceding paragraphs. It however still exhibits a few unsolved difficulties.

Most important one is the relative placement of the isomeric and ground-state branch in both ^{257}Db and ^{253}Lr. In light of recent results from RITU separator [81] where $1/2^{-}[521]$ isomer in ^{255}Lr was assigned to lie below $7/2^{-}[514]$ orbital based on a good quality data, this situation might also apply in case of ^{253}Lr. The indication of coincident 199 keV γ-transition with 9155 keV α-decays would shift $1/2^{-}[521]$ level in this way. This would on the other hand require to situate also $1/2^{-}[521]$ level below the ground-state in ^{249}Md.

Another obstacle represents $9/2^{+}[624]$ level in ^{253}Lr with no support in the data for E1 character of its transition. Possible alternative candidate would be $5/2^{-}[512]$ level predicted to exist in lawrencium isotopes at $E^{*} \sim 0.5$ MeV. This interpretation would also enable the transition $5/2^{-} \rightarrow 7/2^{-}$ to be M1 and highly converted. Also such a state could decay by series of M1 transition via $5/2^{-} \rightarrow 5/2^{-} \rightarrow 3/2^{-} \rightarrow 1/2^{-}$ rotational band to the isomeric state. This could also possibly explain the influence of IC-summing on 9066 keV which in other case could not represent the g.s. to g.s transition. Also questionable is then the ground-state of ^{257}Db considering also no highly favored hindrance factors measured in this work. As seen from Fig. 4.32 the experimental information on odd-A dubnium isotopes is still rather scarce.

Both available theoretical calculations [37] and [38] predict for ^{257}Db different ordering of low lying Nilsson levels as so far acquired experimental data suggested.

Possible alternative candidate could be $9/2^-[505]$ orbital stemming from $1h_{9/2}$ shell. Though the occurrence of this level is not predicted by calculations, it is trespassing the region of Z = 104 shell gap at around $\varepsilon_2 \sim 0.1$ as can be seen from Fig. 4.31. In this situation $1/2^-[521]$ level in ^{257}Db could still retain its isomeric character. Best agreement between the experimental data and calculations, especially of Ref. [37] existed for lawrencium isotopes. This was however endangered by already mentioned experiment on ^{255}Lr [81] which claims different ordering of $1/2^-[521]$ and $7/2^-[514]$ levels. This is also true for mendelevium isotopes where calculations and experimental data also predict the switched ordering of these two levels.

However, the scarce α-γ matrix shown in fig. 4.29 in the energy region 8500 - 9250 keV did not allow to shed much more light onto the topic of low-lying Nilsson levels in ^{253}Lr and/or ^{249}Md. On the other hand presented analysis revealed many interesting features in decay properties of ^{257}Db and its products, that can not be unambiguously clarified based on the quality of available data. These topics with respect to the properties of other odd A odd Z = 99 - 105 isotopes in this region need to be investigated in more detail in future experiments.

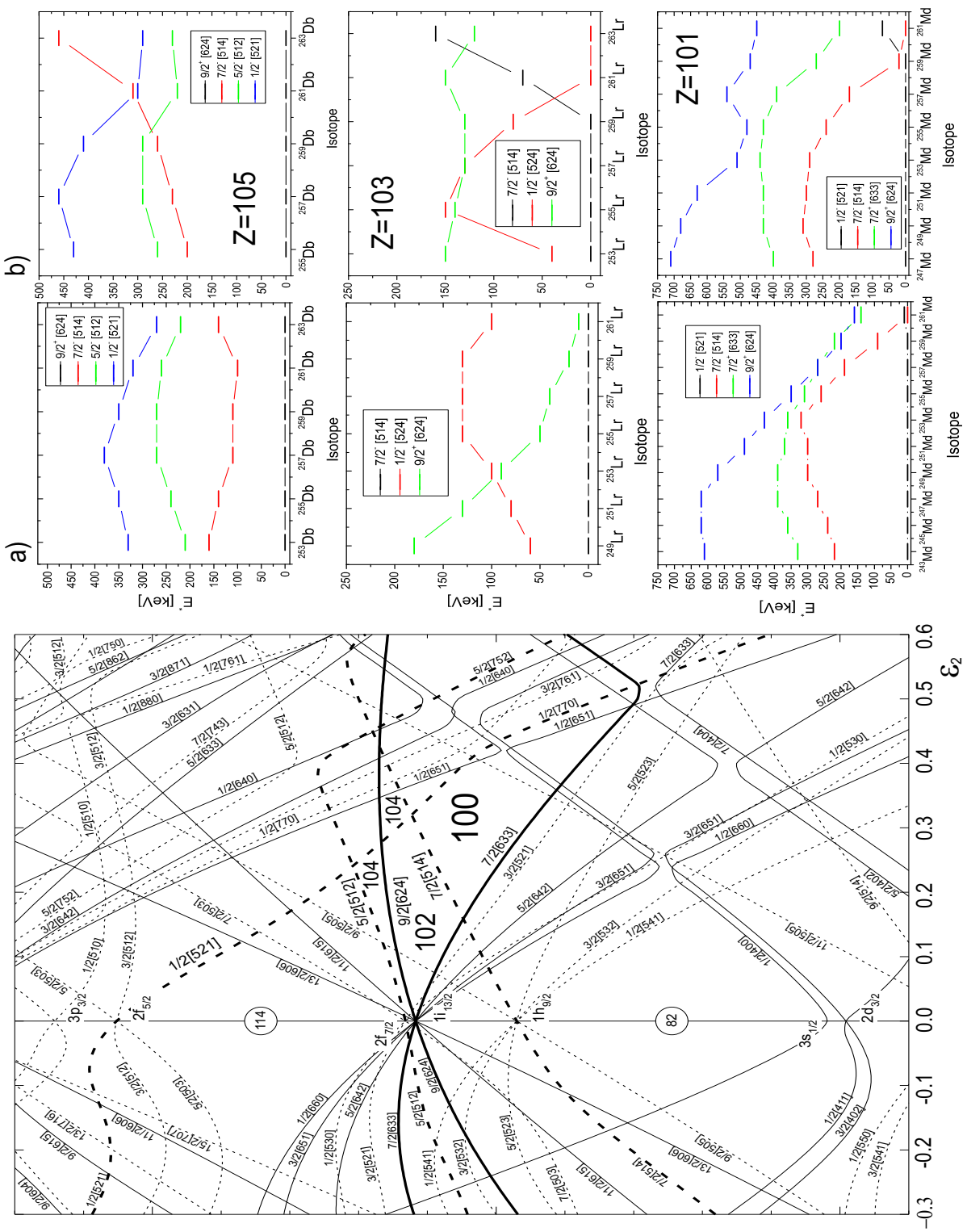

Figure 4.31: Left: Nilsson diagram for protons with $Z > 82$ from [70], Right: theoretical predictions of single particle levels for elements with $Z = 105$, 103 and 101, taken from **a)** Ref. [38], and **b)** Ref. [37].

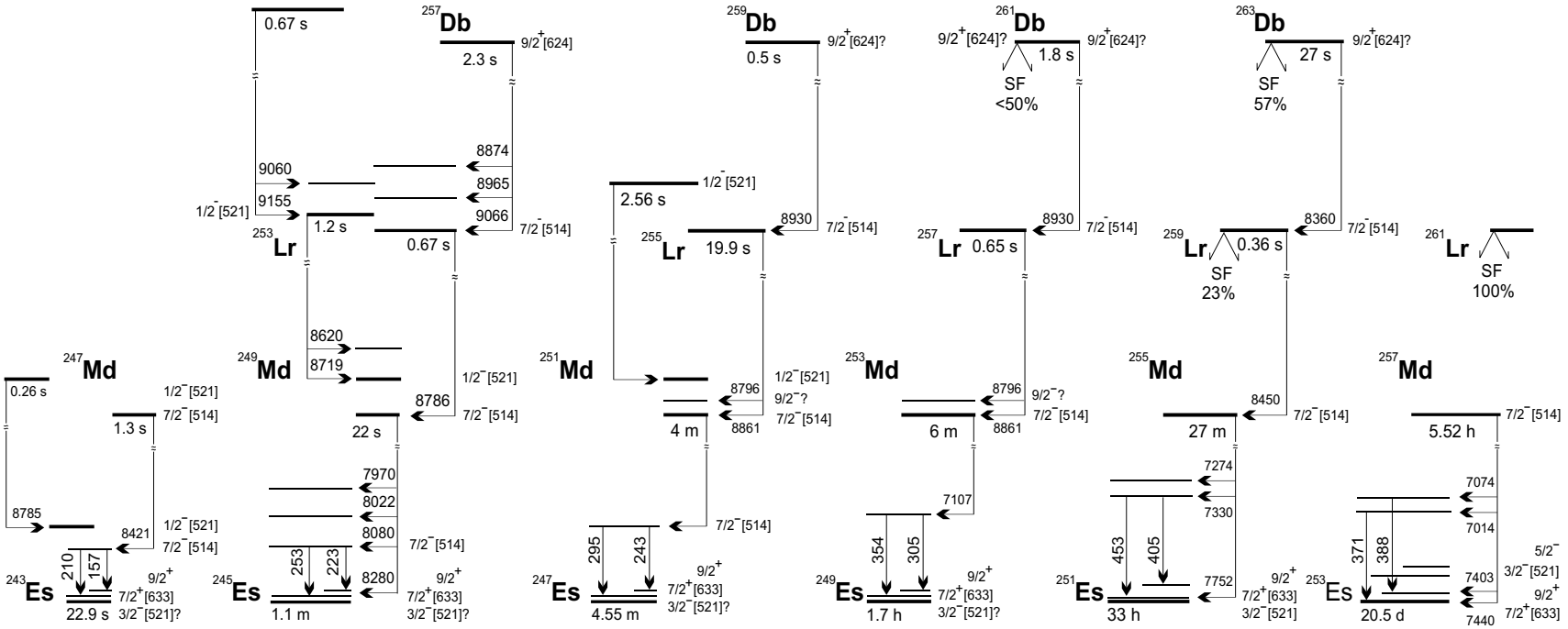

Figure 4.32: Present status of experimentally deduced systematics of the decay chains for odd-A and odd-Z isotopes in the region Z = 99 - 105. Decay path for ^{257}Db is taken from the analysis presented in this work shown in Fig. 4.30. Other data are taken either from [70] or recent publication [A7)]. Only the strongest α-lines and first levels of the rotational bands are drown. for ^{253}Es.

Chapter 5

Discussion and Conclusion

Physical data and its interpretation as presented in this work are based on spectroscopic analysis of experiments performed on velocity filter SHIP at GSI Darmstadt, Germany, throughout the period of years 2003 to 2006. This velocity filter was constructed along with its detection system to be suited for new element production. Later it proved to be excelent tool for performing spectroscopic experiments in the region of nuclei ranging from Z $\sim$ 82 - 112. The isotopes studied within this work were produced by the mechanism of complete fusion reactions with very low cross-sections from pbarn region.

All the analyzed experiments were performed with specific purpose and each of the studied cases presented different challenges. Of uppermost importance was to study low-lying single-particle levels in the odd mass isotopes. The results obtained from these experiments gave new insight and information on nuclear structure in these exotic nuclei.

The decay spectroscopy methods were used to analyze the acquired data. Namely, α-decay spectroscopy combined with the method of generic linking of decay sequences to a single radioactive nucleus by Re-α and α-α correlation analysis. In order to extract more detail information about the nuclear structure of these isotopes, also the methods of prompt and/or delayed α-γ coincidences were used.
Information about these isotopes was obtained within this work:

- ♣ `Decay chain of` ^{261}`Sg:` This work attempted to construct for the first time decay scheme of the isotope ^{261}Sg. New α-lines at 9345 and 9620 keV were measured with collective half-life of $T_{1/2}$ = 184 $\pm$ 5 ms for this isotope. In prompt coincidence with ^{261}Sg the γ-energy of 107 keV was measured de-exciting the level in daughter nucleus ^{257}Rf with probable M1 multipolarity. The K X-rays were measured for the first time for the element as heavy as Z = 104 and the ratio $I_{K_{\alpha_1}}/I_{K_{\alpha_2}}$ = 2.2 $\pm$ 1.2 was obtained which should be constant for all isotopes of element rutherfordium. The improved value on the total cross-section of σ = 2.2 $\pm$ 0.2 nb was calculated with the maximum of measured excitation function at E^* = 16.9 $\pm$ 0.2 MeV using

metallic targets in R-212. This value was later confirmed by measuring σ = 2.02 ± 0.06 nb using the compound PbS targets (see also later discussion).

`Isotope` ^{257}`Rf:` Very complex α-spectrum of this isotope was confirmed with the admixture of its EC-product ^{257}Lr. The difference in its indirect production via the decay of ^{261}Sg is that the α-decay from the assumed $3/2^+$ ground-state of ^{261}Sg into the $11/2^-$ isomer in ^{257}Rf is strongly hindered. In its direct production the α-particles from this $11/2^-$ overlap the energy region of the ground-state transition. This difference allowed in analyzed indirect production experiments to extract the ground-state α-transition resulting in Q_α-value of 9092 keV for ^{257}Rf. From delayed α-X-rays coincidences the half-life of the isomer $5/2^+[622]$ was calculated with $T_{1/2} = 24.6^{+5.0}_{-3.6}$ μs in perfect agreement with the value measured in direct production of ^{253}No at SHIP [45]. Moreover present analysis could unambiguously identify the γ-transition of E_γ = 167 keV with the half-life of $T_{1/2} = 22^{+30}_{-8}$ μs de-exciting the very same isomer with M2 transition to the ground state. Later this year this transition was also confirmed at the direct production of ^{253}No [60] with $T_{1/2}$ = 21.6± 2.2 μs. This finding together with tentatively assigned E2 multipolarity of 283 keV γ-transition populating again $5/2^+[622]$ isomeric level would confirm the general resemblance to the systematics of lighter N = 153 isotones. The sign of observation of isomeric state in ^{253}Md - produced by α-decay of ^{257}Lr was observed with the half-life of $T_{1/2} = 44^{+24}_{-11}$ μs.

♣ `Decay chain of` ^{262}`Bh:` This work can be viewed as a first attempt to study the levels populated by α-decay of ^{262}Bh. About an order of magnitude higher statistics was obtained for this isotope. Altogether eight α-energies coming from the ground state with $T_{1/2} = 135^{+15}_{-12}$ ms were observed along with three α-energies with $T_{1/2} = 13.2^{+1.2}_{-1.0}$ ms of the isomeric state. The γ-transition of 157 keV was measured. Possible transition with E_γ = 360 keV was detected from the level populated by the most energetic α-line of ^{262}Bh ground-state group. Measurements with enabled delayed Re-γ coincidences would be necessary to stabilize the relative position of ground and isomeric states.

`Isotope` ^{258}`Db:` Complex α-spectrum influenced heavily with the summing from internal conversion was observed. The unambiguous presence of the isomeric state could not be confirmed in neither ^{258}Db nor in its daughter ^{254}Lr. Two γ-transitions of E_γ = 157 and 221 keV were measured in prompt coincidence with ^{258}Db α-decays. The later transition could be assigned to be of either E1 or E2 multipolarity populating the ground state in ^{254}Lr. The total Q_α-value of 9460 keV could be calculated based on this observation.

`Isotope` ^{254}`Lr:` The α-spectrum again influenced heavily by internal conversion could be disentangled into possibly five components from observation of

characteristic placement of observed α-γ groups. Three prompt γ-transitions of E_γ = 42, 209 and 306 keV were unambiguously assigned to originate from de-excitation of the levels in the daughter nucleus ^{250}Md. Two most energetic ones were assigned to populate the ground state in ^{250}Md. Resulting Q_α-value 8824 keV is about 225 keV higher than the one calculated solely from the α-decay in previous measurements, indicating strong hindrance for direct α-transition into the ground state. Another γ-transition of E_γ = 165 keV was measured. Its origin in the decay of ^{254}Lr was excluded.

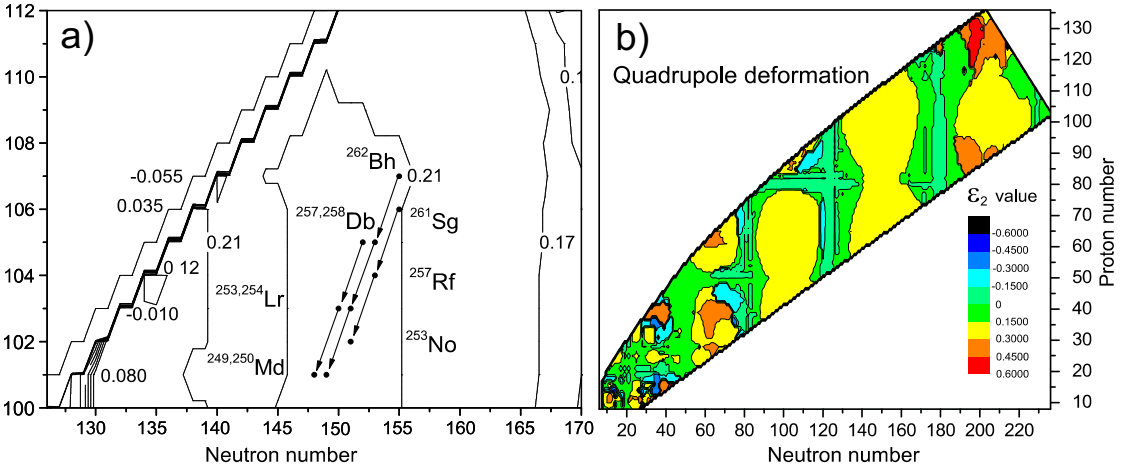

Figure 5.1: **a)** Transfermium region of isotopes with contour plot of quadrupole deformation superimposed over the position of the decay sequences studied in this work.**b)** Chart of nuclides showing the value of their quadrupole deformation parameter ε_2. Plotted data are taken from [79].

♣ `Decay chain of` ^{257}`Db:` Previously unobserved crosscorelations of ^{257}Db ground-state and isomeric-state decay paths were identified at present experiments. This observation would fix the placement of isomer in ^{253}Lr between 0 - 100 keV above its ground-state and the isomer in ^{257}Db between 90 - 190 keV above the ground-state, and thus stabilizing the systematics of for odd-A, odd-Z isotopes with Z = 99 - 105 that are methodically being studied at SHIP. Despite complicated α-pattern possible new α-lines of 8874 keV for ^{257}Db and 8620 keV for its daughter ^{253}Lr could be extracted from the data. Different placement of coincident γ-group with 254 keV energy was assigned in the level scheme of the granddaughter ^{250}Md indicating the break of the systematic trend in lighter mendelevium isotopes.

`Targets:` It was shown in R-212 which was analyzed within this work that the usage of the compound targets is justified in the experiments with heavy ions at

SHIP. This is especially important considering steeply decreasing cross-sections in transfermium region and therefore requirement for increased beam intensities in order to keep the irradiation times within reasonable limits. Beam intensities at UNILAC accelerator used by SHIP separator raise to values up to 1pμA for some used isotopes. The active target cooling with helium jet was studied at SHIP, but was pushed aside by usage of the compound targets withstanding higher beam intensities. R-212 tested these targets based on both fluoride and oxide compounds in reproduction of the cross-section for ^{261}Sg as discussed in detail in section 4.1.4. Moreover these targets were successfully used also in the recent experiment R-238 also analyzed within this work as well as other recent SHIP experiments.

`Experimental future prospects:` In recent experiments at SHIP the free data acquisition started to be performed. This enables to identify by means of α-γ spectroscopy methods the isomeric states decaying by γ-radiation with times longer than few μs. Unfortunately only recent R-238 analyzed in this work was performed with this mode. The isomeric state in ^{253}No could be identified in this way. Usage of this procedure in future experiments gives the possibility that in re-measuring the isotopes the new information will be found considering the isomeric states as predicted by this work. Together with this improvement the electron tagging technique started to be used at SHIP as discussed in section 3.2.3. Future improvements at SHIP should concentrate on the detector set-up, namely at bettering the total efficiency of γ-radiation detection that is at most about $\varepsilon \sim 15$ % for energy region around $E_\gamma \sim 100$ keV at present. This can be achieved by installing more sophisticated CLOVER detectors or their arrays. Their active shielding would be also beneficial from the point of view of lowering the background which is important taking into account low statistics acquired at the experiment in transfermium region. Another useful improvement would be usage of the planar detector whose range of detection efficiency is suitable for low energy region required to detect γs from the conversion on the L(M)-shells that is again of great importance for this region of nuclei. These improvements are however immensely expensive and require major rebuild of the detection system and the chamber and at present stage they are not forethought in detail at present as many technical obstacles have to be overcome.

The last upgrade could be done to the box detector that proved to be a useful tool and within this work it was possible to calibrate it with the resolution down to about 40 keV which is comparable to the PSSD resolution. This was however done using the box detector with many strips of poor quality and no correlation for the angle of implantation with the respect of the emitting position from the PSSD detector. This can be easily implemented into the analysis and could squeeze down its resolution to 20 keV region. This is again of uppermost importance since many of the α-emitters are heavily influenced with the summing from conversion electrons. But these are stopped in the PSSD and contribute only little to the α-spectrum recorded in box, thus giving the opportunity to disentangle the problem of real α-peaks and those created by the summing effect. This work also proved

for example in the analysis of ^{261}Sg and/or ^{258}Db isotopes that this is a serious problem that could be at least partly solved with proposed modification.

All isotopes in the transfermium region of isotopes are predicted to be strongly deformed [78] with the major contribution of the quadrupole term ε_2. This physical quantity is directly connected with ordering of single-particle levels and determines their ordering and energy placement as the levels with particular value of J^π can can change rapidly with small variation of ε_2. Its evolution throughout the periodic table, reaching deeply to the unknown region around Z = 114, N = 182 is shown in Fig. 5.1b). In decay studies the experimental data such as hindrance factors are combined with the Potential-Energy-Surface calculations to estimate the value and the sign of this quantity. But the spectroscopic data alone do not provide any information on the deformation, except for one case, when both the ground-state and 2^+ state are populated. In this case the excitation energy of the 2^+ state can be deduced and by using the rotational formula one can estimate the moment of inertia and hence the ε_2, but no sign again. Even though the deformation can not be measured directly at spectroscopic experiments performed at SHIP, in some of the cases assignments, not of the absolute values but rather general trends can be derived from the combination of evolution of single-particle levels, systematics and calculations. But all such assignments must be considered as tentative.

In case of the single-particle levels assignment for odd-A, odd-N isotones of ^{261}Sg decay chain general experimental systematics was taken into account as well as theoretical calculations of [37] and [38] as discussed in detail in section 4.1.3. It can be concluded that the theoretical predictions in general case provide an useful guide to experimentally observed ordering of particular J^π levels. It seems from recent SHIP data and also from the data in this work that calculations tend to overestimate excitation energies, but this assumption must be taken only as a hint. As this work suggests with recent findings of [65] the ground state of N = 155 isotones seems to change from $1/2^+$ to $3/2^+$ starting from ^{257}No upward including also ^{261}Sg. This can be also expected from the calculations as these levels are less that 50 keV apart as seen in Fig.4.5 however their ordering is interchanged. Biggest discrepancy is observed in N = 151 isotones where calculations fail to predict the existence of the low-lying isomeric state observed in the experimental data throughout all N = 151 isotones, including ^{253}No discussed here. According to present knowledge confirmed in this work this is caused by the placement of $5/2^+[622]$ single-neutron orbital being the second level above $9/2^-[734]$ ground state while calculations predict the second level as $7/2^+[624]$ with the two being about 150 keV apart. All of these features - correct prediction of the ground-states for N = 155 and 153 isotones as well as failure to predict the isomer in N = 151 isotones can be also deduced from simple Nilsson level diagram for neutrons with N $\geq$ 126 shown in Fig. 4.14 based on calculations using simple Wood-Saxon potential. Here also $5/2^+[622]$ single-neutron orbital fails to go above 150 neutron shell up to deformations $\varepsilon_2 < 0.4$ while all the other isotopes in questions, whose placement agrees with predicted deformation of about 0.2 as seen in Fig. 5.1a).

These features stemming from comparison of experimental data and calculations based on macroscopic-microscopic model give evidence for inevitable improvement of these models and their predicting power. Moreover this can be viewed only as a first step, because predicting single-particle levels for odd-A nuclei should be in principle relatively easy compared to predicting the shell structure of odd-odd isotopes. The study of such systems must proceed in the future in and its feasibility even in the heaviest transfermium region was shown also within this work by investigation of ^{262}Bh decay chain.

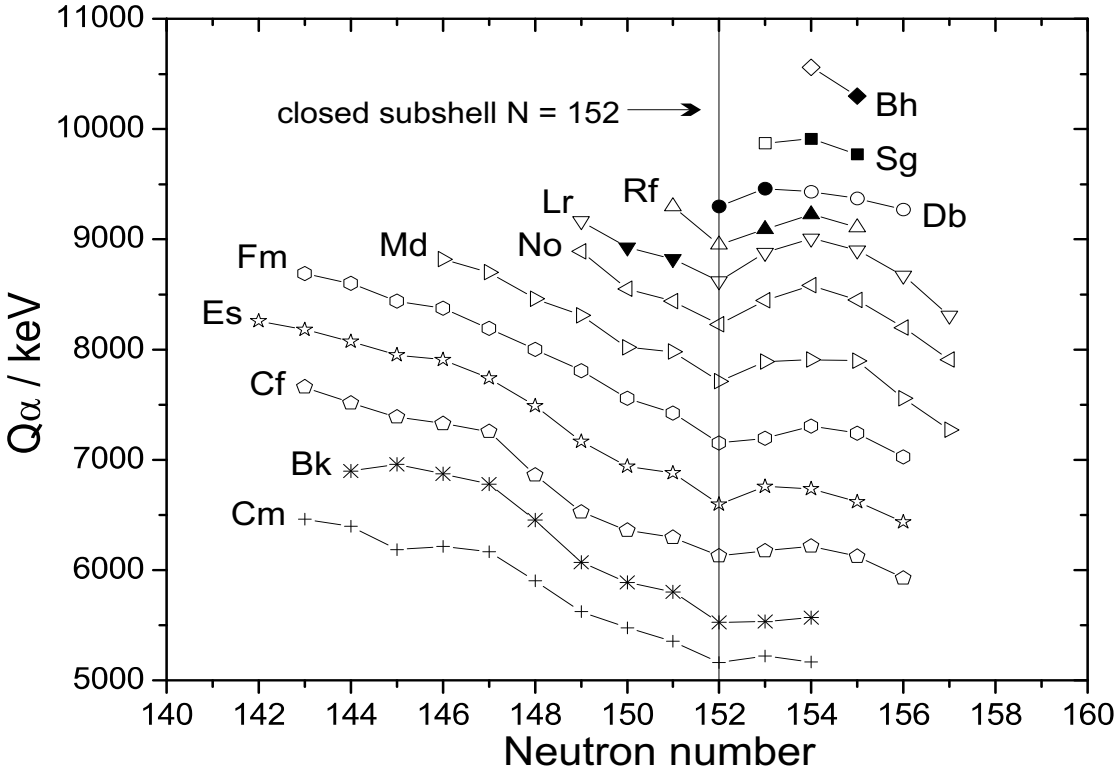

Figure 5.2: Q_α-value systematics for the isotopes of the heaviest elements with Z $\geq$ 96. Open symbols represent the data taken from Ref. [70] and closed symbols are values calculated based on the data derived in this work.

The results concerning improved and newly measured α-decay energies for the isotopes discussed here are put into the perspective of the Q_α-value systematics of the heaviest elements with Z $\geq$ 96 as shown in Fig. 5.2. In the cases of such heavy nuclei the acquired experimental statistics does not always allow to identify the highest α-transition. This is especially true for the odd mass nuclei where g.s. to g.s. transitions are often strongly hindered by unfavorable change of spin and/or parity. Even tougher experimental challenge represent the odd-odd isotopes that are very poorly studied in this region. Despite this, it can be seen that even the heaviest isotopes fit quite well into the general Q_α-trend. It is worth mentioning that also the values for nuclei studied here and depicted with closed symbols in Fig.

5.2 show the behavior characteristic for the local minimum in the Q_α-values at N = 152, clearly pronounced for the lighter systems. This neutron number is associated with the closed neutron subshell and represents the deformed gap in energies of the single-particle levels. Especially in the case of the isotope ^{254}Lr studied here the used α-γ coincident method proved that the ground state transition should be located about 200 keV lower than the level populated by measurable α-transition. Resulting Q_α-value fits well into the systematics, and would otherwise lie below the value calculated for its heavier neighboring isotope at N = 152, thus breaking the general trend. Similar case also applies to ^{258}Db whose Q_α-value $\sim$ 9460 keV was again derived with the help of previously unobserved γ-transition.

It would be beneficial for disentangling the systematics of N = 153 isotones, to which this work contributed by investigation of the decay scheme of ^{261}Sg, to produce the isotope ^{259}Rf. The information about single-particle levels in its daughter ^{255}No is rather scarce representing a missing link between levels assignment in ^{257}Rf and lighter N = 153 isotones which are sufficiently well studied. The reactions on either lead or bismuth targets can not be used to produce this isotope due to lack of suitable projectile nucleus. Thanks to recent experimental advancement at the separator SHIP concerning the usage of radioactive targets from ^{238}U would provide possibility to try the reaction ^{238}U(^{24}Mg,3n)^{259}Rf or ^{238}U(^{25}Mg,4n)^{259}Rf. The first one can most likely run from the PIG source due to high natural abundance of ^{24}Mg. The second would already require the ECR source. The experimental advantages and drawbacks as well as the yield of reaction products in respect to the beam-time request must be carefully checked by calculations.

Data analysis presented in sections 4.2, 4.3.3 and 4.3.4 proved that at reasonably long irradiation times even odd-odd transfermium elements can be studied in detail by α-γ spectroscopy methods. The valuable information concerning the isomeric states, multipolarity of the observed transitions and thus nuclear level can be obtained. This information should serve as a baseline and yet major challenge for theoretical model, which leave the topic of calculations of structure properties of odd-odd nuclei for its difficulty virtually untouched at present.

The results presented in this work contribute to improvement of knowledge on spectroscopic properties of elements in transfermium region. This is valuable not only for continuation of research in the field of superheavy elements but also for bettering the systematics and deepening the knowledge of theoretical properties of neutron deficient elements.

Many of the results obtained raised new questions and interest in these nuclei. In all of the cases presented here, new experiments and further study of these isotopes is needed to fully understand the structure of these nuclei. These studies will helps us to better understand the behavior of the atomic nucleus under extreme conditions. Many of the fundamental questions raised almost 50 years ago still remain unanswered. The spectroscopic studies presented in this thesis contribute a tiny portion to the sea of knowledge bringing the answers a little bit closer.

Appendix A

Publications in refereed articles

1. **Second experiment at VASSILISSA separator on the synthesis of the element 112**
   Yu. Ts. Oganessian, A. V. Yeremin, A. G. Popeko, O. N. Malyshev, A. V. Belozerov, G. V. Buklanov, M. L. Chelnokov, V. I. Chepigin, V. A. Gorshkov, S. Hofmann, M. G. Itkis, A. P. Kabachenko, B. Kindler, G. Münzenberg, R. N. Sagaidak, Š. Šáro, H.-J. Schött, B. Štreicher, A. V. Shutov, A. I. Svirichin and G. K. Vostokin
   Eur. Phys. J. A **19**, 3-6 (2004)

2. **Properties of heavy nuclei measured at the GSI SHIP**
   S. Hofmann, F. P. Heßberger, D. Ackerman, S. Antalic, P. Cagarda, B. Kindler, P. Kuusiniemi, M. Leino, B. Lommel, O. N. Malyshev, R. Mann, G. Münzenberg, A. G. Popeko, Š. Šáro, B. Štreicher, A.V. Yeremin
   Nuclear Physics A **734**, 93-100 (2004)

3. **In-Flight Separation and Mass Selection of Heavy Evaporation Residues**
   Yu. Ts. Oganessian, A. V. Yeremin,A. G. Popeko, O. N. Malyshev, A. V. Belozerov, G. V. Buklanov, M. L. Chelnokov, V. I. Chepigin, V. A. Gorshkov, S. Hofmann, M. G. Itkis, A. P. Kabachenko, B. Kindler, G. Münzenberg, R. N. Sagaidak, Š. Šáro, H. J. Schött, B. Štreicher, A. V. Shutov, A. I. Svirichin and G. K. Vostokin
   Nuclear Physics A **734**, 196-199 (2004)

4. **Cross section systematics for the lightest Bi and Po nuclei produced in complete fusion reactions with heavy irons**
   A. N. Andreyev, D. Ackerman, S. Antalic, I. G. Darby, S. Franchoo, F. P. Heßberger, S. Hofmann, M. Huyse, P. Kuusiniemi, B. Lommel, B. Kindler, R. Mann, G. Münzenberg, R. D. Page, Š. Šáro, B. Sulignano, B. Štreicher, K. Van de Vel, P. Van Duppen, D. R. Wiseman
   Phys. Rev. C **72**, 014612 (2005)

5. **α-decay spectroscopy of the new isotope ^{192}At**
   A. N. Andreyev, S. Antalic, D. Ackerman, S. Franchoo, F. P. Heßberger, S. Hofmann, M. Huyse, I. Kojouharov, B. Kindler, P. Kuusiniemi, S. R. Lesher, B. Lommel, R. Mann, G. Münzenberg, K. Nishio, R. D. Page, J. J. Ressler, B. Štreicher, Š. Šáro, B. Sulignano, P. Van Duppen, D. R. Wiseman
   Phys. Rev. C **73**, 024317 (2006)

6. **α-decay of the new isotope ^{187}Po: Probing prolate structures beyound the neutron mid-shell at N = 104**
   A. N. Andreyev, S. Antalic, D. Ackerman, S. Franchoo, F. P. Heßberger, S. Hofmann, M. Huyse, I. Kojouharov, B. Kindler, P. Kuusiniemi, S. R. Lesher, B. Lommel, R. Mann, G. Münzenberg, K. Nishio, R. D. Page, J. J. Ressler, B. Štreicher, Š. Šáro, B. Sulignano, P. Van Duppen, D. R. Wiseman
   Phys. Rev. C **73**, 044324 (2006)

Following publications deal with the spectroscopy of isotopes in transfermium region from experiments performed at SHIP and have a direct link with the isotopes discussed in this thesis. They are periodicaly refered to in sections 4.1.2, 4.1.3 and 4.4:

7. **Energy systematics of low-lying Nilsson levels in odd-mass einsteinium isotopes**
   F. P. Heßberger, S. Antalic, B. Štreicher, S. Hofmann, D. Ackerman, B. Kindler, I. Kojouharov, P. Kuusiniemi, M. Leino, B. Lommel, R. Mann, K. Nishio, Š. Šáro, B. Sulignano
   Eur. Phys. J. A **26**, 233-239 (2005)

8. **Alpha - gamma decay studies of ^{255}Rf, ^{251}No, and ^{247}Fm**
   F. P. Heßberger, S. Hofmann, D. Ackerman, S. Antalic, B. Kindler, I. Kojouharov, P. Kuusiniemi, M. Leino, B. Lommel, R. Mann, K. Nishio, A. G. Popeko, Š. Šáro, B. Štreicher, B. Sulignano, M. Venhart, A. V. Yeremin
   Submited in Eur. Phys. J. A (2006)

9. **Alpha - gamma decay studies of ^{255}No**
   F. P. Heßberger, S. Hofmann, D. Ackerman, S. Antalic, B. Kindler, I. Kojouharov, P. Kuusiniemi, M. Leino, B. Lommel, R. Mann, K. Nishio, A. G. Popeko, Š. Šáro, B. Štreicher, B. Sulignano, M. Venhart, A. V. Yeremin
   Submited in Eur. Phys. J. A (2006)

10. **Synthesis and properties of the heaviest elements**
    S. Antalic, B. Štreicher, F. P. Heßberger, S. Hofmann, D. Ackerman, Š. Šáro, B. Sulignano,
    Acta Physica Slovaca vol. **56**, 87-90 (2006)

11. **Alpha - gamma decay studies of ^{261}Sg and ^{257}Rf**
    B. Štreicher, F. P. Heßberger, S. Antalic, D. Ackerman, S. Hofmann, Š. Šáro, B. Sulignano,
    In preparation (2006)

Other publications:

1. **Measurement of beam energy in she experiments carried out on the VASSILISSA separator**
   A. I. Svirikhin, A. V. Jeremin, A. G. Popeko, O. N. Malyshev, A. V. Belozerov, V. I. Sagaydak, V. I. Chepigin, A. P. Kabachenko, M. L. Chelnokov, V. A. Gorshkov, A. V. Shutov, B. Štreicher
   Scientific Report 2001-2002 - Dubna, Joint Institute for Nuclear Research, 234 (2003)

2. **Search for element 113**
   S. Hofmann, D. Ackerman, S. Antalic, H. G. Burkhard, P. Cagarda, F. P. Heßberger, B. Kindler, I. Kojouharov, P. Kuusiniemi, M. Leino, B. Lommel, O. N. Malyshev, R. Mann, G. Münzenberg, A. G. Popeko, Š. Šáro, H. J. Schött, B. Štreicher, B. Sulignano, J. Uusitalo, A.V. Yeremin
   GSI Scientific Report 2003, (2004)

3. **Nilsson levels in odd mass odd Z nuclei in the region Z=(99-105)**
   F. P. Heßberger, S. Hofmann, D. Ackerman, S. Antalic, I. Kojouharov, P. Kuusiniemi, R. Mann, K. Nishio, Š. Šáro, B. Štreicher, B. Sulignano, M. Venhart
   GSI Scientific Report 2004, (2005)

4. **Decay spectroscopy of ^{255}No**
   F. P. Heßberger, S. Hofmann, D. Ackerman, S. Antalic, I. Kojouharov, P. Kuusiniemi, R. Mann, K. Nishio, Š. Šáro, B. Štreicher, B. Sulignano, M. Venhart
   GSI Scientific Report 2004, (2005)

5. **Evidence for an isomeric state in ^{251}No**
   B. Sulignano, F. P. Heßberger, S. Hofmann, D. Ackerman, S. Antalic, I. Kojouharov, P. Kuusiniemi, R. Mann, K. Nishio, Š. Šáro, B. Štreicher, M. Venhart
   GSI Scientific Report 2004, (2005)

6. **New isotopes ^{186,187}Po and ^{192}At**
   A. N. Andreyev, S. Antalic, D. Ackerman, S. Franchoo, F. P. Heßberger, S. Hofmann, M. Huyse, I. Kojouharov, B. Kindler, P. Kuusiniemi, S. R. Lesher, B. Lommel, R. Mann, G. Münzenberg, K. Nishio, R. D. Page, J. Ressler, B. Štreicher, B. Sulignano, K. Van de Vel, P. Van Duppen, D. R. Wiseman
   GSI Scientific Report 2004, (2005)

7. **Shape coexistence in Pb-Po region: Properties of new ^{186,187}Po and ^{192}At isotopes**
   B. Štreicher, A. N. Andreyev, S. Antalic, Š. Šáro
   15th Conference of Slovak and Czech Physicists: Proceedings of Abstracts, Košice (2005)

Appendix B

Abbreviations

- antiTOF - In anticoincidence with Time Of Flight system
- SHE - Super Heavy Elements
- SHIP - Separator of Heavy Ion Products
- RITU - Reacoil Ion Transport Unit
- Re - Recoiling Nucleus (Recoil) - also refered to as Evaporation Residue - ER
- CN - Compound Nucleus
- PSSD - Position Sensitive Silicon Detector
- TOF - Time Of Flight
- g.s. - Ground State
- GSI - Gesellschaft Für Schwerionenforschung (Company for Heavy Ion Research)
- JYFL - Jyväskylän Yliopisto - Fysiikan Laitos (University of Jyväskylä - Department of Physics)
- LBNL - Lawrence Barkeley National Laboratory
- JINR - Joint Institute For Nuclear Research
- EC - Electron Capture
- IC - Internal Conversion
- SF - Spontaneous Fission
- UNILAC - Linear Accelerator
- SHO - Simple Harmonic Oscillator

Bibliography

[1] V. M. Strutinsky, Nucl. Phys. A **95**, 420 (1967)

[2] R. Smolanczuk *et al.*, Phys. Rev. C **52**, 1871 (1995)

[3] K. Rutz *et al.*, Phys. Rev. C **56**, 238 (1997)

[4] S. G. Nilsson *et al.*, Phys. Lett. B **28**, 458 (1969)

[5] Yu. Ts. Oganessian, Presentation at the workshop on *The Future of the Superheavy Element Research*, GSI, Darmstadt, February 17 - 18, 2004

[6] S. Hofmann *et al.*, Eur. Phys. J. A **14**, 147-157 (2002)

[7] G. Giardina *et al.*, Eur. Phys. J. A **8**, 205-216 (2000)

[8] F.P.Heßberger, GSI Report, GSI 85-11, (1985)

[9] H. Geiger and J. M. Nuttall, Philos. Mag. **22**, 613 (1911)

[10] G. Gamow, Z. Phys. **52**, 510 (1929)

[11] E. U. Condon and R. W. Gurney, Phys. Rev. **33**, 127 (1929)

[12] J. O. Rasmussen, Phys. Rev. **113**, 1593 (1958)

[13] G. Igo, Phys. Rev. Letters **1**, 72 (1958)

[14] Y. Hatsukawa *et al.*, Phys. Rev. C **42** 674-682 (1990)

[15] D.N. Poenaru *et al.*, J. Physique **41** 589-590 (1980)

[16] E. Rurarz, Acta Physica Polonica B**14** 917 (1983)

[17] M. G. Mayer, Phys. Rev. **75**, 1969 (1949)

[18] O. Haxel, J. H. D. Jensen, H. E. Suess, Phys. Rev. **113**, 1766 (1949)

[19] R. D. Woods and D. S. Saxon, Phys. Rev. **95**, 577-578 (1954)

[20] S. G. Nilsson, Kgl. Dan. Viden. Selsk. Mat. Fys. Medd. 29, No.16 (1955)

[21] P. T. Greenlees, to be published (2006)

[22] G. Münzenberg *et al.*, Nucl. Inst. and Meth. **65**, 161 (1979)

[23] G. Müunzenberg, Rep. Prog. Phys. **51** 57 (1988)

[24] S. Hofmann and G. M*ü*unzenberg, Rev. Mod. Phys. **72** 733 (2000)

[25] G. Münzenberg *et al.*, Nuc. Inst. and Meth. **186** 423-433 (1981)

[26] Š. Šaro *et al.*, Nucl. Instr. and Meth. in Phys. Res. A **381** 520-526, (1996)

[27] B. Kindler *et al.*, AIP Conf. Proc. **680** 781 (2003)

[28] B. Sulignano, PhD. Thesis to be published (2006)

[29] F.P. Heßberger *et al.*, Eur. Phys. J. A **22** 417-427 (2004)

[30] R.D. Herzberg *et al.*, Eur. Phys. J. A **15** 205-208 (2002)

[31] R.D. Herzberg *et al.*, J. Phys. G: Nucl. Part. Phys **30** R123-R141 (2004)

[32] G. N. Flerov *et al.*, Nucl. Phys. A **160** 181 (1971)

[33] A.Ghiorso *et al.*, Phys. Rev. C **4** 1850 (1971)

[34] F.P.Heßberger *et al.*, Eur. Phys. J. A **12** 57 (2001)

[35] F.P. Heßberger *et al.*, Nucl. Instr. Meth. in Phys. Res. B **204** 597 (2003)

[36] K.H. Schmidt *et al.*, Z. Phys. A **316** 19 (1984)

[37] S. Ćwiok *et al.*, Nuc. Phys A **573**, 356-394, (1994)

[38] A. Parkhomenko, A. Sobiczewski, Acta Phys. Polonica **35** 2447-2471 (2004)

[39] H.G. Essel *et al.*, GSI Multi-Branch System User Manual, GSI Darmstadt (2000)

[40] H.G. Essel, GOOSY *Data Acquisition and Analysis*, GSI Darmstadt (1988); URL: `http://www-gsi-vms.gsi.de/anal/home.html`

[41] H.G. Essel, GSI *Object Oriented On-line Off-line system*, GSI Darmstadt (1988); URL: `http://www-gsi-vms.gsi.de/anal/home.html`

[42] R. Brun and F. Rademakers, ROOT - *An Object Oriented Analysis Framework* CERN Geneva (1996); URL: `http://root.cern.ch`

[43] G. Münzenberg *et al.*, Z. Phys. A **322**, 227-235 (1985)

[44] J.F. Ziegler and J.P. Biersack, SRIM-*2003, Stopping and Range of Ions in Matter*, `URL: http://www.srim.org`, (2003)

[45] F.P.Heßberger, Privat communication

[46] G. Münzenberg *et al.*, Z. Phys. A **328**, 49 (1987) (1985)

[47] F.P.Heßberger *et al.*, Z. Phys. A **321**, 317-327 (1985)

[48] F.P.Heßberger *et al.*, Z. Phys. A **359**, 415-425 (1997)

[49] F.P.Heßberger *et al.*, J. Phys. G: Nucl.Part.Phys. **25** 877-879, (1999)

[50] A. Ghiorso *et al.*, Phys. Rev. Lett. **22**, 1317 (1969)

[51] J. Bemis *et al.*, Phys. Rev. Lett. **31**, 647 (1973)

[52] F.P.Heßberger *et al.*, Z. Phys. A **322**, 557 (1985)

[53] I. Ahmad *et al.*, Phys. Rev. C A **68**, 044306 (2003)

[54] S. Antalic, Ph.D Thesis, Comenius University, Bratislava, (2005)

[55] B. Sulignano *et al.*, GSI Scientific Report 2004 (GSI Report 2005-1), 74 (2005)

[56] F.P.Heßberger *et al.*, GSI Scientific Report 2004 (GSI Report 2005-1), 73 (2005)

[57] F.P.Heßberger *et al.*, to be published in Eur. Phys. J. A, (2006)

[58] S. Hofmann *et al.*, Z. Phys. A **358**, 377-378 (1997)

[59] F.P.Heßberger *et al.*, in preparation

[60] S. Antalic, Private communication (2006)

[61] T. Kibédi *et al.*, Proceedings of the International Conference on Nuclear Data for Science and Technology, AIP Conference Series, CP**769**, 268 (2005)

[62] A. A. Chasman *et al.*, Rev. Mod. Phys. **49**, 833 (1977)

[63] G. T. Seaborg and W. D. Loveland, The Elements Beyound Uranium, J. Wiley & Sons, INNC., New-York, Chichester, Brisbane, Toronto, Singapore, (1990)

[64] Y. A. Ellis, M. R. Schmorak, Nucl. Data scheets B8, 345 (1972)

[65] M. Asai *et al.*, Phys. Rev. Lett. **95**, 102502 (2005)

[66] P. Reiter *et al.*, Phys. Rev. Lett. **95**, 032501 (2005)

[67] W. Nazarewicz *et al.*, Nucl. Phys. A **701**, 165c (2002)

[68] A. Parkhomenko, A. Sobiczewski, Acta Phys. Polonica B**36** 3115-3137 (2005)

[69] T. Bengtsson and I. Ragnarsson, Nucl. Phys. A **436**, 14 (1985)

[70] R. B. Firestone and V. S. Shirley, *Table of Isotopes*, 8th edition, John Wiley and Sons, New York, 1996

[71] W. Reisdorf, Z. Phys. A **300**, 227 (1981)

[72] W. Reisdorf and M. Schädel, Z. Phys. A **343**, 47 (1992)

[73] Y. T. Oganessian *et al.*, Nucl. Phys. A **273**, 505 (1976)

[74] G. Münzenberg *et al.*, Z. Phys. A **300**, 107 (1981)

[75] G. Münzenberg *et al.*, Z. Phys. A **333**, 163-175 (1989)

[76] C. M. Folden III *et al.*, Phys. Rev. C **73**, 014611 (2006)

[77] S. Hofmann *et al.*, Eur. Phys. J. A **10**, 5 (2001)

[78] P. Möller *et al.*, Atomic Data Nucl. Data Tables **66**, 131 (1997)

[79] P. Möller *et al.*, Atomic Data Nucl. Data Tables **59**, 185-381 (1995)

[80] I. Ahmad *et al.*, Phys. Rev. C, 044301 (2000)

[81] A. Chatillon *et al.*, to be published in EPJ